

GENETIC TOOLS AND PRIMARY CELL MODELS ENABLE DISCOVERY OF NOVEL
MECHANISMS OF IMMUNE REGULATION IN LUNG HEALTH AND DISEASE.

By

Sean M. Thomas

A DISSERTATION

Submitted to
Michigan State University
in partial fulfillment of the requirements
for the degree of

Microbiology and Molecular Genetics-Doctor of Philosophy

2023

ABSTRACT

Chronic respiratory infections are a leading cause of death worldwide. These can range in cause from genetic, to toxic, to pathogenic, but nearly all are characterized by dysfunction of the pulmonary immune response. Pathogenic respiratory diseases are caused by airborne bacteria or viruses that are inhaled and withstand the lung immune response to establish infection and cause disease. Of pathogenic bacteria, *Mycobacterium tuberculosis* (Mtb), the causative agent of Tuberculosis, is by far the deadliest in terms of global burden, infecting nearly a third of the world's population, and killing 1.5 million per year. Current treatment and prevention strategies of pulmonary tuberculosis are insufficient due to antibiotic resistance and lack of an effective vaccine.

Recently, efforts have been made to address this pandemic through the development of host-directed therapies, which, instead of targeting the bacterium directly, aim to treat disease by modulating host immune responses, allowing them to better control the infection. Development of these therapies requires an intimate understanding of the pathogenesis of Mtb within the lungs, the events that take place during infection, and the immune mechanisms that are responsible for a successful or failed immune response. A significant obstacle in developing novel host-directed therapies for pulmonary tuberculosis has been an inability to effectively and efficiently study the tissues that play significant roles during infection. When Mtb enters the lung, the first cell it interacts with is the alveolar macrophage (AM), where it resides for multiple weeks. Therefore, to develop an understanding of the initial events that occur following exposure to Mtb, we must understand the alveolar macrophage and its

interactions with Mtb. However, an obstacle in this venture has been the scarcity of these cells within the lungs, and the recalcitrance of these cells to ex vivo culture.

In this dissertation, I sought to address this obstacle by developing a novel ex vivo alveolar macrophage model that we can use to expand our understanding of the alveolar macrophage and pulmonary response to disease. We employ CRISPR/Cas9 genetics on a genome-wide scale to identify factors that contribute to the uniqueness of AM biology and pave the way for future genetics approaches to uncover AM-specific mechanisms of pathogen response. We explore the role of the essential cytokine TGF β in this model and uncover a novel mechanism of TLR2-mediated type 1 interferon production that occurs through a mitochondrial anti-viral response pathway and may play a role in IFN β production during Mtb infection. To conclude my studies, I investigate a potential genetic interaction of Caspase1 and the phagocyte oxidase during Mtb infection, and discover an extreme susceptibility of mice that lack both of these factors to tuberculosis. This susceptibility is characterized by dysregulation of cytokine responses and recruitment of permissive granulocytes and highlights the utility of the investigation of genetic interactions as a strategy to uncover novel immune mechanisms of protection during tuberculosis.

Taken together, these studies explore lung biology and the numerous ways that AMs are a unique and important cell population. They underscore the utility of this platform to, when used in combination with functional genetic approaches, broaden our currently inadequate knowledge of pulmonary tuberculosis and lung inflammation.

This dissertation is dedicated to my parents, Gary and Kristin Thomas, for teaching me to strive for more, to my wife, Anna Thomas, for supporting me in everything we endeavor to achieve, and the Cleary and Fata families, for making Michigan home to a Missouri kid that didn't know a soul within 500 miles.

ACKNOWLEDGEMENTS

To my parents: You taught me to reach for the stars, and how to get there. You impressed upon me the value of hard work and made me believe that I could become whatever I wanted. You encouraged me to learn, and learn, and never stop learning. It was this mindset that drove me through college, and now through my PhD.

To Anna: You supported me through the easy times, and the times where I didn't leave the computer for weeks on end from writer's block. You babysat the dogs for whole weeks while I was away at conferences. Speaking of conferences, you took it in stride when I went on a conference less than a week after our wedding, when we should have been on our honeymoon on an island way. Last of all, you're letting me take you away from your friends and family to move to a state in which you know no one. These past five years have been tough, but they've been better with you.

To Andrew. You taught me how to science. When I joined the lab, I had essentially zero research experience, technical experience, scientific reading experience, or really any other relevant experience that might have given me a head start in a PhD program. I made every mistake in the book (and even invented a few new ones for the book), but you were patient and encouraging through it all, helping me slowly learn to be a scientist. Now, as I defend my dissertation and move on, I can without a shred of doubt say that I wouldn't be remotely close to where I am now if it wasn't for your mentoring.

To my guidance committee, Drs. Rob Abramovitch, Jon Hardy, Jim Pestka, and Andrea Doseff: the support, guidance, and insight that you afforded to me during our meetings was invaluable in shaping my research and path towards graduation. During

each of our interactions, the positivity and reinforcement that I received helped reassure me that I was on the right path and working towards a successful and fulfilling PhD experience.

To Larry and Harry: Congratulations, you made it into the acknowledgements. Graduate school (especially getting a PhD) was supposed to be a miserable experience. I was told that I would dread the monotonous slog that was unsuccessful experiments (cloning) and endless reading and writing that I didn't have the motivation for but had to do regardless. That's not what happened, though. You guys made it, dare I say, fun. Misery loves company. Having you two that I could be myself around and candidly share experiences with (both the good ones and the bad ones) made all the difference in the world, and I can only hope that I find colleagues like you in future positions.

TABLE OF CONTENTS

LIST OF ABBREVIATIONS.....	viii
CHAPTER 1: INTRODUCTION.....	1
BIBLIOGRAPHY.....	21
CHAPTER 2: FLAMS: A SELF-REPLICATING EX VIVO MODEL OF ALVEOLAR MACROPHAGES FOR FUNCTIONAL GENETIC STUDIES	40
BIBLIOGRAPHY	80
CHAPTER 3: TGFB PRIMES ALVEOLAR-LIKE MACROPHAGES TO INDUCE TYPE I IFN FOLLOWING TLR2 ACTIVATION	87
BIBLIOGRAPHY	120
CHAPTER 4: RAPID LETHALITY OF MICE LACKING PHAGOCYTE OXIDASE AND CASPASE1/11 FOLLOWING <i>MYCOBACTERIUM TUBERCULOSIS</i> INFECTION. ...	125
BIBLIOGRAPHY	153
CHAPTER 5: CONCLUDING REMARKS AND FUTURE DIRECTIONS	158
BIBLIOGRAPHY	168

LIST OF ABBREVIATIONS

AECII	Type II alveolar epithelial cells
AM	Alveolar macrophage
ASC	Apoptosis-associated speck-like protein containing a CARD
BCG	Bacillus Calmette–Guérin
BMDM	Bone marrow-derived macrophage
CARD	Caspase activation and recruitment domain
CGD	Chronic Granulomatous Disease
CLR	C-type lectin receptor
cSiO ₂	Crystalline silica
DAMP	Damage-associated molecular pattern
FACS	Fluorescence activated cell sorting
FLAM	Fetal liver-derived alveolar-like macrophage
GSEA	Gene set enrichment analysis
HDT	Host-directed therapy
HSC	Hematopoietic stem cell
IFN	Interferon
IPF	Idiopathic pulmonary fibrosis
IRF	Interferon regulatory factor
ISG	Interferon-stimulated gene
LAP	Latency-associated peptide
LPS	Lipopolysaccharide
M-CSF	Macrophage colony-stimulating factor

MAVS	Mitochondrial antiviral-signaling protein
MHCII	Major histocompatibility complex II
MSMD	Mendelian Susceptibility to Mycobacterial Disease
NLR	Nod-like receptor
Mab	<i>Mycobacterium abcessus</i>
Mtb	<i>Mycobacterium tuberculosis</i>
PAMP	Pathogen-associated molecular pattern
PAP	Pulmonary alveolar proteinosis
PPAR	Peroxisome proliferator-activating receptor
PRR	Pattern recognition receptors
PYD	Pyrin domain
RLR	RIG-I like receptor
RNS	Reactive nitrogen species
ROS	Reactive oxygen species
T7SS	Type VII secretion system
TDM	Trehelose dimycolate
TB	Tuberculosis
TCR	T-cell receptor
TGFβ	Transforming growth factor beta
TLR	Toll-like receptor
TIDE	Tracking of Indels by Decomposition
TLR	Toll-like receptor
TNF	Tumor necrosis factor

TRM	Tissue resident macrophage
cSiO ₂	Crystalline silica
SLE	Systemic Lupus Erythematosus

CHAPTER 1: INTRODUCTION

OUR LUNGS AND THE AIR WE BREATHE

Our lungs work at the interface between our bodies and the outside world. Their purpose is to facilitate gas exchange in our blood by bringing in oxygen and expelling carbon dioxide. This function requires that lungs be both highly vascular but also exposed to the oxygen-containing external environment. As a result, blood vessels and lymphatic tissue comes into close proximity to inhaled foreign matter that occupies the air we breathe. This matter can range from harmless particles of debris that can be easily cleared, to pathogens, allergens, and toxicants that can damage the lungs and cause disease. For this reason, the surface-air interface must be strictly surveilled by immune cells that sample their surrounding environment, searching for this foreign matter. These cells then must determine the threat of these particulates and tightly regulate their responses to harmless, and harmful antigens.

MACROPHAGES IN THE LUNGS

Like nearly all organs, the lungs are occupied by numerous immune cell populations that serve to sense and respond to antigens and coordinate an appropriate immune response when necessary. These immune populations can be divided into two categories: innate immune cells, which initiate rapid responses to a vast array of antigens and alert the body to a threat, and adaptive immune cells, which activate in response to innate immune signaling and mount delayed, but highly specific and robust responses. One important class of innate immune cells is the macrophage. Macrophages are the bodies primary resident mononuclear phagocytes that serve numerous critical functions throughout the body including tissue development, tissue

repair, homeostasis and innate immune signaling(1–12). In their immune capacity, macrophages detect, engulf (phagocytose), digest, and present antigens that are encountered to elicit adaptive immune responses if necessary. Concerning lung immunity, there are two primary macrophage populations: alveolar macrophages (AMs) and infiltrating/recruited macrophages(13, 14). AMs are tissue-resident macrophages that play a key role in maintaining lung homeostasis by clearing surfactant and patrolling the alveoli to directly sense and respond to inhaled matter before it enters the body(15–17). Infiltrating or recruited macrophages, however, reside within the circulation during homeostasis and are not localized to the lung, but are recruited there during disease(1, 13). These two macrophages are highly distinct populations that fill unique niches through diverse regulation of metabolic and inflammatory pathways.

MACROPHAGE DEVELOPMENT AND HETEROGENEITY

Macrophages throughout the body can broadly be separated into two classes: circulating, bone marrow-derived monocytes (BMDMs), and tissue-resident macrophages (TRMs) (18). Circulating macrophages arise throughout life from hematopoietic stem cells (HSCs), a process called hematopoiesis, and develop into monocytes, when, as their name suggests, they circulate in the bloodstream for a brief period before dying or being recruited to a tissue to develop into mature macrophages(19–21). The functions of these macrophages are directed by transient, local signals and can range from driving inflammation and anti-microbial functions to resolving inflammation and repairing tissue damage following inflammation. TRMs, unlike circulating macrophages, exist at homeostasis in mature, functional states(22,

23). There are numerous distinct TRM populations within the body that reside exclusively in their respective tissues. In addition to alveolar macrophages in the lung, there are Kupffer cells in the liver, microglia in the brain, and red pulp macrophages in the spleen, among many others. Each of these TRMs are unique in their tissue-specific functions but have the shared characteristic of developing from stem cells in the yolk sac and seeding their respective tissues during fetal development(22, 24). Once in these tissues, unlike circulating monocytes, these TRM populations proliferate and are self-maintained throughout life, independent from hematopoiesis. Also unlike circulating monocytes, TRMs more tightly regulate inflammation and disease response pathways. As circulating monocytes are primarily functional in tissue when they've been recruited due to existing inflammation, they need to more rapidly and robustly induce the pro/anti-inflammatory responses as dictated by the already-present immune cells(13, 25–29). TRMs, being constitutively present and active in their tissue, must more tightly regulate inflammation and disease response pathways. As inflammation is damaging to both pathogen and host, driving an unnecessarily robust inflammatory response to a tolerable stimulus is detrimental to the host. This is especially important in the case of alveolar macrophages. Since the air we breathe is laden with inert and non-pathogenic particles, AMs must determine if what they engulf is pathogenic or not, and strictly control their inflammatory responses to the countless antigens that they encounter. This careful regulation of inflammation is likely due in part to expression of the transcription factor PPAR γ , dependence on the immune-modulating cytokine TGF β , and the reliance of AMs on fatty acid metabolism for the generation of energy(30–39). Comparatively, inflammatory bone marrow-derived macrophages express far less PPAR γ during

homeostasis and while contributing to inflammation. They also primarily employ glycolysis as a means to generate metabolic intermediates, with a shift to fatty acid metabolism being associated with an anti-inflammatory BMDM phenotype(40–48). These numerous and significant differences highlight the need to study circulating macrophage and individual TRM populations in their own context, so that we can specifically understand the ontogeny-related and environmental factors that allow these populations to function in such a distinct manner.

BONE MARROW-DERIVED MACROPHAGES VS ALVEOLAR MACROPHAGES FOR EX VIVO STUDY

Compared to BMDMs, our understanding of what makes AMs unique and how they control their biology and inflammatory processes is remarkably limited. BMDMs are well characterized due to both the ease of accessibility to large numbers of primary cells, and the existence of numerous immortalized BMDM (iBMDM) models that faithfully recapitulate BMDM biology and permit large scale *in vitro* replication and experimentation. Tens of millions of primary BMDMs can be acquired in less than a week by extracting crude bone marrow from a single mouse and incubating it with cell culture media containing macrophage colony-stimulating factor (M-CSF, a cytokine that matures the HSCs into macrophages)(49–51). These strategies allow for rapid and extensive exploration of BMDM immune regulation and responses using large scale - omics and genetic manipulation studies, such as CRISPR-Cas9-mediated genetic knockout, that require extended culture ex-vivo(52–54). AMs, however, are much more difficult to study ex vivo, as they develop quickly after birth and exist exclusively in

relatively small numbers in a complex and heterogenous tissue. Isolation of this cell population from murine lungs is a tedious and time-consuming process that yields prohibitively low numbers of viable cells ($5 \times 10^4 - 2 \times 10^5$ cells/mouse)(55, 56).

Additionally, macrophages that are recovered from the lung are highly unstable ex vivo, and quickly lose their AM-like properties in traditional cell culture media(55). For these reasons, our current understanding of suitable growth conditions for primary AMs renders them largely unsuitable for ex-vivo studies exploring AM biology. Due to the aforementioned problems with primary AMs and the availability and accessibility of BMDMs and iBMDMs, the BMDM models have largely been the basis of study in understanding general macrophage biology and inflammatory responses. While informative, these studies do not necessarily capture the numerous unique and important differences between BMDMs and AMs(5, 13, 14, 25, 26, 29, 36, 39, 46, 47). Therefore, there is a need for the development of an accessible alveolar macrophage-like cell model that can stably be maintained ex vivo in high quantities for extended periods of time.

In 2013, a research group led by Marina Freudenberg at the Max Planck Institute in Hamburg, Germany, attempted to resolve this problem by leveraging the tissue ontogeny of alveolar macrophages to create a fetal-liver derived macrophage that possessed AM-like characteristics at steady state and in response to inflammatory stimuli(57). These cells developed ex-vivo after mechanical disruption of the fetal liver when cultured in traditional cell culture media and GM-CSF. In this study, Fejer et al showed that in response to lipopolysaccharide (LPS) or the mycobacterial cell wall component trehalose dimycolate (TDM), fetal-liver derived macrophages expressed

AM-like cytokine profiles and displayed highly distinct transcription profiles compared to bone marrow monocytes in response to LPS. Overall, this new cell model was a promising candidate for the study of AM biology ex vivo. Such a model would allow for exploration and genetic dissection of lung biology and regulation of pulmonary inflammation, so that we can better understand factors contributing to lung inflammation and disease.

CHRONIC LUNG DISEASES ARE A MAJOR GLOBAL PUBLIC HEALTH CONCERN

Chronic respiratory diseases are diseases of the lung that can persist anywhere on the scale of years to being lifelong conditions. They are diverse and multifactorial in their etiology, but primarily arise due to dysregulation of immune function in the lungs. Chronic respiratory diseases are a major public health concern and leading cause of mortality in the United States and worldwide. Respiratory infections and non-communicable chronic respiratory diseases account for 2 of the top 5 causes of death worldwide, with a global burden of 3.59 million and 3.54 million deaths caused per year, respectively(58, 59). These diseases can be the result of genetic mutation, environmental exposure to toxins (such as crystalline silica (cSiO₂)), or infection with pathogenic bacteria or viruses that are able to withstand the immune response and drive chronic inflammation. The most notable and impactful of these chronic lung disease-causing bacteria is *Mycobacterium tuberculosis* (Mtb), a hardy bacterium that is highly effective in suppressing and evading host immune responses to establish chronic pulmonary infections.

GLOBAL BURDEN AND CHALLENGES OF TUBERCULOSIS

Mycobacterium tuberculosis, the causative agent of tuberculosis (TB), is an intracellular, obligate human pathogen responsible for the death of over 1.5 million people per year, making it the number one cause of death due to infectious disease and the 13th leading cause of all deaths in the world(60). It's estimated that over 10.5 million individuals become infected with Mtb every year, with the majority of these infections occurring in sub-Saharan Africa and southeast Asia where funding for the prevention, diagnosis, and treatment of TB is inadequate, and access to clinics is limited. The most effective vaccine available, the Bacillus Calmette–Guérin (BCG) vaccine, is a live, attenuated version of the closely related *M. bovis* that lacks a virulence factor necessary for infection(61–63). However, this vaccine is ineffective in preventing pulmonary tuberculosis in adults and cannot be used in patients that are clinically immunosuppressed, and as such, plays a limited role in controlling tuberculosis transmission. Treatment of drug-susceptible forms of the disease is prohibitive, costing on average ~\$20,000 USD and involving a 2-month regimen of the first line antibiotics isoniazid, rifampin, pyrazinamide, and ethambutol, followed by 4-month regimen of isoniazid and rifampin if the infection is improving(64, 65). The already extensive time and resource cost of treatment further rises in the case of drug-resistant infections, with the most extensively drug-resistant infections requiring decades of treatment that cost hundreds of thousands of dollars and carry a low rate of success(66). Unfortunately, drug resistance among Mtb isolates is rising due to ineffective antibiotic prescription, non-compliance with the arduous and lengthy treatment plans, and mutation of bacterial drug targets during infection(67, 68).

HOST-DIRECTED THERAPIES AS A NOVEL ANTI-TB THERAPEUTIC STRATEGY

The increase in antibiotic resistant Mtb infections highlights the need for alternative treatment options that employ novel mechanisms to target infections. An emerging strategy in the fight against tuberculosis is host-directed therapy (HDT). Unlike traditional anti-tuberculosis therapies that directly target the pathogen, HDTs aim to bolster the existing host defenses to allow for better control of disease, either by controlling harmful inflammation, or by better equipping host cells to eradicate the infection. Many current anti-tuberculosis HDTs are targeted at controlling the hyper-active inflammatory response that occurs during infection and is responsible for disease. Promising progress has been made in the use of anti-inflammatory therapies such as corticosteroids, phosphodiesterase inhibitors, or non-steroid cox-inhibitors to systemically dampen immune responses, leading to less severe disease(69–75). Alternatively, vitamin D therapies have been shown to decrease bacterial burden by amplifying certain inflammatory responses within infected animals, but clinical trials using Vitamin D gave mixed results(76–80). While these therapies have potential to help control TB, their non-specific and systemic effects make them unsuitable for large-scale use; broadly anti-inflammatory drugs will permit increased Mtb growth and susceptibility to co-infections, while generalized inflammation-amplifying strategies allow for higher killing of the bacteria at the cost of the health of the patient. However, there are a handful of more directed HDTs that are being explored for use against TB. Imatinib, an FDA approved ABL tyrosine kinase inhibitor for use against poxvirus, has been shown to improve TB in mice through increased acidification of Mtb-containing

phagosomes(81, 82). Lipid metabolism has also been a target in HDT through the use of statins, or mepenzolate bromide, molecules that reduce cholesterol levels and blocks Mtb-driven lipid accumulation, respectively(83, 84). However, these compounds have only been tested in mouse models, and further work is needed to identify their utility as future therapies. The shortcomings of current and potential HDTs highlight the need to uncover more specific and effective host-directed anti-TB therapies.

Creating therapies that specifically target Mtb infections requires a high level of understanding of the events that occur during these infections, and the interactions between host immune cells and bacteria throughout the course of disease. Understanding these interactions will inform decisions regarding both which pathways should be targeted, how they can be targeted, and at what point during infection treatment is likely to be most effective.

PATHOGEN RECOGNITION AND INITIAL TRANSCRIPTIONAL RESPONSES

To understand how Mtb evades the host immune response and establishes infection, we must first explore the events and processes that take place during an intact, effective host response to bacterial pathogens in the lung. The immune response is initiated by contact and recognition of bacteria by patrolling phagocytes, typically macrophages(85). These macrophages express pattern recognition receptors (PRRs) that recognize and bind to bacteria-derived pathogen-associated molecular patterns (PAMPs) or host cell-derived damage-associated molecular patterns (DAMPs)(86). There are 4 classes of PRRs that each sense various PAMPs and DAMPs at different

locations within the cell. These are: toll-like receptors (TLRs), C-type lectin receptors (CLRs), nucleotide-binding oligomerization domain (NOD)-like receptors (NLRs), and retinoic acid-inducible gene I (RIG-I)-like receptors (RLRs)(87–91). TLRs are membrane bound on the plasma membrane or in endosome and sense diverse ligands to activate proinflammatory transcription factors AP-1, NFκB, or interferon response factors (IRFs)(92–99). CLRs are located on the plasma membrane, sense pathogen-derived glycans and induce activation of the transcription factors NFκB, AP-1 and NFAT(100–103). NLRs are located in the cytoplasm and sense various PAMPs to drive NFκB and AP-1 activation as well as activation of numerous inflammasomes(104–108). RLRs are located in the cytoplasm and sense viral RNA to drive type 1 interferon responses through mitochondrial antiviral-signaling protein (MAVS). An important PRR that doesn't necessarily fall into any of the above-mentioned categories is cGAS, which is similar to RLRs in that it senses cytosolic nucleic acids to induce type 1 interferon responses. Unlike RLRs however the cGAS pathway senses DNA and activates STING through cGAMP production, which drives interferon signaling(109–111). A relatively conserved function of these PRRs is their ability to induce activation of the transcription factors NFκB and AP-1(112–115). These transcription factors induce the production of proinflammatory cytokines such as IL-1, TNFα, and IL-6. TNFα and IL-6 are functional cytokines immediately following translation, but IL-1 is translated as an inactive precursor that must be proteolytically cleaved to become active. In macrophages, this enzymatic activation is achieved as a function of an inflammasome(116, 117).

INFLAMMASOMES

Inflammasomes are cytosolic oligomers that proteolytically cleave precursor cytokines into their mature forms for secretion in response to PRR activation(116, 118). There are numerous canonical inflammasomes that sense and respond to various stimuli, but they all share a similar 3-part structure. The first part is the sensor, which is a PRR that varies between inflammasomes, detects specific ligands and initiates inflammasome activation. Each sensor contains a pyrin domain (PYD), which functions as a binding point for the second subunit, the apoptosis-associated speck-like protein containing a CARD (ASC). ASC is the adapter protein which contains PYD and caspase activation and recruitment domain (CARD) domains to facilitate oligomerization of the sensor and recruitment and activation of the third functional subunit of the inflammasome, caspase-1. Active caspase-1 cleaves pro-IL1, pro-IL18, and Gasdermin D, resulting in pore formation in the plasma membrane and secretion of the mature cytokines, often resulting in the pro-inflammatory form of programmed cell death, pyroptosis(119, 120).

PATHOGEN UPTAKE, PHAGOSOME MATURATION AND ANTIGEN PRESENTATION

In addition to initiating inflammatory signals through pathogen recognition, phagocytosis of the pathogen is a major component of the macrophage's response to pathogenic bacteria. During CLR or opsonin-mediated recognition, the macrophages use actin polymerization to reorganize the plasma membrane around the bacterium, creating a phagocytic cup(121–124). The distal portions of the phagocytic cup then

fuse, resulting in an intracellular, membrane-bound, bacteria-containing organelle called the phagosome(125). The phagosome then undergoes a series of transformations and fuses with early and late endosomes, resulting in toxification of the maturing phagosome through vacuolar-ATPase mediated acidification, phagocyte oxidase-mediated reactive oxygen species (ROS)-generation, and recruitment of cathepsins and hydrolases(126–129). Finally, the late phagosome fuses with lysosomes to become the highly anti-microbial phagolysosome. Lysosomes contain numerous acid-activated hydrolytic enzymes that degrade the contents of the phagolysosome following fusion(126, 130). The macrophage then loads the degraded microbial fragments onto major histocompatibility complex II (MHCII) molecules, which are transported to the exterior of the cell(131, 132). During this process, the macrophage travels through the lymphatic system to a nearby draining lymph node, where it interacts with a vast array of T cells. The extracellular MHCII on the macrophage surface then binds to CD4+T cell receptors (TCRs) that are specific for the presented antigen(133–135). This interaction, along with the interactions of PRR-induced costimulatory molecules and TCR-associated cognate receptors, activate the T-cell(136–139). These pathogen-specific activated CD4+T cells then polarize to the antibacterial Th1 subtype, rapidly proliferate, and produce large amounts of IL-2 and IFN γ (136, 140). IFN γ activates surrounding macrophages to further upregulate antimicrobial and antigen-presentation pathways and has been shown to play an important role in protection to tuberculosis, as patients with deficiencies in IFN γ signaling are diagnosed with Mendelian Susceptibility to Mycobacterial Disease (MSDM), and as the name suggests, are highly susceptible to tuberculosis and nontubercular mycobacterial infections(141–148). IFN γ is also

produced by other cells, including innate lymphoid cells, which are present in the lung at homeostasis, suggesting a potential role of IFN γ during initial immune signaling as well as during CD4 $^+$ T cell activation(149, 150).

THE BALANCE OF DISEASE RESISTANCE AND DISEASE TOLERANCE

The production of inflammatory cytokines and antimicrobial pathways such as TNF α , IFN γ , and ROS generation are all aimed at limiting bacterial burden. As such, they are termed disease resistance mechanisms and were traditionally thought to be the sole means of surviving disease. These resistance mechanisms come at a cost, however, as they also damage the surrounding tissue. In fact, with some exception in regards to persistent cough, hypersensitive immune reactions are likely responsible for all symptoms of pulmonary tuberculosis infections, rather than toxins or effectors from the bacteria itself(151–155). To counteract the tissue-destructive effects of disease resistance responses and pathogen-mediated damage, the body also possesses tolerance responses, which can be just as important as resistance mechanisms when considering disease outcome. This two-pronged defense strategy, first observed in plants, can be thought of as a balancing act by the immune system(156, 157). If resistance mechanisms outweigh tolerance mechanisms, the resulting tissue damage can result in poor prognosis, regardless of bacterial burden. Inversely, if tolerance mechanisms play too large of a roll, antimicrobial responses will be muted, and the infection will progress relatively unchecked, which is also detrimental to the host(158). As resistance mechanisms have largely been the focus of susceptibility studies, work uncovering/identifying tolerance mechanisms is lacking. Typically, these mechanisms

can be dissected by both measuring disease state and pathogen burden simultaneously: resistance mechanisms can be identified by a susceptibility characterized by increased pathogen load, while tolerance mechanisms control disease state with no change in pathogen load(159–161). To further complicate matters, dissection of these two phenotypes can be complicated: loss of a gene or pathway of interest may lead to increased bacterial burden; this could indicate that said gene is involved in bacterial resistance and thus directly resulting in decreased bacterial killing, or it could play a role in tolerance, and the increased bacterial burden is a result of the bacteria taking advantage of extensive tissue necrosis. This dichotomy in disease responses can inform strategies in discovering novel host-directed therapeutics; combining knowledge of both the stage of infection during which the pathway of interest is proposed to be a candidate for therapy and the mechanism by which said pathway protects against disease can inform us about the likelihood of targeted therapy being beneficial. Thus, to identify optimal pathways to target with host-directed therapies, we must understand the immunological and pathological events surrounding infection with Mtb and the progression of tuberculosis.

THE INFECTIOUS CYCLE OF TUBERCULOSIS

Tuberculosis primarily manifests as a multi-stage, dynamic, pulmonary infection(162). The initial stage of infection, called active tuberculosis, is established when an individual inhales airborne, Mtb-containing droplets. Once the bacterium is in the lung, it is recognized by PRRs on the surface of the tissue-resident lung macrophage population, alveolar macrophages (AMs) and is phagocytosed(163–171).

Thus, the battle between AM and Mtb begins. This process, while not fully understood in AMs, is well characterized from both the host and pathogen perspective in bone marrow-derived macrophages (BMDMs) due to its relative simplicity compared to later stages of infection.

Mtb possesses an arsenal of virulence factors that arrest phagosome maturation and subsequently inhibit phagolysosome fusion while blocking macrophage anti-bacterial responses. One of the most studied, ESX-1, is a type 7 secretion systems (T7SS), which is a specialized class of secretion systems unique to mycobacteria and limited gram-positive bacteria(172, 173). ESX-1 effectors cause phagosome membrane damage, resulting in secretion of bacterial effectors into the cytosol and are essential for Mtb virulence(172). ESX-1 secreted factors are responsible for the induction of type-1 IFNs, either through direct secretion of Mtb DNA or ESX-1 mediated mitochondrial damage, which are typically activated in response to cytosolic DNA, a common occurrence during viral infections(174, 175). This decoy anti-viral response inhibits cellular IFN γ -mediated antibacterial responses and allows for persistence within the macrophage(174). Additionally, secreted factors from ESX-3, another virulence-associated T7SS, specifically block action of ESCRT machinery, therefore inhibiting phagolysosome fusion(176, 177). Many of the complex mycolic acids and lipid moieties on the surface of Mtb also are sensed by the toll like receptor TLR2, which induces production of the anti-inflammatory cytokine IL-10 and inhibits MHCII production, further suppressing macrophage activation and antigen presentation(178, 179).

These immune-evasion mechanisms, among many others, allow the bacteria to reside and replicate within the immunologically silenced macrophage for up to 2 weeks.

During this replication period, the bacteria secrete factors through ESX-1 that induce translocation of the infected macrophage from the alveolar lumen into the lung interstitium, leading to the recruitment of local immune populations to the infected AMs which form an early cellular aggregate and mark the initiation of the adaptive immune response to infection(163, 180). This immune response is characterized by the formation of the highly structured and dynamic granuloma that is visible by chest radiograph and is characteristic of Mtb infection(181, 182).

Infected patients can have many granulomas during an infection, each of which likely arise from a single bacterium and are structurally unique, with some common characteristics(183, 184). The center of the granuloma is a highly inflammatory necrotic core, which is composed of infected macrophages and multi-nucleated giant cells. Surrounding this inner layer are uninfected phagocytes such as foam cells, neutrophils, macrophages, and dendritic cells. The outer layer of the granuloma is comprised of recruited lymphocytes and serves an anti-inflammatory role, protecting the surrounding tissue from the inflammatory center(184). The purpose of the granuloma is two-fold: the necrotic center aims to sterilize the infection by killing the bacteria, but if that is unsuccessful, the surrounding cells function to physically wall off the infection and prevent it from disseminating. The latter function is the most important, however, as Mtb survives within the center of the granuloma by entering a dormant, non-replicative state that renders it resistant to the antibacterial mechanisms that the immune system employs (and many antibiotics)(185–189).

An effective immune response contains the infection within these granulomas for decades, surrounding them with fibrotic scar tissue to “heal” them. This is considered

the latent stage of infection and is asymptomatic. The majority of patients remain at this stage for the duration of their lives. However, patients that are immunocompromised or immunosuppressed may never resolve the infection and healthy patients that are latently infected but become immunosuppressed may eventually progress to the reactivation stage of infection(190–195). During this stage, cellular immunity within the granuloma fails, and Mtb comes out of dormancy and begins replicating again, resulting in a renewed inflammatory response that results in cavitation of the granuloma into either the airways or circulatory system(196–199). Granulomas that cavitate into the airways cause coughing, a phenomenon that may in part be mediated by neurologically active Mtb secreted factors, and the production of Mtb-laden droplets that are infectious(155). Granulomas that cavitate into circulatory system lead to dissemination of the disease, and can result in infection of virtually any organ(200–202).

WHEN, WHERE AND HOW TO FOCUS ANTI-TB HOST-DIRECTED THERAPY EFFORTS

The dynamic and complicated course of events that occur during Mtb infection results in numerous questions to be answered when exploring strategies for uncovering targets for potential anti-TB HDTs. The physical inaccessibility and non-replicative dormancy of Mtb during latent infection, and the already-severe disease and immune exhaustion that is present during the reactivation stage of infection suggest that targeting latent or reactivated infections for host-directed therapy would be highly complicated and have a low chance success(185, 187, 199). However, given the immune potential of uninfected or recently infected individuals, the relative simplicity

from a cell-population standpoint during early infection, and how little is known regarding the AM-specific interactions with Mtb, the initial stages of infection are an attractive target for the development of novel, host-directed therapies(17, 163, 203). If we can use genetic manipulation and genetic interaction studies to understand the inflammatory networks involved in protection during Mtb infection and why AMs are unable to control Mtb growth following initial exposure, we will be better able to target deficient anti-microbial pathways for therapy.

DISSERTATION DIRECTION AND OVERVIEW

In this dissertation, I seek to fill a gap in knowledge regarding alveolar macrophages and the genetic immune networks that control protection during Mtb infection, so that we may better prevent and eliminate pulmonary TB infections by identifying potential targets for host-directed therapy.

To begin this work, I investigate the previously described ex vivo alveolar macrophage like cell model alveolar macrophage biology and regulation of AM inflammatory pathways both during and independent of Mtb infection. I discover that the cytokine TGF β is required to fully develop and maintain fetal-liver derived macrophages into AM-like cells during ex vivo culture. I then employ this model in a previously impossible manner by using CRISPR-Cas9 genetic editing to dissect cytokine responses to the environmental toxin crystalline silica and employ a forward genetic screen to identify genetic pathways that are necessary for the surface expression of an AM-specific surface protein.

I then sought to further understand the impact of TGF β on the inflammatory profiles of these ex vivo AM-like cells. Whole-transcriptome sequencing and cytokine secretion analysis highlight global changes in metabolic and inflammatory pathways in cells that have been cultured in TGF β . We use synthetic TLR agonists to uncover alternative signaling through TLR2 and results in a muted global inflammatory response, with the exception of IFN β , which is exacerbated and is known to be detrimental during pulmonary TB infection. We again use genetic studies to dissect the mechanisms behind this increased IFN β production and discover that it occurs through a novel TLR2/MAVS signaling axis, further highlighting the unique inflammatory regulation of AMs.

To finish, I expound on previous work that identified a protective role of the NADPH phagocyte oxidase during Mtb infection. Loss of this phagocyte oxidase was shown to result in uncontrolled inflammasome and Caspase-1 activation and IL-1 β production, resulting in a loss in disease tolerance and susceptibility to infection, independent of bacterial burden. We explore this interaction between the phagocyte oxidase and Caspase1 by characterizing Mtb infection in cells and lacking both components, and uncover a novel synthetic lethal genetic interaction characterized by aberrant cytokine production, increased bacterial burden, and hyper-susceptibility of infected mice to TB.

BIBLIOGRAPHY

1. Murray PJ, Wynn TA. 2011. Protective and pathogenic functions of macrophage subsets. *Nature Reviews Immunology* 2011 11:11 11:723–737.
2. Schulz D, Severin Y, Zanotelli VRT, Bodenmiller B. 2019. In-Depth Characterization of Monocyte-Derived Macrophages using a Mass Cytometry-Based Phagocytosis Assay. *Sci Rep* 9.
3. Jäger AV, Arias P, Tribulatti MV, Brocco MA, Pepe MV, Kierbel A. 2021. The inflammatory response induced by *Pseudomonas aeruginosa* in macrophages enhances apoptotic cell removal. *Sci Rep* 11.
4. Wang Y, Zhao M, Liu S, Guo J, Lu Y, Cheng J, Liu J. 2020. Macrophage-derived extracellular vesicles: diverse mediators of pathology and therapeutics in multiple diseases. *Cell Death Dis* 11.
5. Hill DA, Lim HW, Kim YH, Ho WY, Foong YH, Nelson VL, Nguyen HCB, Chegireddy K, Kim J, Habertheuer A, Vallabhajosyula P, Kambayashi T, Won KJ, Lazar MA. 2018. Distinct macrophage populations direct inflammatory versus physiological changes in adipose tissue. *Proc Natl Acad Sci U S A* 115:E5096–E5105.
6. Zhang C, Yang M, Ericsson AC. 2021. Function of Macrophages in Disease: Current Understanding on Molecular Mechanisms. *Front Immunol* 12:635.
7. Herzog C, Garcia LP, Keatinge M, Greenald D, Moritz C, Peri F, Herrgen L. 2019. Rapid clearance of cellular debris by microglia limits secondary neuronal cell death after brain injury in vivo. *Development (Cambridge)* 146.
8. Orecchioni M, Ghosheh Y, Pramod AB, Ley K. 2019. Macrophage polarization: Different gene signatures in M1(Lps+) vs. Classically and M2(LPS-) vs. Alternatively activated macrophages. *Front Immunol* 10.
9. Kratz M, Coats BR, Hisert KB, Hagman D, Mutskov V, Peris E, Schoenfelt KQ, Kuzma JN, Larson I, Billing PS, Landerholm RW, Crouthamel M, Gozal D, Hwang S, Singh PK, Becker L. 2014. Metabolic dysfunction drives a mechanistically distinct proinflammatory phenotype in adipose tissue macrophages. *Cell Metab* 20:614–625.
10. Vannella KM, Wynn TA. 2017. Mechanisms of Organ Injury and Repair by Macrophages*. *Annu Rev Physiol* 79:593–617.
11. Watanabe S, Alexander M, Misharin A v., Budinger GRS. 2019. The role of macrophages in the resolution of inflammation. *J Clin Invest* 129:2619.
12. van Furth R, Cohn ZA. 1968. The origin and kinetics of mononuclear phagocytes. *J Exp Med* 128:415–435.

13. Hou F, Xiao K, Tang L, Xie L. 2021. Diversity of Macrophages in Lung Homeostasis and Diseases. *Front Immunol* 12:3930.
14. Shi T, Denney L, An H, Ho LP, Zheng Y. 2021. Alveolar and lung interstitial macrophages: Definitions, functions, and roles in lung fibrosis. *J Leukoc Biol* 110:107–114.
15. Misharin A v., Budinger GRS, Perlman H. 2011. The lung macrophage: A jack of all trades. *Am J Respir Crit Care Med* 184:497–498.
16. Byrne AJ, Mathie SA, Gregory LG, Lloyd CM. 2015. Pulmonary macrophages: Key players in the innate defence of the airways. *Thorax* 70:1189–1196.
17. Hu G, Christman JW. 2019. Editorial: Alveolar Macrophages in Lung Inflammation and Resolution. *Front Immunol* 10:2275.
18. Ginhoux F, Schultze JL, Murray PJ, Ochando J, Biswas SK. 2015. New insights into the multidimensional concept of macrophage ontogeny, activation and function. *Nature Immunology* 2015 17:1 17:34–40.
19. Gonzalez-Mejia ME, Doseff AI. 2009. Regulation of monocytes and macrophages cell fate. *Front Biosci (Landmark Ed)* 14:2413–2431.
20. Geissmann F, Jung S, Littman DR. 2003. Blood monocytes consist of two principal subsets with distinct migratory properties. *Immunity* 19:71–82.
21. Parihar A, Eubank TD, Doseff AI. 2010. Monocytes and Macrophages Regulate Immunity through Dynamic Networks of Survival and Cell Death. *J Innate Immun* 2:204.
22. Ginhoux F, Guilliams M. 2016. Tissue-Resident Macrophage Ontogeny and Homeostasis. *Immunity* 44:439–449.
23. Hashimoto D, Chow A, Noizat C, Teo P, Beasley MB, Leboeuf M, Becker CD, See P, Price J, Lucas D, Greter M, Mortha A, Boyer SW, Forsberg EC, Tanaka M, van Rooijen N, García-Sastre A, Stanley ER, Ginhoux F, Frenette PS, Merad M. 2013. Tissue-resident macrophages self-maintain locally throughout adult life with minimal contribution from circulating monocytes. *Immunity* 38:792–804.
24. Gomez Perdiguero E, Klapproth K, Schulz C, Busch K, Azzoni E, Crozet L, Garner H, Trouillet C, de Bruijn MF, Geissmann F, Rodewald HR. 2015. Tissue-resident macrophages originate from yolk-sac-derived erythro-myeloid progenitors. *Nature* 518:547–551.
25. Kumar V. 2020. Pulmonary Innate Immune Response Determines the Outcome of Inflammation During Pneumonia and Sepsis-Associated Acute Lung Injury. *Front Immunol* 11:1722.

26. Mould KJ, Barthel L, Mohning MP, Thomas SM, McCubbrey AL, Danhorn T, Leach SM, Fingerlin TE, O'Connor BP, Reisz JA, D'Alessandro A, Bratton DL, Jakubzick C v., Janssen WJ. 2017. Cell origin dictates programming of resident versus recruited macrophages during acute lung injury. *Am J Respir Cell Mol Biol* 57:294–306.
27. Misharin A v., Morales-Nebreda L, Reyfman PA, Cuda CM, Walter JM, McQuattie-Pimentel AC, Chen CI, Anekalla KR, Joshi N, Williams KJN, Abdala-Valencia H, Yacoub TJ, Chi M, Chiu S, Gonzalez-Gonzalez FJ, Gates K, Lam AP, Nicholson TT, Homan PJ, Soberanes S, Dominguez S, Morgan VK, Saber R, Shaffer A, Hinchcliff M, Marshall SA, Bharat A, Berdnikovs S, Bhorade SM, Bartom ET, Morimoto RI, Balch WE, Sznajder JI, Chandel NS, Mutlu GM, Jain M, Gottardi CJ, Singer BD, Ridge KM, Bagheri N, Shilatifard A, Budinger GRS, Perlman H. 2017. Monocyte-derived alveolar macrophages drive lung fibrosis and persist in the lung over the life span. *Journal of Experimental Medicine* 214:2387–2404.
28. Shi T, Denney L, An H, Ho LP, Zheng Y. 2021. Alveolar and lung interstitial macrophages: Definitions, functions, and roles in lung fibrosis. *J Leukoc Biol* 110:107–114.
29. Liao X, Shen Y, Zhang R, Sugi K, Vasudevan NT, Amer Alaiti M, Sweet DR, Zhou L, Qing Y, Gerson SL, Fu C, Wynshaw-Boris A, Hu R, Schwartz MA, Fujioka H, Richardson B, Cameron MJ, Hayashi H, Stamler JS, Jain MK. 2018. Distinct roles of resident and nonresident macrophages in nonischemic cardiomyopathy. *Proc Natl Acad Sci U S A* 115:E4661–E4669.
30. Ginhoux F. 2014. Fate PPAR-titoning: PPAR-gamma “instructs” alveolar macrophage development. *Nat Immunol*2014/10/21. 15:1005–1007.
31. Reddy RC. 2008. Immunomodulatory role of PPAR-gamma in alveolar macrophages. *J Investig Med*2008/03/05. 56:522–527.
32. Baker AD, Malur A, Barna BP, Ghosh S, Kavuru MS, Malur AG, Thomassen MJ. 2010. Targeted PPAR{gamma} deficiency in alveolar macrophages disrupts surfactant catabolism. *J Lipid Res*2010/01/13. 51:1325–1331.
33. Croasdell A, Duffney PF, Kim N, Lacy SH, Sime PJ, Phipps RP. 2015. PPARgamma and the Innate Immune System Mediate the Resolution of Inflammation. *PPAR Res*2015/12/30. 2015:549691.
34. Hou Y, Moreau F, Chadee K. 2012. PPARgamma is an E3 ligase that induces the degradation of NFkappaB/p65. *Nat Commun*2012/12/20. 3:1300.
35. Yu X, Buttgerit A, Lelios I, Utz SG, Cansever D, Becher B, Greter M. 2017. The Cytokine Tgfβ Promotes the Development and Homeostasis of Alveolar Macrophages. *Immunity*2017/11/12. 47:903-912 e4.

36. Svedberg FR, Brown SL, Krauss MZ, Campbell L, Sharpe C, Clausen M, Howell GJ, Clark H, Madsen J, Evans CM, Sutherland TE, Ivens AC, Thornton DJ, Grecis RK, Hussell T, Cunoosamy DM, Cook PC, MacDonald AS. 2019. The lung environment controls alveolar macrophage metabolism and responsiveness in type 2 inflammation. *Nat Immunol* 20:571–580.
37. Gao X, Zhu B, Wu Y, Li C, Zhou X, Tang J, Sun J. 2022. TFAM-Dependent Mitochondrial Metabolism Is Required for Alveolar Macrophage Maintenance and Homeostasis. *The Journal of Immunology* 208:1456–1466.
38. Pearce EL, Pearce EJ. 2013. Metabolic pathways in immune cell activation and quiescence. *Immunity* 38:633–643.
39. Woods PS, Kimmig LM, Meliton AY, Sun KA, Tian Y, O’Leary EM, Gökalp GA, Hamanaka RB, Mutlu GM. 2020. Tissue-resident alveolar macrophages do not rely on glycolysis for LPS-induced inflammation. *Am J Respir Cell Mol Biol* 62:243–255.
40. Johnson AR, Qin Y, Cozzo AJ, Freerman AJ, Huang MJ, Zhao L, Sampey BP, Milner JJ, Beck MA, Damania B, Rashid N, Galanko JA, Lee DP, Edin ML, Zeldin DC, Fueger PT, Dietz B, Stahl A, Wu Y, Mohlke KL, Makowski L. 2016. Metabolic reprogramming through fatty acid transport protein 1 (FATP1) regulates macrophage inflammatory potential and adipose inflammation. *Mol Metab* 5:506–526.
41. Malandrino MI, Fucho R, Weber M, Calderon-Dominguez M, Mir JF, Valcarcel L, Escoté X, Gómez-Serrano M, Peral B, Salvadó L, Fernández-Veledo S, Casals N, Vázquez-Carrera M, Villarroya F, Vendrell JJ, Serra D, Herrero L. 2015. Enhanced fatty acid oxidation in adipocytes and macrophages reduces lipid-induced triglyceride accumulation and inflammation. *Am J Physiol Endocrinol Metab* 308:E756–E769.
42. Wang F, Zhang S, Vuckovic I, Jeon R, Lerman A, Folmes CD, Dzeja PP, Herrmann J. 2018. Glycolytic Stimulation Is Not a Requirement for M2 Macrophage Differentiation. *Cell Metab* 28:463-475.e4.
43. Im SS, Yousef L, Blaschitz C, Liu JZ, Edwards RA, Young SG, Raffatellu M, Osborne TF. 2011. Linking lipid metabolism to the innate immune response in macrophages through sterol regulatory element binding protein-1a. *Cell Metab* 13:540–549.
44. Batista-Gonzalez A, Vidal R, Criollo A, Carreño LJ. 2020. New Insights on the Role of Lipid Metabolism in the Metabolic Reprogramming of Macrophages. *Front Immunol* 10:2993.
45. Min BK, Park S, Kang HJ, Kim DW, Ham HJ, Ha CM, Choi BJ, Lee JY, Oh CJ, Yoo EK, Kim HE, Kim BG, Jeon JH, Hyeon DY, Hwang D, Kim YH, Lee CH, Lee T, Jungwhan K, Choi YK, Park KG, Chawla A, Lee J, Harris RA, Lee IK. 2019.

- Pyruvate dehydrogenase kinase is a metabolic checkpoint for polarization of macrophages to the M1 phenotype. *Front Immunol* 10.
46. Wang T, Liu H, Lian G, Zhang SY, Wang X, Jiang C. 2017. HIF1 α -Induced Glycolysis Metabolism Is Essential to the Activation of Inflammatory Macrophages. *Mediators Inflamm* 2017.
 47. Freemerman AJ, Johnson AR, Sacks GN, Milner JJ, Kirk EL, Troester MA, Macintyre AN, Goraksha-Hicks P, Rathmell JC, Makowski L. 2014. Metabolic reprogramming of macrophages: Glucose transporter 1 (GLUT1)-mediated glucose metabolism drives a proinflammatory phenotype. *Journal of Biological Chemistry* 289:7884–7896.
 48. Viola A, Munari F, Sánchez-Rodríguez R, Scolaro T, Castegna A. 2019. The metabolic signature of macrophage responses. *Front Immunol* 10:1462.
 49. Austin PE, McCulloch EA, Till JE. 1971. Characterization of the factor in L-cell conditioned medium capable of stimulating colony formation by mouse marrow cells in culture. *J Cell Physiol* 77:121–133.
 50. Richard Stanley E. 1985. The macrophage colony-stimulating factor, CSF-1. *Methods Enzymol* 116:564–587.
 51. Johnson BK, Thomas SM, Olive AJ, Abramovitch RB. 2021. Macrophage Infection Models for Mycobacterium tuberculosis. *Methods in Molecular Biology* 2314:167–182.
 52. Jinek M, Chylinski K, Fonfara I, Hauer M, Doudna JA, Charpentier E. 2012. A programmable dual-RNA-guided DNA endonuclease in adaptive bacterial immunity. *Science* (1979) 337:816–821.
 53. Maddalo D, Manchado E, Concepcion CP, Bonetti C, Vidigal JA, Han YC, Ogradowski P, Crippa A, Rekhman N, Stanchina E de, Lowe SW, Ventura A. 2014. In vivo engineering of oncogenic chromosomal rearrangements with the CRISPR/Cas9 system. *Nature* 2014 516:7531 516:423–427.
 54. Ran FA, Hsu PD, Wright J, Agarwala V, Scott DA, Zhang F. 2013. Genome engineering using the CRISPR-Cas9 system. *Nat Protoc* 8:2281–2308.
 55. Nayak DK, Mendez O, Bowen S, Mohanakumar T. 2018. Isolation and In Vitro Culture of Murine and Human Alveolar Macrophages. *J Vis Exp* 2018:57287.
 56. Cohen AB, Cline MJ. 1971. The human alveolar macrophage: isolation, cultivation in vitro, and studies of morphologic and functional characteristics. *J Clin Invest* 50:1390–1398.
 57. Fejer G, Wegner MD, Györy I, Cohen I, Engelhard P, Voronov E, Manke T, Ruzsics Z, Dölken L, da Costa OP, Branzk N, Huber M, Prasse A, Schneider R,

- Apte RN, Galanos C, Freudenberg MA. 2013. Nontransformed, GM-CSF-dependent macrophage lines are a unique model to study tissue macrophage functions. *Proc Natl Acad Sci U S A* 110:E2191–E2198.
58. Bochen Cao by, Stevens GA, Ho J, Ma Fat D, Cao Gretchen Stevens BA, Ma D, Estevez D, Daher J, Ferlay J, Gacic-Dobo M, Gerland P, Glaziou P, Hug L, Ilaych K, Jakob R, Liu L, Lozano R, Mahy M, Mathers C, Moller A-B, Msemburi W, Naghavi M, Noor A, Patel MK, You D. 2000. Global Health Estimates Technical Paper.
 59. Murphy SL, Kochanek KD, Xu J, Arias E. 2020. Mortality in the United States, 2020 Key findings Data from the National Vital Statistics System.
 60. Geneva: World Health Organization. 2022. Global tuberculosis report 2022.
 61. Peck M, Gacic-Dobo M, Diallo MS, Nedelec Y, Sodha S v, Wallace AS. 2019. Global Routine Vaccination Coverage, 2018. *MMWR Morb Mortal Wkly Rep* 68:937–942.
 62. Abubakar I, Pimpin L, Ariti C, Beynon R, Mangtani P, Sterne J, Fine P, Smith P, Lipman M, Elliman D, Watson J, Drumright L, Whiting P, Vynnycky E. 2013. Systematic review and meta-analysis of the current evidence on the duration of protection by bacillus Calmette-Guérin vaccination against tuberculosis. *Health Technol Assess* 17:1–4.
 63. Pym AS, Brodin P, Brosch R, Huerre M, Cole ST. 2002. Loss of RD1 contributed to the attenuation of the live tuberculosis vaccines *Mycobacterium bovis* BCG and *Mycobacterium microti*. *Mol Microbiol* 46:709–717.
 64. Nahid P, Dorman SE, Alipanah N, Barry PM, Brozek JL, Cattamanchi A, Chaisson LH, Chaisson RE, Daley CL, Grzemska M, Higashi JM, Ho CS, Hopewell PC, Keshavjee SA, Lienhardt C, Menzies R, Merrifield C, Narita M, O'Brien R, Peloquin CA, Raftery A, Saukkonen J, Schaaf HS, Sotgiu G, Starke JR, Migliori GB, Vernon A. 2016. Executive Summary: Official American Thoracic Society/Centers for Disease Control and Prevention/Infectious Diseases Society of America Clinical Practice Guidelines: Treatment of Drug-Susceptible Tuberculosis. *Clinical Infectious Diseases* 63:853–867.
 65. Aslam M v., Owusu-Edusei K, Marks SM, Asay GRB, Miramontes R, Kolasa M, Winston CA, Dietz PM. 2018. Number and cost of hospitalizations with principal and secondary diagnoses of tuberculosis, United States. *Int J Tuberc Lung Dis* 22:1495–1504.
 66. Marks SM, Flood J, Seaworth B, Hirsch-Moverman Y, Armstrong L, Mase S, Salcedo K, Oh P, Graviss EA, Colson PW, Armitige L, Revuelta M, Sheeran K. 2014. Treatment practices, outcomes, and costs of multidrug-resistant and extensively drug-resistant tuberculosis, United States, 2005-2007. *Emerg Infect Dis* 20:812–821.

67. Dean AS, Tosas Auguste O, Glaziou P, Zignol M, Ismail N, Kasaeva T, Floyd K. 2022. 25 years of surveillance of drug-resistant tuberculosis: achievements, challenges, and way forward. *Lancet Infect Dis* 22:e191–e196.
68. Castelnuovo B. 2010. A review of compliance to anti tuberculosis treatment and risk factors for defaulting treatment in Sub Saharan Africa. *Afr Health Sci* 10:320.
69. Thwaites GE, Bang ND, Dung NH, Quy HT, Oanh DTT, Thoa NTC, Hien NQ, Thuc NT, Hai NN, Lan NTN, Lan NN, Duc NH, Tuan VN, Hiep CH, Chau TTH, Mai PP, Dung NT, Stepniewska K, White NJ, Hien TT, Farrar JJ. 2004. Dexamethasone for the treatment of tuberculous meningitis in adolescents and adults. *N Engl J Med* 351:1741–1751.
70. Vilaplana C, Marzo E, Tapia G, Diaz J, Garcia V, Cardona PJ. 2013. Ibuprofen therapy resulted in significantly decreased tissue bacillary loads and increased survival in a new murine experimental model of active tuberculosis. *J Infect Dis* 208:199–202.
71. Koo MS, Manca C, Yang G, O'Brien P, Sung N, Tsenova L, Subbian S, Fallows D, Muller G, Ehrt S, Kaplan G. 2011. Phosphodiesterase 4 inhibition reduces innate immunity and improves isoniazid clearance of *Mycobacterium tuberculosis* in the lungs of infected mice. *PLoS One* 6.
72. Maiga M, Agarwal N, Ammerman NC, Gupta R, Guo H, Maiga MC, Lun S, Bishai WR. 2012. Successful shortening of tuberculosis treatment using adjuvant host-directed therapy with FDA-approved phosphodiesterase inhibitors in the mouse model. *PLoS One* 7.
73. Bafica A, Scanga CA, Serhan C, Machado F, White S, Sher A, Aliberti J. 2005. Host control of *Mycobacterium tuberculosis* is regulated by 5-lipoxygenase-dependent lipoxin production. *J Clin Invest* 115:1601–1606.
74. Mayer-Barber KD, Andrade BB, Oland SD, Amaral EP, Barber DL, Gonzales J, Derrick SC, Shi R, Kumar NP, Wei W, Yuan X, Zhang G, Cai Y, Babu S, Catalfamo M, Salazar AM, Via LE, Barry CE, Sher A. 2014. Host-directed therapy of tuberculosis based on interleukin-1 and type I interferon crosstalk. *Nature* 511:99–103.
75. Meintjes G, Wilkinson RJ, Morroni C, Pepper DJ, Rebe K, Rangaka MX, Oni T, Maartens G. 2010. Randomized placebo-controlled trial of prednisone for paradoxical tuberculosis-associated immune reconstitution inflammatory syndrome. *AIDS* 24:2381–2390.
76. Nursyam EW, AZ, & RCM. 2006. The effect of vitamin D as supplementary treatment in patients with moderately advanced pulmonary tuberculous lesion. *Acta Med Indones* 38:3–5.

77. Morcos MM, Gabr AA, Samuel S, Kamel M, el Baz M, el Beshry M, Michail RR. 1998. Vitamin D administration to tuberculous children and its value. *Boll Chim Farm* 137:157–164.
78. Wejse C, Gomes VF, Rabna P, Gustafson P, Aaby P, Lisse IM, Andersen PL, Glerup H, Sodemann M. 2009. Vitamin D as supplementary treatment for tuberculosis: a double-blind, randomized, placebo-controlled trial. *Am J Respir Crit Care Med* 179:843–850.
79. Coussens AK, Wilkinson RJ, Hanifa Y, Nikolayevskyy V, Elkington PT, Islam K, Timms PM, Venton TR, Bothamley GH, Packe GE, Darmalingam M, Davidson RN, Milburn HJ, Baker L v., Barker RD, Mein CA, Bhaw-Rosun L, Nuamah R, Young DB, Drobniowski FA, Griffiths CJ, Martineau AR. 2012. Vitamin D accelerates resolution of inflammatory responses during tuberculosis treatment. *Proc Natl Acad Sci U S A* 109:15449–15454.
80. Martineau AR, Timms PM, Bothamley GH, Hanifa Y, Islam K, Claxton AP, Packe GE, Moore-Gillon JC, Darmalingam M, Davidson RN, Milburn HJ, Baker L v., Barker RD, Woodward NJ, Venton TR, Barnes KE, Mullett CJ, Coussens AK, Rutterford CM, Mein CA, Davies GR, Wilkinson RJ, Nikolayevskyy V, Drobniowski FA, Eldridge SM, Griffiths CJ. 2011. High-dose vitamin D(3) during intensive-phase antimicrobial treatment of pulmonary tuberculosis: a double-blind randomised controlled trial. *Lancet* 377:242–250.
81. Reeves PM, Bommarius B, Lebeis S, McNulty S, Christensen J, Swimm A, Chahroudi A, Chavan R, Feinberg MB, Veach D, Bornmann W, Sherman M, Kalman D. 2005. Disabling poxvirus pathogenesis by inhibition of Abl-family tyrosine kinases. *Nat Med* 11:731–739.
82. Napier RJ, Rafi W, Cheruvu M, Powell KR, Zaunbrecher MA, Bornmann W, Salgame P, Shinnick TM, Kalman D. 2011. Imatinib-sensitive tyrosine kinases regulate mycobacterial pathogenesis and represent therapeutic targets against tuberculosis. *Cell Host Microbe* 10:475–485.
83. Singh V, Jamwal S, Jain R, Verma P, Gokhale R, Rao KVS. 2012. Mycobacterium tuberculosis-driven targeted recalibration of macrophage lipid homeostasis promotes the foamy phenotype. *Cell Host Microbe* 12:669–681.
84. Parihar SP, Guler R, Khutlang R, Lang DM, Hurdal R, Mhlanga MM, Suzuki H, Marais AD, Brombacher F. 2014. Statin therapy reduces the mycobacterium tuberculosis burden in human macrophages and in mice by enhancing autophagy and phagosome maturation. *J Infect Dis* 209:754–763.
85. Zhang H, He F, Li P, Hardwidge PR, Li N, Peng Y. 2021. The Role of Innate Immunity in Pulmonary Infections. *Biomed Res Int* 2021.
86. Janeway CA. 1989. Approaching the asymptote? Evolution and revolution in immunology. *Cold Spring Harb Symp Quant Biol* 54 Pt 1:1–13.

87. Gack MU. 2014. Mechanisms of RIG-I-Like Receptor Activation and Manipulation by Viral Pathogens. *J Virol* 88:5213–5216.
88. Drickamer K, Taylor ME. 1993. Biology of animal lectins. *Annu Rev Cell Biol*. *Annu Rev Cell Biol* <https://doi.org/10.1146/annurev.cb.09.110193.001321>.
89. Hao L, Nei M. 2004. Genomic organization and evolutionary analysis of Ly49 genes encoding the rodent natural killer cell receptors: rapid evolution by repeated gene duplication. *Immunogenetics* 56:343–354.
90. Rock FL, Hardiman G, Timans JC, Kastelein RA, Bazan JF. 1998. A family of human receptors structurally related to *Drosophila* Toll. *Proc Natl Acad Sci U S A* 95:588–593.
91. Lange C, Hemmrich G, Klostermeier UC, López-Quintero JA, Miller DJ, Rahn T, Weiss Y, Bosch TCG, Rosenstiel P. 2011. Defining the origins of the NOD-like receptor system at the base of animal evolution. *Mol Biol Evol* 28:1687–1702.
92. Kawai T, Akira S. 2010. The role of pattern-recognition receptors in innate immunity: update on Toll-like receptors. *Nature Immunology* 2010 11:5 11:373–384.
93. Bernard JJ, Cowing-Zitron C, Nakatsuji T, Muehleisen B, Muto J, Borkowski AW, Martinez L, Greidinger EL, Yu BD, Gallo RL. 2012. Ultraviolet radiation damages self noncoding RNA and is detected by TLR3. *Nature Medicine* 2012 18:8 18:1286–1290.
94. Mancuso G, Gambuzza M, Midiri A, Biondo C, Papasergi S, Akira S, Teti G, Beninati C. 2009. Bacterial recognition by TLR7 in the lysosomes of conventional dendritic cells. *Nature Immunology* 2009 10:6 10:587–594.
95. Guiducci C, Gong M, Cepika AM, Xu Z, Tripodo C, Bennett L, Crain C, Quartier P, Cush JJ, Pascual V, Coffman RL, Barrat FJ. 2013. RNA recognition by human TLR8 can lead to autoimmune inflammation. *J Exp Med* 210:2903.
96. Hidmark A, von Saint Paul A, Dalpke AH. 2012. Cutting Edge: TLR13 Is a Receptor for Bacterial RNA. *The Journal of Immunology* 189:2717–2721.
97. Yarovinsky F, Zhang D, Andersen JF, Bannenberg GL, Serhan CN, Hayden MS, Hieny S, Sutterwala FS, Flavell RA, Ghosh S, Sher A. 2005. Immunology: TLR11 activation of dendritic cells by a protozoan profilin-like protein. *Science* (1979) 308:1626–1629.
98. Andrade WA, Souza MDC, Ramos-Martinez E, Nagpal K, Dutra MS, Melo MB, Bartholomeu DC, Ghosh S, Golenbock DT, Gazzinelli RT. 2013. Combined Action of Nucleic Acid-Sensing Toll-like Receptors and TLR11/TLR12 Heterodimers Imparts Resistance to *Toxoplasma gondii* in Mice. *Cell Host Microbe* 13:42–53.

99. Botos I, Segal DM, Davies DR. 2011. The Structural Biology of Toll-like Receptors. *Structure* 19:447–459.
100. Ali MF, Driscoll CB, Walters PR, Limper AH, Carmona EM. 2015. β -Glucan-Activated Human B Lymphocytes Participate in Innate Immune Responses by Releasing Proinflammatory Cytokines and Stimulating Neutrophil Chemotaxis. *J Immunol* 195:5318–5326.
101. Mansour MK, Tam JM, Khan NS, Seward M, Davids PJ, Puranam S, Sokolovska A, Sykes DB, Dagher Z, Becker C, Tanne A, Reedy JL, Stuart LM, Vyas JM. 2013. Dectin-1 activation controls maturation of β -1,3-glucan-containing phagosomes. *J Biol Chem* 288:16043–16054.
102. Brown GD, Willment JA, Whitehead L. 2018. C-type lectins in immunity and homeostasis. *Nature Reviews Immunology* 2018 18:6 18:374–389.
103. Drummond RA, Gaffen SL, Hise AG, Brown GD. 2014. Innate Defense against Fungal Pathogens. *Cold Spring Harb Perspect Med* 5:1–19.
104. Willingham SB, Allen IC, Bergstralh DT, Brickey WJ, Huang MT-H, Taxman DJ, Duncan JA, Ting JP-Y. 2009. NLRP3 (NALP3, cryopyrin) facilitates in vivo caspase-1, necrosis, & HMGB1 release via inflammasome-dependent and – independent pathways. *J Immunol* 183:2008.
105. Inohara N, Koseki T, del Peso L, Hu Y, Yee C, Chen S, Carrio R, Merino J, Liu D, Ni J, Núñez G. 1999. Nod1, an Apaf-1-like Activator of Caspase-9 and Nuclear Factor- κ B. *Journal of Biological Chemistry* 274:14560–14567.
106. Zhang Q, Zmasek CM, Dishaw LJ, Gail MG, Ye Y, Litman GW, Godzik A. 2008. Novel genes dramatically alter regulatory network topology in amphioxus. *Genome Biol* 9:1–9.
107. Franchi L, Warner N, Viani K, Nuñez G. 2009. Function of Nod-like Receptors in Microbial Recognition and Host Defense. *Immunol Rev* 227:106.
108. Franchi L, Muñoz-Planillo R, Núñez G. 2012. Sensing and reacting to microbes through the inflammasomes. *Nature Immunology* 2012 13:4 13:325–332.
109. Ablasser A, Goldeck M, Cavlar T, Deimling T, Witte G, Röhl I, Hopfner KP, Ludwig J, Hornung V. 2013. cGAS produces a 2'-5'-linked cyclic dinucleotide second messenger that activates STING. *Nature* 498:380–384.
110. Diner EJ, Burdette DL, Wilson SC, Monroe KM, Kellenberger CA, Hyodo M, Hayakawa Y, Hammond MC, Vance RE. 2013. The innate immune DNA sensor cGAS produces a noncanonical cyclic dinucleotide that activates human STING. *Cell Rep* 3:1355–1361.

111. Ishikawa H, Ma Z, Barber GN. 2009. STING regulates intracellular DNA-mediated, type I interferon-dependent innate immunity. *Nature* 461:788–792.
112. Pichlmair A, Schulz O, Tan CP, Näslund TI, Liljeström P, Weber F, Reis E Sousa C. 2006. RIG-I-mediated antiviral responses to single-stranded RNA bearing 5'-phosphates. *Science* 314:997–1001.
113. Kato H, Takeuchi O, Sato S, Yoneyama M, Yamamoto M, Matsui K, Uematsu S, Jung A, Kawai T, Ishii KJ, Yamaguchi O, Otsu K, Tsujimura T, Koh CS, Reis E Sousa C, Matsuura Y, Fujita T, Akira S. 2006. Differential roles of MDA5 and RIG-I helicases in the recognition of RNA viruses. *Nature* 441:101–105.
114. Yoneyama M, Kikuchi M, Natsukawa T, Shinobu N, Imaizumi T, Miyagishi M, Taira K, Akira S, Fujita T. 2004. The RNA helicase RIG-I has an essential function in double-stranded RNA-induced innate antiviral responses. *Nat Immunol* 5:730–737.
115. Goubau D, Deddouche S, Reis e Sousa C. 2013. Cytosolic sensing of viruses. *Immunity* 38:855–869.
116. Schroder K, Tschopp J. 2010. The inflammasomes. *Cell* 140:821–832.
117. Thornberry NA, Bull HG, Calaycay JR, Chapman KT, Howard AD, Kostura MJ, Miller DK, Molineaux SM, Weidner JR, Aunins J, Elliston KO, Ayala JM, Casano FJ, Chin J, Ding GJF, Egger LA, Gaffney EP, Limjuco G, Palyha OC, Raju SM, Rolando AM, Salley JP, Yamin TT, Lee TD, Shively JE, MacCross M, Mumford RA, Schmidt JA, Tocci MJ. 1992. A novel heterodimeric cysteine protease is required for interleukin-1 beta processing in monocytes. *Nature* 356:768–774.
118. Martinon F, Burns K, Tschopp J. 2002. The inflammasome: a molecular platform triggering activation of inflammatory caspases and processing of proIL-beta. *Mol Cell* 10:417–426.
119. Fink SL, Cookson BT. 2006. Caspase-1-dependent pore formation during pyroptosis leads to osmotic lysis of infected host macrophages. *Cell Microbiol* 8:1913–1926.
120. Bergsbaken T, Fink SL, Cookson BT. 2009. Pyroptosis: host cell death and inflammation. *Nat Rev Microbiol* 7:99–109.
121. Rosales C. 2007. Fc receptor and integrin signaling in phagocytes. *Signal Transduct* 7:386–401.
122. Brown GD, Taylor PR, Reid DM, Willment JA, Williams DL, Martinez-Pomares L, Wong SYC, Gordon S. 2002. Dectin-1 Is A Major β -Glucan Receptor On Macrophages. *J Exp Med* 196:407.

123. Taylor PR, Tsoni SV, Willment JA, Dennehy KM, Rosas M, Findon H, Haynes K, Steele C, Botto M, Gordon S, Brown GD. 2007. Dectin-1 is required for β -glucan recognition and control of fungal infection. *Nat Immunol* 8:31.
124. Diakonova M, Bokoch G, Swanson JA. 2002. Dynamics of Cytoskeletal Proteins during Fcy Receptor-mediated Phagocytosis in Macrophages. *Mol Biol Cell* 13:402.
125. Marion S, Mazzolini J, Herit F, Bourdoncle P, Kambou-Pene N, Hailfinger S, Sachse M, Ruland J, Benmerah A, Echard A, Thome M, Niedergang F. 2012. The NF- κ B Signaling Protein Bcl10 Regulates Actin Dynamics by Controlling AP1 and OCRL-Bearing Vesicles. *Dev Cell* 23:954–967.
126. Marshansky V, Futai M. 2008. The V-type H⁺-ATPase in vesicular trafficking: targeting, regulation and function. *Curr Opin Cell Biol* 20:415–426.
127. Levin R, Grinstein S, Canton J. 2016. The life cycle of phagosomes: formation, maturation, and resolution. *Immunol Rev* 273:156–179.
128. Brozna JP, Hauff NF, Phillips WA, Johnston RB. 1988. Activation of the respiratory burst in macrophages. Phosphorylation specifically associated with Fc receptor-mediated stimulation. *The Journal of Immunology* 141:1642–1647.
129. Minakami R, Sumimoto H. 2006. Phagocytosis-coupled activation of the superoxide-producing phagocyte oxidase, a member of the NADPH oxidase (Nox) family. *Int J Hematol* 84:193–198.
130. Nauseef WM. 2014. Myeloperoxidase in human neutrophil host defence. *Cell Microbiol* 16:1146–1155.
131. Castellino F, Germain RN. 1995. Extensive trafficking of MHC class II-invariant chain complexes in the endocytic pathway and appearance of peptide-loaded class II in multiple compartments. *Immunity* 2:73–88.
132. Roche PA, Cresswell P. 1990. Invariant chain association with HLA-DR molecules inhibits immunogenic peptide binding. *Nature* 345:615–618.
133. Jakubzick C, Gautier EL, Gibbings SL, Sojka DK, Schlitzer A, Johnson TE, Ivanov S, Duan Q, Bala S, Condon T, vanRooijen N, Grainger JR, Belkaid Y, Ma'ayan A, Riches DWH, Yokoyama WM, Ginhoux F, Henson PM, Randolph GJ. 2013. Minimal Differentiation of Classical Monocytes as They Survey Steady-State Tissues and Transport Antigen to Lymph Nodes. *Immunity* 39:599–610.
134. von Andrian UH, Mempel TR. 2003. Homing and cellular traffic in lymph nodes. *Nature Reviews Immunology* 2003 3:11 3:867–878.
135. Calabro S, Tortoli M, Baudner BC, Pacitto A, Cortese M, O'Hagan DT, de Gregorio E, Seubert A, Wack A. 2011. Vaccine adjuvants alum and MF59 induce

- rapid recruitment of neutrophils and monocytes that participate in antigen transport to draining lymph nodes. *Vaccine* 29:1812–1823.
136. Acuto O, Michel F. 2003. CD28-mediated co-stimulation: a quantitative support for TCR signalling. *Nat Rev Immunol* 3:939–951.
 137. Watts TH. 2005. TNF/TNFR family members in costimulation of T cell responses. *Annu Rev Immunol* 23:23–68.
 138. Hutloff A, Dittrich AM, Beier KC, Eljaschewitsch B, Kraft R, Anagnostopoulos I, Kroczek RA. 1999. ICOS is an inducible T-cell co-stimulator structurally and functionally related to CD28. *Nature* 397:263–266.
 139. Jenkins MK, Khoruts A, Ingulli E, Mueller DL, McSorley SJ, Lee Reinhardt R, Itano A, Pape KA. 2001. In vivo activation of antigen-specific CD4 T cells. *Annu Rev Immunol* 19:23–45.
 140. Lugo-Villarino G, Maldonado-López R, Possemato R, Peñaranda C, Glimcher LH. 2003. T-bet is required for optimal production of IFN-gamma and antigen-specific T cell activation by dendritic cells. *Proc Natl Acad Sci U S A* 100:7749–7754.
 141. Boehm U, Klamp T, Groot M, Howard JC. 1997. Cellular responses to interferon-gamma. *Annu Rev Immunol* 15:749–795.
 142. Melzer T, Duffy A, Weiss LM, Halonen SK. 2008. The gamma interferon (IFN-gamma)-inducible GTP-binding protein IGTP is necessary for toxoplasma vacuolar disruption and induces parasite egression in IFN-gamma-stimulated astrocytes. *Infect Immun* 76:4883–4894.
 143. Prete G del. 1992. Human Th1 and Th2 lymphocytes: their role in the pathophysiology of atopy. *Allergy*. <https://doi.org/10.1111/j.1398-9995.1992.tb00662.x>.
 144. Bustamante J, Boisson-Dupuis S, Abel L, Casanova JL. 2014. Mendelian susceptibility to mycobacterial disease: Genetic, immunological, and clinical features of inborn errors of IFN- γ immunity. *Semin Immunol*. NIH Public Access <https://doi.org/10.1016/j.smim.2014.09.008>.
 145. Ramirez-Alejo N, Santos-Argumedo L. 2014. Innate defects of the IL-12/IFN- γ axis in susceptibility to infections by mycobacteria and salmonella. *Journal of Interferon and Cytokine Research*. *J Interferon Cytokine Res* <https://doi.org/10.1089/jir.2013.0050>.
 146. Casanova JL, Jouanguy E, Lamhamedi S, Blanche S, Fischer A. 1995. Immunological conditions of children with BCG disseminated infection [16]. *Lancet*. *Lancet* [https://doi.org/10.1016/S0140-6736\(95\)91421-8](https://doi.org/10.1016/S0140-6736(95)91421-8).

147. Levin M, Newport MJ, Kalabalikis P, Klein N, D'Souza S, Brown IN, Lenicker HM, Vassallo Agius P, Davies EG, Thrasher A, Blackwell JM. 1995. Familial disseminated atypical mycobacterial infection in childhood: a human mycobacterial susceptibility gene? *The Lancet* 345:79–83.
148. Casanova JL, Abel L. 2002. Genetic dissection of immunity to mycobacteria: The human model. *Annu Rev Immunol*. *Annu Rev Immunol* <https://doi.org/10.1146/annurev.immunol.20.081501.125851>.
149. Weizman O et al, Adams NM, Schuster IS, Krishna C, Pritykin Y, Lau C, Degli-Esposti MA, Leslie CS, Sun JC, O'Sullivan TE. 2017. ILC1 Confer Early Host Protection at Initial Sites of Viral Infection. *Cell* 171:795-808.e12.
150. Bernink JH, Peters CP, Munneke M, te Velde AA, Meijer SL, Weijer K, Hreggvidsdottir HS, Heinsbroek SE, Legrand N, Buskens CJ, Bemelman WA, Mjösberg JM, Spits H. 2013. Human type 1 innate lymphoid cells accumulate in inflamed mucosal tissues. *Nat Immunol* 14:221–229.
151. van Crevel R, Karyadi E, Netea MG, Verhoef H, Nelwan RHH, West CE, van der Meer JWM. 2002. Decreased plasma leptin concentrations in tuberculosis patients are associated with wasting and inflammation. *J Clin Endocrinol Metab* 87:758–763.
152. Deng Z, Zhou W, Sun J, Li C, Zhong B, Lai K. 2018. IFN- γ enhances the cough reflex sensitivity via calcium influx in vagal sensory neurons. *Am J Respir Crit Care Med* 198:868–879.
153. Choudry NB, Fuller RW, Pride NB. 2012. Sensitivity of the Human Cough Reflex: Effect of Inflammatory Mediators Prostaglandin E2, Bradykinin, and Histamine. <https://doi.org/10.1164/ajrccm/1401137> 140:137–141.
154. WOOD WB, KAISER HK. 1962. Pathogenesis of Fever. *Clinical Manual of Fever in Children* 57:53.
155. Ruhl CR, Pasko BL, Khan HS, Kindt LM, Stamm CE, Franco LH, Hsia CC, Zhou M, Davis CR, Qin T, Gautron L, Burton MD, Mejia GL, Naik DK, Dussor G, Price TJ, Shiloh MU. 2020. Mycobacterium tuberculosis Sulfolipid-1 Activates Nociceptive Neurons and Induces Cough. *Cell* 181:293-305.e11.
156. Roy BA, Kirchner JW. 2000. Evolutionary dynamics of pathogen resistance and tolerance. *Evolution (N Y)* 54:51–63.
157. Schafer JF. 1971. Tolerance to Plant Disease. *Annu Rev Phytopathol* 9:235–252.
158. Schneider DS, Ayres JS. 2008. Two ways to survive infection: what resistance and tolerance can teach us about treating infectious diseases. *Nat Rev Immunol* 8:889–895.

159. Pamplona A, Ferreira A, Balla J, Jeney V, Balla G, Epiphanio S, Chora Â, Rodrigues CD, Gregoire IP, Cunha-Rodrigues M, Portugal S, Soares MP, Mota MM. 2007. Heme oxygenase-1 and carbon monoxide suppress the pathogenesis of experimental cerebral malaria. *Nat Med* 13:703–710.
160. Ayres JS, Freitag N, Schneider DS. 2008. Identification of *Drosophila* mutants altering defense of and endurance to *Listeria monocytogenes* infection. *Genetics* 178:1807–1815.
161. Li C, Corraliza I, Langhorne J. 1999. A Defect in Interleukin-10 Leads to Enhanced Malarial Disease in *Plasmodium chabaudi chabaudi* Infection in Mice. *Infect Immun* 67:4435.
162. Pai M, Behr MA, Dowdy D, Dheda K, Divangahi M, Boehme CC, Ginsberg A, Swaminathan S, Spigelman M, Getahun H, Menzies D, Raviglione M. 2016. Tuberculosis. *Nature Reviews Disease Primers* 2:1 2:1–23.
163. Cohen SB, Gern BH, Delahaye JL, Adams KN, Plumlee CR, Winkler JK, Sherman DR, Gerner MY, Urdahl KB. 2018. Alveolar Macrophages Provide an Early *Mycobacterium tuberculosis* Niche and Initiate Dissemination. *Cell Host Microbe* 24:439-446.e4.
164. Ferwerda G, Kullberg BJ, de Jong DJ, Girardin SE, Langenberg DML, van Crevel R, Ottenhoff THM, van der Meer JWM, Netea MG. 2007. *Mycobacterium paratuberculosis* is recognized by Toll-like receptors and NOD2. *J Leukoc Biol* 82:1011–1018.
165. Yadav M, Schorey JS. 2006. The beta-glucan receptor dectin-1 functions together with TLR2 to mediate macrophage activation by mycobacteria. *Blood* 108:3168–3175.
166. Geurtsen J, Chedammi S, Mesters J, Cot M, Driessen NN, Sambou T, Kakutani R, Ummels R, Maaskant J, Takata H, Baba O, Terashima T, Bovin N, Vandenbroucke-Grauls CMJE, Nigou J, Puzo G, Lemassu A, Daffé M, Appelmelk BJ. 2009. Identification of mycobacterial alpha-glucan as a novel ligand for DC-SIGN: involvement of mycobacterial capsular polysaccharides in host immune modulation. *J Immunol* 183:5221–5231.
167. Kang PB, Azad AK, Torrelles JB, Kaufman TM, Beharka A, Tibesar E, DesJardin LE, Schlesinger LS. 2005. The human macrophage mannose receptor directs *Mycobacterium tuberculosis* lipoarabinomannan-mediated phagosome biogenesis. *J Exp Med* 202:987–999.
168. Davila S, Hibberd ML, Dass RH, Wong HEE, Sahiratmadja E, Bonnard C, Alisjahbana B, Szeszko JS, Balabanova Y, Drobniewski F, van Crevel R, van de Vosse E, Nejentsev S, Ottenhoff THM, Seielstad M. 2008. Genetic association and expression studies indicate a role of toll-like receptor 8 in pulmonary tuberculosis. *PLoS Genet* 4.

169. Bafica A, Scanga CA, Feng CG, Leifer C, Cheever A, Sher A. 2005. TLR9 regulates Th1 responses and cooperates with TLR2 in mediating optimal resistance to *Mycobacterium tuberculosis*. *J Exp Med* 202:1715–1724.
170. Tapping RI, Tobias PS. 2003. Mycobacterial lipoarabinomannan mediates physical interactions between TLR1 and TLR2 to induce signaling. *J Endotoxin Res* 9:264–268.
171. Underhill DM, Ozinsky A, Smith KD, Aderem A. 1999. Toll-like receptor-2 mediates mycobacteria-induced proinflammatory signaling in macrophages. *Proc Natl Acad Sci U S A* 96:14459–14463.
172. Stanley SA, Raghavan S, Hwang WW, Cox JS. 2003. Acute infection and macrophage subversion by *Mycobacterium tuberculosis* require a specialized secretion system. *Proc Natl Acad Sci U S A* 100:13001–13006.
173. Spencer BL, Doran KS. 2022. Evolving understanding of the type VII secretion system in Gram-positive bacteria. *PLoS Pathog* 18:e1010680.
174. Lienard J, Mover E, Valfridsson C, Sturegård E, Carlsson F. 2016. ESX-1 exploits type I IFN-signalling to promote a regulatory macrophage phenotype refractory to IFN γ -mediated autophagy and growth restriction of intracellular mycobacteria. *Cell Microbiol* 18:1471–1485.
175. Khan S, Godfrey V, Zaki MH. 2019. Cytosolic Nucleic Acid Sensors in Inflammatory and Autoimmune Disorders. *Int Rev Cell Mol Biol* <https://doi.org/10.1016/bs.ircmb.2018.10.002>.
176. Mehra A, Zahra A, Thompson V, Sirisaengtaksin N, Wells A, Porto M, Köster S, Penberthy K, Kubota Y, Dricot A, Rogan D, Vidal M, Hill DE, Bean AJ, Philips JA. 2013. *Mycobacterium tuberculosis* type VII secreted effector EsxH targets host ESCRT to impair trafficking. *PLoS Pathog* 9.
177. Portal-Celhay C, Tufariello JM, Srivastava S, Zahra A, Klevorn T, Grace PS, Mehra A, Park HS, Ernst JD, Jacobs WR, Philips JA. 2016. *Mycobacterium tuberculosis* EsxH inhibits ESCRT-dependent CD4 $^{+}$ T-cell activation. *Nat Microbiol* 2.
178. Fortune SM, Solache A, Jaeger A, Hill PJ, Belisle JT, Bloom BR, Rubin EJ, Ernst JD. 2004. *Mycobacterium tuberculosis* Inhibits Macrophage Responses to IFN- γ through Myeloid Differentiation Factor 88-Dependent and -Independent Mechanisms. *The Journal of Immunology* 172:6272–6280.
179. Pai RK, Convery M, Hamilton TA, Boom WH, Harding C v. 2003. Inhibition of IFN- γ -induced class II transactivator expression by a 19-kDa lipoprotein from *Mycobacterium tuberculosis*: a potential mechanism for immune evasion. *J Immunol* 171:175–184.

180. Cambier CJ, Takaki KK, Larson RP, Hernandez RE, Tobin DM, Urdahl KB, Cosma CL, Ramakrishnan L. 2013. Mycobacteria manipulate macrophage recruitment through coordinated use of membrane lipids. *Nature* 2013 505:7482–7487.
181. Pande T, Pai M, Khan FA, Denkinger CM. 2015. Use of chest radiography in the 22 highest tuberculosis burden countries. *Eur Respir J* 46:1816–1819.
182. Case-Finding, | An Evaluation of Various Techniques | American Review of Tuberculosis.
<https://www.atsjournals.org/doi/epdf/10.1164/art.1939.39.2.256?role=tab>. Retrieved 16 February 2023.
183. Martin CJ, Cadena AM, Leung VW, Lin PL, Maiello P, Hicks N, Chase MR, Flynn JAL, Fortune SM. 2017. Digitally barcoding *Mycobacterium tuberculosis* reveals *In vivo* infection dynamics in the macaque model of tuberculosis. *mBio* 8.
184. Sholeye AR, Williams AA, Loots DT, Tutu van Furth AM, van der Kuip M, Mason S. 2022. Tuberculous Granuloma: Emerging Insights From Proteomics and Metabolomics. *Front Neurol* 13:527.
185. Mailaender C, Reiling N, Engelhardt H, Bossmann S, Ehlers S, Niederweis M. 2004. The MspA porin promotes growth and increases antibiotic susceptibility of both *Mycobacterium bovis* BCG and *Mycobacterium tuberculosis*. *Microbiology (Reading)* 150:853–864.
186. McCune RM, Feldmann FM, Lambert HP, McDermott W. 1966. Microbial persistence. I. The capacity of tubercle bacilli to survive sterilization in mouse tissues. *J Exp Med* 123:445–468.
187. Xie Z, Siddiqi N, Rubin EJ. 2005. Differential Antibiotic Susceptibilities of Starved *Mycobacterium tuberculosis* Isolates. *Antimicrob Agents Chemother* 49:4778.
188. Rao SPS, Alonso S, Rand L, Dick T, Pethe K. 2008. The protonmotive force is required for maintaining ATP homeostasis and viability of hypoxic, nonreplicating *Mycobacterium tuberculosis*. *Proc Natl Acad Sci U S A* 105:11945–11950.
189. Wayne LG, Hayes LG. 1996. An *in vitro* model for sequential study of shutdown of *Mycobacterium tuberculosis* through two stages of nonreplicating persistence. *Infect Immun* 64:2062–2069.
190. Selwyn PA, Hartel D, Lewis VA, Schoenbaum EE, Vermund SH, Klein RS, Walker AT, Friedland GH. 1989. A prospective study of the risk of tuberculosis among intravenous drug users with human immunodeficiency virus infection. *N Engl J Med* 320:545–550.

191. Lönnroth K, Williams BG, Cegielski P, Dye C. 2010. A consistent log-linear relationship between tuberculosis incidence and body mass index. *Int J Epidemiol* 39:149–155.
192. Sidhu A, Verma G, Humar A, Kumar D. 2014. Outcome of latent tuberculosis infection in solid organ transplant recipients over a 10-year period. *Transplantation* 98:671–675.
193. Raanan R, Zack O, Ruben M, Perluk I, Moshe S. 2022. Occupational Silica Exposure and Dose–Response for Related Disorders—Silicosis, Pulmonary TB, AIDs and Renal Diseases: Results of a 15-Year Israeli Surveillance. *Int J Environ Res Public Health* 19.
194. Yang Q, Lin M, He Z, Liu X, Xu Y, Wu J, Sun F, Jiang T, Gao Y, Huang X, Zhang W, Ruan Q, Shao L. 2022. Mycobacterium tuberculosis Infection among 1,659 Silicosis Patients in Zhejiang Province, China . *Microbiol Spectr* 10.
195. Rehm J, Samokhvalov A v., Neuman MG, Room R, Parry C, Lönnroth K, Patra J, Poznyak V, Popova S. 2009. The association between alcohol use, alcohol use disorders and tuberculosis (TB). A systematic review. *BMC Public Health* 9.
196. van Pinxteren LAH, Cassidy JP, Smedegaard BHC, Agger EM, Andersen P. Control of latent Mycobacterium tuberculosis infection is dependent on CD8 T cells <https://doi.org/10.1002/1521-4141>.
197. Scanga CA, Mohan VP, Yu K, Joseph H, Tanaka K, Chan J, Flynn JAL. 2000. Depletion of CD4(+) T cells causes reactivation of murine persistent tuberculosis despite continued expression of interferon gamma and nitric oxide synthase 2. *J Exp Med* 192:347–358.
198. Scanga CA, Mohan VP, Joseph H, Yu K, Chan J, Flynn JL. 1999. Reactivation of latent tuberculosis: variations on the Cornell murine model. *Infect Immun* 67:4531–4538.
199. Flynn JL, Chan J. 2001. Tuberculosis: Latency and Reactivation. *Infect Immun* 69:4195.
200. Peto HM, Pratt RH, Harrington TA, LoBue PA, Armstrong LR. 2009. Epidemiology of extrapulmonary tuberculosis in the United States, 1993-2006. *Clin Infect Dis* 49:1350–1357.
201. MacPherson AMC. 1942. Primary Tuberculosis of the Lung and some of its Consequences. *Postgrad Med J* 18:139–141.
202. Wallgren A. 1948. The time-table of tuberculosis. *Tubercle* 29:245–251.

203. Shi T, Denney L, An H, Ho LP, Zheng Y. 2021. Alveolar and lung interstitial macrophages: Definitions, functions, and roles in lung fibrosis. *J Leukoc Biol* 110:107–114.

CHAPTER 2: FLAMS: A SELF-REPLICATING EX VIVO MODEL OF ALVEOLAR MACROPHAGES FOR FUNCTIONAL GENETIC STUDIES

PUBLICATION NOTICE

The following chapter has been published by *ImmunoHorizons* and is available through the *ImmunoHorizons* website at “S. Thomas*, K. Wierenga*, J. Pestka, A. Olive, *Fetal Liver–Derived Alveolar-like Macrophages: A Self-Replicating Ex Vivo Model of Alveolar Macrophages for Functional Genetic Studies*, *ImmunoHorizons*, <https://doi.org/10.4049/immunoHorizons.2200011>.” * indicates that these authors contributed equally to this work.

ABSTRACT

Alveolar macrophages (AMs) are tissue resident cells in the lungs derived from the fetal liver that maintain lung homeostasis and respond to inhaled stimuli. While the importance of AMs is undisputed, they remain refractory to standard experimental approaches and high-throughput functional genetics as they are challenging to isolate and rapidly lose AM properties in standard culture. This limitation hinders our understanding of key regulatory mechanisms that control AM maintenance and function. Here, we describe the development of a new model, fetal liver-derived alveolar-like macrophages (FLAMs), which maintains cellular morphologies, expression profiles, and functional mechanisms similar to murine AMs. FLAMs combine treatment with two key cytokines for AM maintenance, GM-CSF and TGF β . We leveraged the long-term stability of FLAMs to develop functional genetic tools using CRISPR-Cas9-mediated gene editing. Targeted editing confirmed the role of AM-specific gene *Marco* and the IL-1 receptor *Il1r1* in modulating the AM response to crystalline silica. Furthermore, a genome-wide knockout library using FLAMs identified novel genes required for surface expression of the AM marker Siglec-F, most notably those related to the peroxisome. Taken together, our results suggest that FLAMs are a stable, self-replicating model of AM function that enables previously impossible global genetic approaches to define the underlying mechanisms of AM maintenance and function.

INTRODUCTION

Tissue resident immune cells regulate homeostasis and control local inflammation to external stimuli. A subset of these immune cells are tissue resident

macrophages (TRMs) that sample the environment and initiate host responses (1). Distinct TRM populations exist in specific tissues including the liver (Kupffer cells), the skin (Langerhans cells), the brain (microglia), and the lungs (alveolar macrophages [AMs]). These distinct TRMs all have unique functions that are regulated by the local environment and are required for tissue maintenance (2, 3).

As the first line of defense in the airways, AMs are particularly important for tuning the host immune response in the lungs (4). AMs can be distinguished from other macrophage populations in the lung by the surface expression of the sialic acid receptor Siglec-F, the scavenger receptor MARCO, and the integrin CD11c in addition to the high expression and activity of the transcription factor PPAR γ , which drives many AM-specific genes (5, 6). AMs are a long-lived and self-replicating and, like most TRMs, are derived from embryonic precursors (7). AMs arise from fetal liver monocytes, which migrate to the lung and develop into mature AMs in the presence of cytokines such as GM-CSF and TGF β shortly after birth (8–10). The continued presence of these factors is necessary for the maintenance and self-renewal of AMs in the lung, in part by promoting expression and activation of PPAR γ (10, 11). Genes and pathways induced by this receptor are involved in lipid metabolism and induction of scavenger receptors that promote phagocytosis (12). This is critical for the AM roles of maintaining surfactant homeostasis, efferocytosis of cellular debris, and phagocytosis of inhaled microbes and particles in the alveolar space (12, 13). Impaired clearance of surfactant by AMs can result in the pathophysiological condition known as pulmonary alveolar proteinosis (PAP) (14). In addition, reduced AM efferocytosis and phagocytosis has been observed

in patients with asthma, COPD, and cystic fibrosis, likely contributing to the sustained inflammation and susceptibility to infection observed in these diseases (15–19).

Despite the paramount importance of AMs for lung health, there continue to be key gaps in our understanding of how they are maintained and function to regulate the host response in the lungs. One hurdle towards a mechanistic understanding of AMs is that experiments employing primary AMs require large numbers of animals to isolate a small number of cells that do not robustly proliferate or maintain AM-like functions *ex vivo* (20). This limitation has prevented genetic approaches from being employed to better understand AM maintenance and function. As a result, many *ex vivo* studies investigating responses to airborne particles and microbes rely on bone-marrow derived macrophages (BMDMs) or transformed macrophage cell lines as surrogates of AM biology (21–23). While these macrophage models are useful, they do not faithfully recapitulate all AM functions (24–26). A recent alternative approach cultured cells from the murine fetal liver in the presence of GM-CSF to generate AM-like cells that are functionally and phenotypically like AMs (25). This approach enabled the isolation of large numbers of AM-like cells that might be amenable to tractable genetic approaches. However, we found here that fetal liver-derived cells cultured in GM-CSF alone lost their AM-like morphology, phenotype, and surface marker expression over time, suggesting that GM-CSF is insufficient to maintain the AM-like phenotype. A recent study found that AMs could be continuously cultured *ex vivo* in the presence of GM-CSF and TGF β (27), which is consistent with reports that TGF β promotes AM development and maintains AM function both *in vivo* and *ex vivo* (10).

Here, we found that growing fetal liver cells in both GM-CSF and TGF β results in a long-term stable population of cells that are phenotypically and functionally similar to AMs. Using these fetal liver-derived alveolar-like macrophages (FLAMs), we developed targeted and global genetic tools to dissect regulatory networks that are required to maintain AM-like cells and function. Employing targeted gene-editing, we show here that directed mutations are readily introduced in FLAMs to query specific AM functions. We further demonstrate the utility of FLAMs by using genome-wide CRISPR-Cas9 knockout screen to identify genes that are required for the surface expression of the AM-specific marker Siglec-F. The screen identified key pathways used to maintain Siglec-F expression and the AM-like state including the observation that peroxisome biogenesis plays a central role in maintaining AM functions. Together our results show that FLAMs enable the global dissection of AM regulatory mechanisms at a previously impossible scale.

RESULTS

Fetal liver-derived cells and AMs cultured in GM-CSF alone do not stably express lineage-specific markers over time.

The development of a genetically tractable AM *ex vivo* model requires a stable population that maintains AM-like phenotypes and functions long-term. As a first step, we examined the long-term stability of AM-like cells using a previously described method culturing fetal liver derived cells in the cytokine GM-CSF (25). Consistent with previous reports, we found that fetal liver cells grown in GM-CSF phenotypically and morphologically resemble AMs (25, 28, 29). Fetal liver cells grown for 2 weeks *ex vivo*

in the presence of GM-CSF adopt a distinct fried-egg-like morphology akin to AMs (**Figure 2.1A**). Scanning electron microscopy revealed that the surfaces of both AM and low passage fetal liver cells (<1 month of culture) have numerous outer membrane ruffles (**Figure 2.1B**). However, high passage fetal liver cells (>1 month of culture) underwent a morphological shift from an AM-like, ovoid morphology with numerous outer plasma membrane ruffles, to a smaller, fusiform morphology with loss of membrane ruffles (**Figure 2.1A and 2.1B**). Thus, in our hands, the morphology of fetal liver derived cells grown in recombinant GM-CSF are not stable long-term.

We further examined whether changes in surface markers or gene expression varied as fetal liver cells were cultured over time. Using flow cytometry, we found similarity between AMs and low passage fetal liver cells with high surface expression of Siglec-F and CD11c and low expression of CD14. However, high passage fetal liver cells showed low expression of SiglecF and CD11c, while expressing high levels of CD14 (**Figure 2.1C**). Similarly, when we quantified gene expression, we observed that low passage fetal liver cells and AMs express high levels of *Pparg*, *Car4*, *Il1a* and *Fabp4* (a transcriptional target of PPARg) and low levels of CD14, while high passage fetal liver cells expressed very low levels of the AM-associated transcripts but high levels of CD14 (**Figure 2.1D**). We observed similar results with AMs isolated from the lungs (**Figure S1A and B**). To exclude the possibility of contaminating cells outcompeting the alveolar-like cells over long-term culture we used fluorescence activated cell sorting (FACS) to isolate a pure Siglec-F positive population of cells that were then cultured in GM-CSF media. We continued to observe a decline in Siglec-F and CD11c in these cells (**Figure S1C**). Together these data suggest that prolonged

culture of fetal liver-derived cells in GM-CSF media results in a decline in AM-like properties.

Fetal liver-derived cells grown in GM-CSF and TGF- β are phenotypically similar to AMs long-term.

We next pursued strategies to improve the stability of AM-specific phenotypes of fetal liver-derived cells grown *ex vivo*. Based on a prior report that the cytokine TGF β is critical to AM development and homeostasis (10), we hypothesized that the addition of TGF β to our culture system would maintain cells in an AM-like state. We first tested whether the addition of TGF β alters the expression of AM-associated genes. Fetal liver cells in GM-CSF media were treated for 24 hours with 10 ng/mL TGF β , which we found induced the genes *Pparg*, *Car4* a transcriptional target of PPAR- γ , and *Itgax* (**Figure S2A**), all of which are highly expressed by AMs (**Figure 2.1D**). We next examined if continued supplementation with TGF β stabilizes the AM-like phenotypes of fetal liver cells long-term. Fetal liver-derived cells were cultured in GM-CSF media or GM-CSF media containing 20 ng/mL TGF β . After 15 passages (approximately 2 months of culturing), cells grown in the presence of TGF β retained a round, AM-like morphology (**Figure 2.2A**) and continued expressing AM-identifying genes (**Figure 2.2B**). Conversely, fetal liver-derived cells cultured without TGF β lost the expression of AM-identifying genes *Siglecf*, *Marco* and *Pparg* and began expressing *Cd14*, which is a common marker for monocyte-derived macrophages recruited to the lung (30) (**Figure 2.2B**).

We next determined if fetal liver-derived cells grown in the absence of TGF β would revert to the AM-like state upon the addition of TGF β . Fetal liver cells grown in the absence of TGF β were cultured with and without TGF β for 6 days and the expression of Siglec-F and CD14 was quantified by flow cytometry (**Figure S2B**). In parallel, fetal liver cells maintained in TGF β were cultured for six days in the presence or absence of TGF β . We observed that while the removal of TGF β resulted in a significant decrease in Siglec-F and an increase in CD14, there was no change in expression upon the addition of TGF β to fetal liver cells that previously lost AM-like marker expression. When we examined the gene expression of *Tgf β 1* and the TGF β receptors, *Tgf β 1* and *Tgf β 2* we observed a significant decrease in expression of the *Tgf β 1* (**Figure 2.2B, Figure S2C**). These data suggest that the loss of AM-like potential of fetal liver cells grown in the absence of TGF β is not reversible.

We next quantified changes in the surface expression of Siglec-F and CD14 by flow cytometry in the fetal liver-derived cells grown in the presence and absence of TGF β . Consistent with our gene expression analysis we observed that fetal liver-derived cells lose the expression of Siglec-F and gain the expression of CD14 over time (**Figure 2.2C and 2D**). In contrast, fetal liver-derived cells grown with TGF β maintained over 80% of cells with high levels of Siglec-F expression and low levels of CD14. Thus, culturing fetal-liver cells in both GM-CSF and TGF β results in the stable gene expression of self-replicating cells that phenotypically resemble AMs.

Fetal liver-derived cells grown in GM-CSF and TGF- β are functionally similar to AMs in response to cSiO₂ relative to phagocytosis, IL-1 cytokine release, and death.

To assess the functional similarity of fetal liver-derived cells grown in TGF β with AMs, we assessed the response of cells to crystalline silica (cSiO₂), a respirable particle associated with silicosis and autoimmunity (31, 32). Cells were exposed to various concentrations of cSiO₂ for 8 hours. SYTOX Green, a membrane impermeable nucleic acid stain, was included to assess lytic cell death. AMs and low passage fetal liver-derived cells grown with and without TGF β showed similar rates of cSiO₂ engulfment and cell death (**Figure 2.3A**). However, late passage fetal liver-derived cells without TGF β exhibited poor phagocytosis, and as a result, tolerated the presence of cSiO₂ without inducing cell death. This unresponsiveness is prevented by TGF β , as late passage fetal liver-derived cells effectively phagocytosed cSiO₂ (**Figure 2.3A and 2.3B**). Rates of phagocytosis by BMDMs were comparable to AMs but were accompanied by a two-fold increase in cell death. Thus, fetal liver-derived cells grown in TGF β and GM-CSF are functionally stable long-term and recapitulate phagocytosis and cell death kinetics similarly to AMs.

IL-1a is associated with the inflammatory response to particle-induced inflammation. *In vivo* and *ex vivo* studies suggest AMs are the primary source of IL-1a in the lung following inhalation of cSiO₂, likely as a result of cell death (33, 34). Initial characterizations of fetal liver-derived cells grown in GM-CSF (35) showed they respond to LPS like AMs by producing high levels of IL-1a and low levels of IL-10 in contrast BMDMs that make little IL-1a. We replicated these experiments and observed similar

results with low passage fetal liver-derived cells producing high levels of IL-1a and low levels of IL-10 in response to LPS (**Figure S2D**). We next tested how the IL-1a response to cSiO₂ differed over-time in fetal liver-derived cells grown in the presence and absence of TGFβ. We found that high levels of IL-1a were released both low and high passage fetal liver-derived cells grown in both GM-CSF and TGFβ following cSiO₂ exposure for 8 hours, similar to AMs (**Figure 2.3C**). In contrast, we observed that cSiO₂ induced IL-1a release from low passage fetal liver-derived cells grown in GM-CSF alone but not late passage cells. Late passage cells grown in GM-CSF alone instead phenocopied BMDMs and released no detectable IL-1a following cSiO₂ exposure. Release of IL-1β in these cells may be indicative of inflammasome activation, which is a major mechanism of AM toxicity following exposure to cSiO₂. We found cSiO₂ exposure to elicit modest IL-1β release from low passage fetal liver-derived cells grown without TGFβ, and from both low and high passage fetal liver-derived cells grown with TGFβ. We further observed a slight, though not significant, increase in IL-1β release in AMs following cSiO₂ exposure (**Figure 2.3C**). cSiO₂-induced IL-1β release was not evident from BMDMs or late MPI cells. Taken together, these experiments show that growth of fetal-liver cells in both GM-CSF and TGFβ recapitulates many aspects of AM physiology and function as stable, long-term, self-propagating cells. We call these cells Fetal Liver-derived Alveolar Macrophages (FLAMs).

CRISPR-Cas9 editing in FLAMs enables disruption of AM-specific responses to cSiO₂.

A significant hinderance in the study of AMs is their intractability to standard genetic approaches. This shortcoming has limited the understanding of pathways and regulators that control AM maintenance and function. We hypothesized that FLAMs could be leveraged to dissect AM functional mechanisms. To test this hypothesis we developed CRISPR-Cas9 mediated gene-editing tools by generating FLAMs from Cas9⁺ mice (36, 37). Using these cells, we targeted *Marco* and *Il1r1*, two genes associated with phagocytosis and inflammatory responses to cSiO₂ in AMs (38, 39). Each gene was targeted using two independent sgRNAs per gene by lentiviral transduction. Following selection of successfully transduced cells, we evaluated the editing efficiency of each target genes using Tracking of Indels by DEcomposition (TIDE) analysis. We observed robust editing for both sgRNAs with at least one sgRNA per gene reaching over 95% editing efficiency (see methods). Thus, FLAMs are amenable to genetic targeting by CRISPR-Cas9.

Given the scavenger receptor MARCO has been shown to be involved in cSiO₂ uptake and toxicity while IL1R1 is known to amplify inflammatory cues, we hypothesized that cells deficient in MARCO and IL1R1 expression would have a reduced inflammatory response to cSiO₂ (38, 40). We therefore tested whether FLAMs targeted for *Marco* or *Il1r1* would differentially respond to cSiO₂ exposure compared to wild-type. We exposed control FLAMs and sgMarco or sgIl1r1 FLAMs to two different cSiO₂ concentrations and quantified cell death. While we observed no change in cell death in sgIl1r1 FLAMs compared to control FLAMs, a significant reduction in cell death in

sgMarco FLAMs was observed following high cSiO₂ exposure (**Figure 2.4A**). We next examined the production of IL1 following exposure of cells to cSiO₂. We found reduced cSiO₂-induced IL-1a and IL-1 β production by sgMarco and sgI1r1 FLAMs compared to control FLAMs (**Figure 2.4B and 2.4C**). Therefore, FLAMs are genetically tractable and can be used to dissect AM-specific functions.

Forward genetic screen in FLAMs identifies regulators of the AM surface marker Siglec-F.

The genetic tractability of FLAMs opens the possibility of performing forward genetic screens in an AM context, which was previously unviable. We recently developed a screening platform in immortalized bone marrow macrophages (iBMDMs) that uses cell sorting of CRISPR-Cas9 targeted cells to enrich for genes that positively or negatively regulate the surface expression of important immune molecules (41). We hypothesized this screening pipeline could be leveraged to dissect pathways responsible for the unique expression profiles seen in AMs and FLAMs. As a first step to test this hypothesis, we dissected the changes in the surface expression of Siglec-F when targeted using CRISPR-Cas9. Among macrophages, Siglec-F is uniquely expressed on the surface of AMs, yet how Siglec-F is regulated remains entirely unknown. Given that Siglec-F expression is lost as cells lose their AM-like phenotypes, globally understanding Siglec-F regulation in FLAMs may inform key gene networks in AMs. To test the dynamic range of Siglec-F expression on FLAMs, we targeted Siglec-F with two independent sgRNAs in both Cas9⁺ FLAMs and iBMDMs. Again, extensive editing for both sgRNAs was observed with one sgRNA reaching over 99% editing

efficiency. As expected, control iBMDMs showed no surface Siglec-F expression and targeting Siglec-F showed no observable change by flow cytometry (**Figure 2.5A**). In contrast, we observed robust Siglec-F expression on control FLAMs while *sgSiglecF* FLAMs showed a greater than 100-fold reduction in MFI (**Figure 2.5B**). This dynamic range is comparable to other surface markers we previously screened in iBMDMs, suggesting that Siglec-F is an ideal target for a genetic screen in FLAMs (41).

To globally identify genes that contribute to Siglec-F surface expression on FLAMs, we generated a genome-wide knockout library. FLAMs from Cas9⁺ mice were transduced with sgRNAs from the pooled Brie library (42) which contains 4 independent sgRNAs per mouse coding gene. In parallel to the library, we grew control Cas9⁺ fetal liver cells with GM-CSF alone to monitor the loss of Siglec-F expression in the absence of TGF β signaling (**Figure 2.5C and 5D**). When control cells lost Siglec-F expression, genomic DNA from the FLAMs knockout library was purified and the sgRNAs were quantified by deep sequencing. The library coverage was confirmed to have minimal skew. We then conducted a forward genetic screen using FACS to isolate the Siglec-F^{high} and Siglec-F^{low} cells from the loss-of-function FLAM library (**Figure 2.5C**).

Following genomic DNA extraction, sgRNA abundances for each sorted population were determined by deep sequencing. To test for statistical enrichment of sgRNAs and genes, we used the modified robust rank algorithm (α -RRA) employed by Model-based Analysis of Genome-wide CRISPR/Cas9 Knockout (MAGeCK). MAGeCK first ranks sgRNAs by effect and then filters low ranking sgRNAs to improve gene significance testing (43). To identify genes that are required for Siglec-F expression we compared the enrichment of sgRNAs in the Siglec-F^{low} population to the Siglec-F^{high} population.

The a-RRA analysis identified over 300 genes with a p-value <0.01 and the second ranked gene in this analysis was the target of the screen Siglec-F (**Figure 2.5E** and **Table S1**). Guide-level analysis showed agreement with all four sgRNAs targeting Siglec-F, with each showing a ten-fold enrichment in the Siglec-F^{low} population (**Figure 2.5F** and **Table S1**). The high ranking of Siglec-F gives high confidence in genome-wide screen results.

Stringent analysis revealed an enrichment of genes with no previously described role in Siglec-F regulation including the TGF β response regulator USP9x (44) (**Figure 2.6A**). To identify pathways that were associated among these genes, we filtered the ranked list to include genes that had a fold change of >4 with at least 2 out of 4 sgRNAs and used DAVID analysis to identify pathways and functions that were enriched in our datasets. The top enriched KEGG pathway was the peroxisome, with all core components of peroxisome biogenesis identified as positive regulators of Siglec-F (**Figure 2.6B**). We further examined other peroxisome-associated (PEX) genes and found that 11 out of 15 PEX genes present in our library were altered greater than two-fold (**Figure 2.6C**). KEGG pathway analysis identified a significant enrichment in genes associated with lipid metabolism, including glycerophospholipid, inositol phosphate, and ether lipids. KEGG analysis also found an enrichment of the phagosome pathway which identified several surface receptors associated with phagocytosis in this pathway, including the IgG Fc Receptor 4, the mannose-6-phosphate receptor, and the oxidized low-density lipoprotein receptor, suggesting surface proteins associated with phagocytosis directly modulate the stability of Siglec-F (**Figure 2.6D**). Examination of enriched UniProt keyword terms using DAVID analysis found a strong enrichment of

proteins with oxidoreductase function including several genes associated with cytochromes P450 (CYP), a key regulator of xenobiotic, fatty acid, and hormone metabolism, known to be important in the lung environment (45). Thus, bioinformatic analysis of the top positive regulators of Siglec-F identified pathways that are associated with AM functions.

We next used gene set enrichment analysis (GSEA) to identify functional enrichments from the entire ranked screen dataset. GSEA identified the peroxisome as a top enriched KEGG pathway consistent with the DAVID analysis (**Figure 2.6E**). This analysis also identified a strong enrichment for oxidative phosphorylation, which is consistent with the key metabolic changes in AMs compared to BMDMs (46), and a significant enrichment for GPI anchor synthesis as negative regulators of Siglec-F surface expression (**Figure 2.6E**). We also noted that mTORC1 signaling was enriched as a negative regulator, in line with previous reports that mTORC1 is required to maintain AMs in the lungs (47). Taken together, our forward genetic screen not only identified Siglec-F, the screen target, but also identified positive and negative regulators of Siglec-F expression that are associated with known AM-functions as well as novel AM regulators. Thus, FLAMs are a tractable genetic platform that enables the detailed interrogation of AM regulatory functions and mechanisms.

DISCUSSION

As long-lived resident macrophages in the lungs, AMs have unique phenotypes and functions shaped by the alveolar environment (48). However, experimental limitations hinder our understanding of AM-specific functional mechanisms. Developing

ex vivo models that recapitulate AM phenotypes would overcome the challenges associated with isolating and maintaining AMs from the lungs of mice. Since AMs are derived from fetal liver monocytes, previous studies tested the culture of fetal liver cells with GM-CSF (49). These culture conditions result in self-replicating AM-like cells, but in our hands, the AM-like phenotype was not stable long-term. While low passage fetal liver cells grown in GM-CSF are useful for some experimental approaches, the instability of the AM phenotype precludes functional genetic studies (50, 51). To stabilize the AM-like phenotype of fetal liver-derived cells we supplemented the growth media with TGF β , a key cytokine for AM maintenance in the lungs, in a model we term FLAMs (10). Here we showed that FLAMs recapitulate many aspects of AM biology, are stable long-term, and are genetically tractable, making them a useful tool to dissect the regulation of AM maintenance and function.

We demonstrated that that even after one month of culture ' FLAMs efficiently phagocytose cSiO₂ particles, produce inflammatory cytokines like IL-1a, and die similarly to AMs. Our results are consistent with two recent reports that examined how TGF β modulates macrophages *ex vivo* (10, 50, 51). These reports showed that TGF β can induce/maintain AM-like phenotypes *ex vivo* using AMs directly from the lungs of mice or purified cells from the bone-marrow. Future studies will be needed to directly compare how distinct sources of AM-like cells grown in GM-CSF and TGF β are functionally similar or distinct. There are other key differences in these approaches beyond the source of cells, including the use of the PPAR γ agonist rosiglitazone. Our data strongly suggest that fetal liver cells do not require rosiglitazone to maintain PPAR γ activity. Another advantage of FLAMs is the low cost, low technology threshold

and high yield of cells that can be isolated from any genetically modified mouse, including mice with embryonic lethality. Another key advantage of FLAMs is genetic toolbox that we have developed here. Using targeted gene-editing we showed that directed mutations can be easily generated in FLAMs to probe specific AM functions. Furthermore, we generated a genome-wide knockout library in FLAMs and completed the first forward genetic screen in AM-like cells. This proof-of-concept genome-wide screen in FLAMs now enables our innovative tools to be broadly used to understand AM biology in previously impossible detail. Thus, FLAMs recapitulate *ex vivo* AMs even after extended culturing and are suitable for dissecting AM responses and regulation.

How AMs control their functional responses and how this differs from other macrophage populations remains unclear. Here we observed both phenotypic and functional differences among AMs, FLAMs, and BMDMs in line with previous studies (25, 28, 29). While BMDMs express high levels of CD14, AMs and FLAMs express high levels of Siglec-F and MARCO. When cells were exposed to cSiO₂, we observed differences in cell death kinetics and IL-1 cytokine responses. Though BMDMs were able to engulf cSiO₂ particles at a rate comparable to AMs and FLAMs, they quickly succumbed to cell death, while AMs and FLAMs remained viable many hours following cSiO₂ phagocytosis. A delay in cell death may be important for appropriate clearance of particles, potentially allowing the AMs to be transported out of the alveoli before they die (52). AMs and AM-like cells also released significantly more IL-1 α and IL-1 β than BMDMs in response to cSiO₂. These data are consistent with studies showing high levels of IL-1 α produced by AMs compared to other cells in the lung and other macrophage sub-types (25, 28, 33, 34, 49) and the known role of cSiO₂ in inducing IL-

1 β release (39). Our findings indicate that MARCO may be a key player in driving the IL-1 cytokine response in AMs as MARCO-deficient FLAMs showed increased viability and decreased IL-1 production following cSiO₂ exposure. These results are in line with previous studies implicating MARCO in the uptake of cSiO₂ and other particles in AMs (40, 53). In the future, FLAMs will be used to dissect the underlying mechanisms of MARCO regulation to understand how MARCO drives distinct inflammatory responses following phagocytosis of cSiO₂ and other pathogenic cargo. Knocking out the IL-1 receptor also reduced IL-1 cytokine release, which points to a feed-forward mechanism to amplify this inflammatory response in AMs.

In addition to MARCO, AMs express other markers that are used to define AM populations. However, the regulation of these other AM markers, like Siglec-F, remains entirely unknown. Siglec-F is a surface-expressed immunoglobulin protein that binds sialic acid residues on glycolipids and glycoproteins, but its function in AMs is largely unknown. In addition to AMs, Siglec-F is expressed on eosinophils, where it limits inflammation by modulating cell death pathways (54). The only studies examining Siglec-F in AMs demonstrated that Siglec-F does not regulate phagocytic activity (55). Our forward genetic screen in FLAMs defined regulators of Siglec-F surface expression and uncovered hundreds of candidate genes that may contribute to Siglec-F expression. Our results not only identified Siglec-F as the second ranked candidate, but we identified other genes that likely modulate Siglec-F expression or trafficking. These genes include transcription factors like Fos and NFkB2 and surface receptors like M6PR. Our screen candidates are likely to include both direct regulators of Siglec-F expression and indirect regulators that maintain the AM-like state. In support of this

prediction, we identified USP9x, a known regulator of TGF β signaling as a strong positive regulator of Siglec-F expression (44). In addition, we identified the enrichment of functional pathways previously associated with AM function including the peroxisome, lipid metabolism, oxidative phosphorylation and CYP. Given the previous links among PPAR transcription factors, peroxisome biogenesis, and lipid metabolism, our data strongly suggest FLAMs recapitulate the metabolic makeup of AMs which is central to their gene regulation (12, 46, 56). In further relation to the metabolic state of FLAMs, we identified several CYP family members among our top candidates which regulate vitamin A and all-trans retinoic acid, known modulators of AM function (57, 58). Based on these findings, we posit that PPAR γ expression drives lipid metabolism to induce the AM-specific transcriptional profile, resulting in Siglec-F expression. Future studies will be centered on testing this model and deeply validating the genetic screen to uncover novel regulatory mechanisms in FLAMs.

FLAMs are a promising model to study AM biology, yet some limitations remain. While FLAMs maintain many AM-like phenotypes long-term, we observed variable expression of the AM marker CD11c over time. This suggests that there are other signals in addition to GM-CSF and TGF β that are needed to fully recapitulate AM functionality *ex vivo*. The alveolar space is a highly complex microenvironment, with constant crosstalk between AMs and other cells (48). For example, our data show that FLAMs express TGF β , yet this is not sufficient to maintain AM-like functions and continued *Tgf β 1* and *Tgf β 2* expression. Given TGF β is known to amplify *Tgf β 1* and *Tgf β 2* this suggests that the TGF β produced by FLAMs is not biologically active. *In vivo*, latent TGF β released by AMs is activated by α -V- β -6 integrins expressed on the

type II alveolar epithelial cells (AECII), resulting in increased levels of the active protein which can signal in an autocrine manner to maintain the unique phenotype of AMs (59). This feed-forward loop is absent *ex vivo*, which may explain why addition of exogenous active TGF β prevents the loss of the AM-like phenotype in FLAMs. Other signals provided by AECII cells and others such as lung-resident basophils likely regulate AM maintenance, but these signals are not modeled in our system (60). In the future the potential to combine the genetic tractability of FLAMs with *in vivo* transfer models may enable detailed dissection of this cross-regulation systematically. Intranasal transfer of TGF β -cultured AMs was recently shown to repopulate the alveolar space. It will be important to test if FLAMs could be similarly instilled into lungs lacking endogenous AMs, enabling rapid *in vivo* studies to better understand AM-maintenance within the lung environment (27).

In summary, we developed FLAMs, a stable *ex vivo* model that can be used to study lung development, immunology, and toxicology. FLAMs are likely to shed new light on processes unique to AMs, like phagocytosis, efferocytosis and the removal of inhaled particles, by employing targeted or genome-wide genetic approaches. Taken together, the optimization and application of FLAMs provides an exciting, innovative model to thoroughly investigate AM biology.

ACKNOWLEDGEMENTS

We would like to acknowledge Dr. Jack Harkema, Dr. Melissa Bates, Dr. Mikhail Givralin, Dr. Alexander Misharin, and the members of the Olive and Pestka lab for helpful discussions and input. We thank the MSU flow cytometry core for their help with

instrumentation and analysis and Carol Flegler of the MSU Center of Advanced Microscopy for assistance in scanning electron microscopy.

MATERIALS AND METHODS

Animals

Experimental protocols were approved by the Institutional Animal Care and Use Committee at MSU (AUF # PROTO201800113). 6-8 week old C57Bl6 mice (cat # 000664) and Cas9⁺ mice (cat # 026179) were obtained from Jackson Laboratories (Bar Harbor, ME). Mice were given free access to food and water under controlled conditions (humidity: 40–55%; lighting: 12 hour light/dark cycles; and temperature: 24±2°C) as described previously (61, 62). Pregnant dams at 8-10 weeks of age and 14-18 gestational days were euthanized to obtain murine fetuses. AMs were isolated from male and female mice older than 10 weeks of age. BMDMs were obtained from male and female mice 6 weeks of age and older.

FLAMs cell isolation and culture

Fetal liver derived cells were obtained as previously described (35). Briefly, pregnant dams were euthanized by CO₂ inhalation for 10 min to ensure death to neonates, which are resistant to anoxia. Cervical dislocation was used as a secondary form of death for the dam. Fetuses were immediately removed, and loss of maternal blood supply served as a secondary form of death for the fetuses. Cells were cultured in complete Roswell Park Memorial Institute medium (RPMI, Thermo Fisher) containing 10% fetal bovine serum (FBS, R&D Systems), 1% penicillin-streptomycin (P/S, Thermo Fisher), 30 ng/mL recombinant mGM-CSF (Peprotech), and 20 ng/mL recombinant hTGFβ1 (Peprotech)

included where indicated. Media was refreshed every 2-3 days. When cells reached 70-90% confluency, they were lifted by incubating for 10 minutes with 37°C phosphate-buffered saline (PBS) containing 10 mM EDTA, followed by gentle scraping. After approximately 1 week, adherent cells adopted a round, AM-like morphology. At this time, stocks were frozen for future use. Thawed stocks were plated in untreated Petri dishes with either GM-CSF or GM-CSF and TGF β (20 ng/mL recombinant hTGF β 1 [Peprotech]) and sub-cultured as described above.

AM isolation and culture

Mice were euthanized by CO₂ exposure followed by exsanguination via the inferior vena cava. Lungs were lavaged as previously described (20). Cells were then resuspended in RPMI media containing 30 ng/mL GM-CSF and plated in untreated 48- or 24- well plates. AMs were lifted from plates using Accutase™ (BioLegend) and seeded for experiments.

BMDM isolation and culture

C57BL/6J mice were euthanized by CO₂ exposure followed by cervical dislocation. Both femurs were cut on one end to expose the bone marrow, placed cut side down in 0.6 mL tubes, and centrifuged at 16,000 xg for 25 seconds. Marrow from multiple mice was pooled, dissociated to a single cells suspension in sterile PBS and pelleted by centrifuging at 220 xg for 5 min. The pellet was resuspended in mouse RBC lysis buffer (Alfa Aeser) and incubated at room temperature for 5 minutes. The RBC lysis buffer was diluted with 2 volumes of PBS and the cell suspension passed through a nylon 70

mm filter (Corning). Cells were pelleted a second time and resuspended in RPMI media containing 10% FBS, 1% P/S, and 20% L929 media (63). Approximately 5×10^6 cells were plated per dish in 10 cm untreated petri dishes. Media was refreshed every 2-3 days. Cells were used for assays when fully differentiated after 7 days.

Flow cytometry

Plated cells were lifted in warm PBS with 10 mM EDTA for 5-10 minutes and washed twice in PBS before fluorescent antibody labeling. Immediately following isolation, AMs were resuspended in PBS and filtered through a 70 μ m basket filter and incubated with an antibody cocktail of PE CD170, APC CD11c, APC-Cyanine7 CD14, and FC Block (Biolegend; 1:400 in PBS) for 20 min at room temperature in light-free condition.

Immunochemically labeled cells were washed three times with PBS, resuspended in PBS, and passed through a 70 mm nylon filter immediately prior to analysis. Flow cytometry was performed on a LSR II Flow Cytometer (BD Biosciences) at the Michigan State University Flow Cytometry Core.

qPCR

RNA was isolated from $\sim 5 \times 10^5$ cells using RNeasy mini kits (Qiagen), typically yielding 100-400 ng RNA. RNA was then reverse transcribed to cDNA using a High-Capacity cDNA reverse transcription kit (Thermo Fisher) on a Stratagene Robocycler 40.

Quantitative real-time qPCR was performed using specific Taqman probes (Thermo Fisher) for TGF β 1 (*Tgf β 1*), TGF β receptors (*Tgf β 1*, *Tgrbr1*), selected genes used to distinguish AMs from other macrophage populations (*Cd14*, *Siglecf*, *Marco*, *Pparg* *Car4*,

Fabp4, *Itgax*), and cytokines (*Il1a*, *Il1b*, *Il10*) on an Applied Biosystems™ QuantStudio™ 7 real-time PCR system. Data were analyzed with Applied Biosystems™ Thermo Fisher Cloud using the RQ software and the relative quantification method. *Gapdh* was used as the housekeeping gene. Relative copy number (RCN) for each gene was normalized to expression of *Gapdh* and calculated as described previously (64).

Scanning electron microscopy

Suspensions of AMs or FLAMs were diluted to 2.5×10^5 cells/mL, and 100 μ L pipetted directly upon glass 12 mm diameter, 0.13-0.16 mm thick circular coverslips (Electron Microscopy Sciences), which were placed in the bottom of 6-well plates. Cells were allowed to settle for 2-3 minutes, then 1 mL of media was added to fill the well. To fix cells, the coverslips were removed from the wells, submerged in 4% glutaraldehyde in 0.1 M sodium phosphate buffer at pH 7.4 and placed in a graded ethanol series (25%, 50%, 75%, 95%) for 10 min at each step followed by 3 minutes changes in 100% ethanol.

Samples were critical point dried in a Leica Microsystems model EM CPD300 critical point drier (Leica Microsystems, Vienna, Austria) using CO₂ as the transitional fluid. Coverslips were then mounted on aluminum stubs using epoxy glue (System's Three Quick Cure 5, Systems Three Resins, Auburn WA). Samples were coated with osmium at ~10 nm thickness in an NEOC-AT osmium chemical vapor deposition coater (Meiwafosis Co, Osaka, Japan) and examined in a JEOL 7500F (field emission emitter) scanning electron microscope (JEOL, Tokyo, Japan).

cSiO₂ phagocytosis assay

To assess phagocytosis of cSiO₂ particles, FLAMs, AMs, and BMDMs were seeded at 0.25 cells/cm² in 48- or 96-well plates to observe engulfment of surrounding silica particles. The following day, the media was removed, wells were rinsed 1x with sterile PBS, media replaced with FluoroBrite DMEM (Thermo Fisher) containing 10% FBS and 200 nM SYTOX Green nucleic acid stain (Thermo Fisher). cSiO₂ was then added dropwise to a final density of 25-100 mg/cm². Cells were imaged over time on an EVOS FL2 fluorescent microscope (Thermo Fisher) with an on-stage, temperature control CO₂ incubator and 2-4 images were acquired per well. SYTOX Green detected on the GFP light cube.

Images were analyzed using analysis pipelines built in the CellProfiler software (65). cSiO₂ engulfment was assessed by quantifying the number of cSiO₂-filled cells, which have a higher pixel intensity than non-cSiO₂-filled cells due to the accumulation of the particles. To avoid counting aggregated cSiO₂ particles, a threshold was applied to capture only shapes with high solidity and low compactness. Cell death was quantified by counting SYTOX Green⁺ cells, respectively.

ELISAs

Cells were treated with cSiO₂ for 8 hours or LPS for 24 hours at the indicated concentrations. Cell-free supernatant was collected and the cytokines IL-1a, IL-1β, and IL-10 were analyzed using DuoSet ELISA kits (R&D Systems) per the manufacturer's instructions.

CRISPR Targeted Knockouts

sgRNA cloning sgOpti was a gift from Eric Lander & David Sabatini (Addgene plasmid #85681) (66). Individual sgRNAs were cloned as previously described (67) . In short, sgRNA targeting sequences were annealed and phosphorylated then cloned into a dephosphorylated and BsmBI (New England Biolabs) digested SgOpti. sgRNA constructs were then packaged into lentivirus as previously described and used to transduce early passage FLAMs. Two days later, transductants were selected with puromycin. After one week of selection, gDNA was isolated from each targeted FLAM, and PCR was used to amplify edited regions and sanger sequencing was used to quantify indels. Two sgRNAs were targeted per gene and one targeted line was selected for follow up study with editing efficiency >98% for each gene.

Construction of genome-wide loss-of-function library and Siglec-F Screen

The mouse BRIE knockout CRISPR pooled library was a gift of David Root and John Doench (Addgene #73633) (68). Using the BRIE library, 4 sgRNAs targeting every coding gene in mice in addition to 1000 non-targeting controls (78,637 sgRNAs total) were packaged into lentivirus using HEK293T cells and transduced Cas9⁺ FLAMs at a low multiplicity of infection (MOI <0.3). Two days later these cells were selected with puromycin. We then passaged the transduced library in TGF β in parallel with non-transduced cells of the same passage without TGF β . When the non-transduced cells grown in the absence of Tgf β showed reduced Siglec-F expression by flow cytometry we isolated gDNA from the library for sequencing and found high coverage and distribution, with only 1000 sgRNAs not found in the input library. In parallel, the

transduced library was fixed, and fluorescence activated cell sorting (FACS) was used to isolate the Siglec^F^{high} and Siglec^F^{low} bins using a BioRad S3e cell sorter. Genomic DNA was isolated from each sorted population from two biological replicate experiments using a homemade modified salt precipitation method previously described (69). Amplification of sgRNAs by PCR was performed as previously described using Illumina compatible primers from IDT (68), and amplicons were sequenced on an Illumina NovaSeq 6000 at the RTSF Genomics Core at Michigan State University. Sequence reads were first trimmed to remove any adapter sequence and to adjust for p5 primer stagger. We used MAGeCK to map reads to the sgRNA library index without allowing for any mismatch. Subsequent sgRNA counts were median normalized to control sgRNAs in MAGeCK to account for variable sequencing depth. To test for sgRNA and gene enrichment, we used the 'test' command in MAGeCK to compare the distribution of sgRNAs in the Siglec^F^{high} and Siglec^F^{low} bins.

Bioinformatic analysis

Both DAVID analysis and GSEA analysis were used to identify enriched pathways and protein families that were enriched in the data set. Genes were ranked in MAGeCK using RRA and the top enriched positive regulators (4-fold change with at least 2 sgRNAs) were used as a "candidate list" in both DAVID analysis using default settings (70). Functional analysis and functional annotation analysis were completed, and top enriched pathways and protein families were identified. For GSEA analysis, the "GSEA Preranked" function was used to complete functional enrichment using default settings for KEGG, Reactome and GO terms.

Data availability

Raw sequencing data in FASTQ and processed formats will be available for download from NCBI Gene Expression Omnibus (GEO) and available upon request.

Statistical analysis and data visualization

Statistical analysis and data visualization were performed using Prism Version 8 (GraphPad) or R studio as indicated in the figure legends. SYTOX⁺ and cSiO₂-filled cells were quantified using CellProfiler. Data are presented, unless otherwise indicated, as the mean \pm the standard deviation. For parametric data, one-way ANOVA followed by Tukey's post-hoc test was used to identify significant differences between multiple groups, and Student's t-tests were used to compare two groups. Non-parametric one-way ANOVAs and Mann-Whitney U tests were used to compare multiple groups and two groups, respectively, for non-parametric data.

FIGURES

Figure 2.1 Fetal liver macrophages cultured with GM-CSF lose their AM-like phenotype over time. Fetal liver cells were cultured with GM-CSF and analyzed at indicated passage. AMs were isolated and analyzed immediately. **(A)** AMs, passage (P) 2 fetal liver cells, and P37 fetal liver cells were lifted from culture and imaged on a EVOS FL Auto 2 fluorescence microscope at $\times 60$ original magnification. **(B)** AMs, P3 fetal liver cells, and P15 fetal liver cells were fixed and imaged by scanning electron microscopy at $\times 4500$, $\times 4000$, and $\times 2200$, respectively. **(C)** AMs (gray), P4 fetal liver macrophages (blue), and P15 fetal liver macrophages (red) were assessed for surface expression of the markers CD14, Siglec-F, and CD11c by flow cytometry. **(D)** Gene expression of indicated genes in AMs, early fetal liver macrophages (P1), and late fetal liver macrophages (P18) was quantified by qPCR. Data were compared using one-way ANOVA followed by a Tukey multiple comparison test. Bars labeled with unique letters are significantly different ($p < 0.05$). Results are representative of two or three independent experiments.

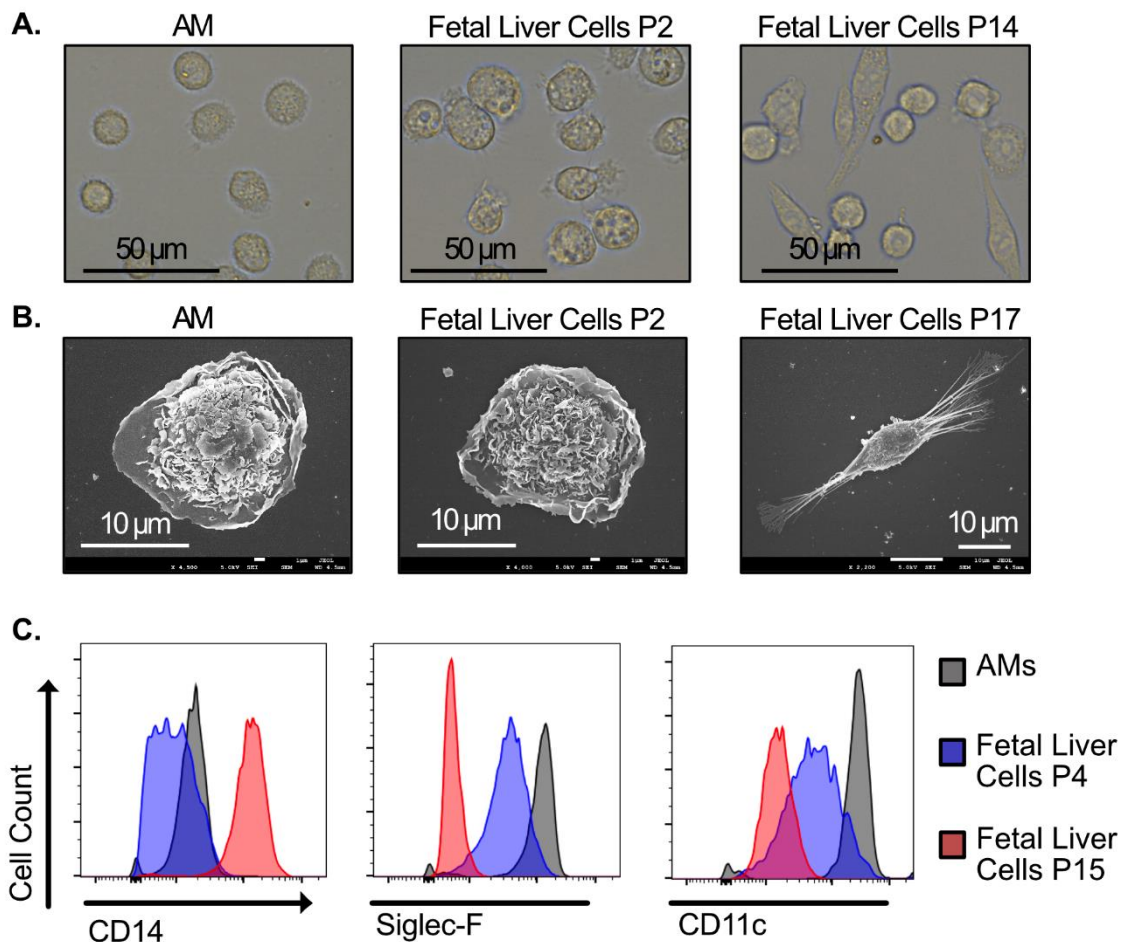


Figure 2.1 (cont'd)

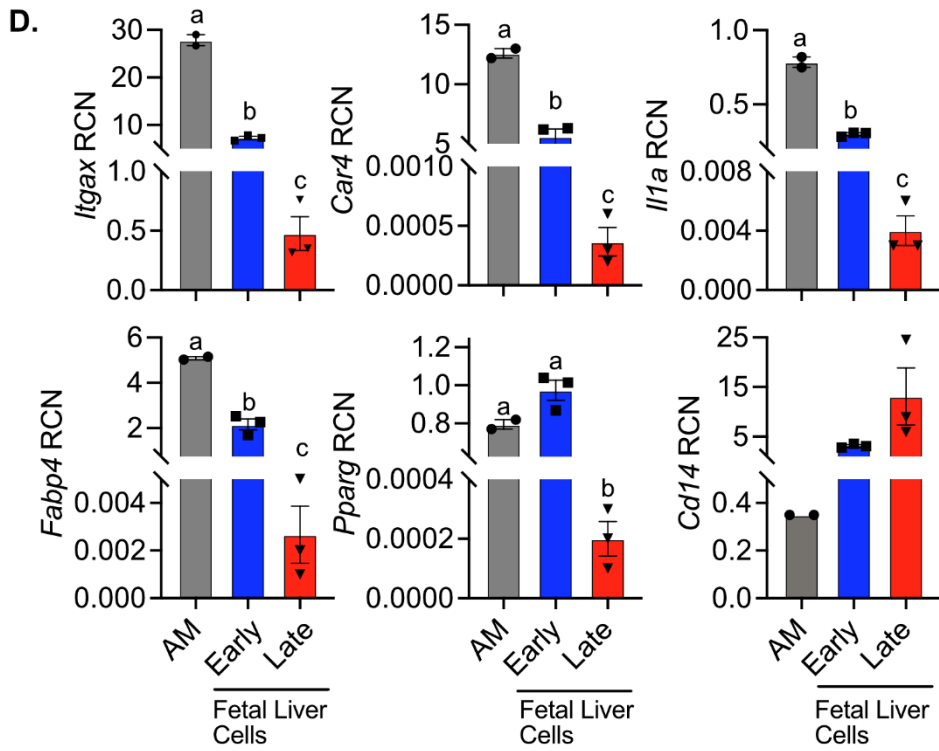


Figure 2.2 Culturing fetal liver cells with TGF- β and GM-CSF maintains AM-like phenotypes long-term. Fetal liver cells were cultured with or without TGF β for the indicated passages. **(A)** Passage (P) 15 cells cultured with and without TGF β were imaged on a EVOS FL Auto 2 fluorescence microscope at $\times 60$ original magnification. Cells with a clearly visible spindleoid morphology are marked with arrows. **(B)** At the indicated passage, RNA was extracted from a subset of cells for gene expression analysis. Expression of the indicated genes are quantified as relative copy number (RCN) compared with *Gapdh*. Asterisks indicate significant differences in gene expression of cells cultured with and without TGF β cells at the same passage number, as determined by a Student *t* test. * $p < 0.05$. **(C)** At the indicated passage, cells were analyzed by flow cytometry for the surface expression of CD14 and Siglec-F. Representative biaxial plots from triplicate samples are shown. **(D)** Quantification of the mean fluorescence intensity (MFI) and percent of cells positive of CD14 and Siglec-F surface expression from cells in (C) expressed as MFI (left) and percent positive (right). Results are representative of at least two independent experiments. **** $p < 0.0001$ by one-way ANOVA with a Tukey correction for multiple comparisons.

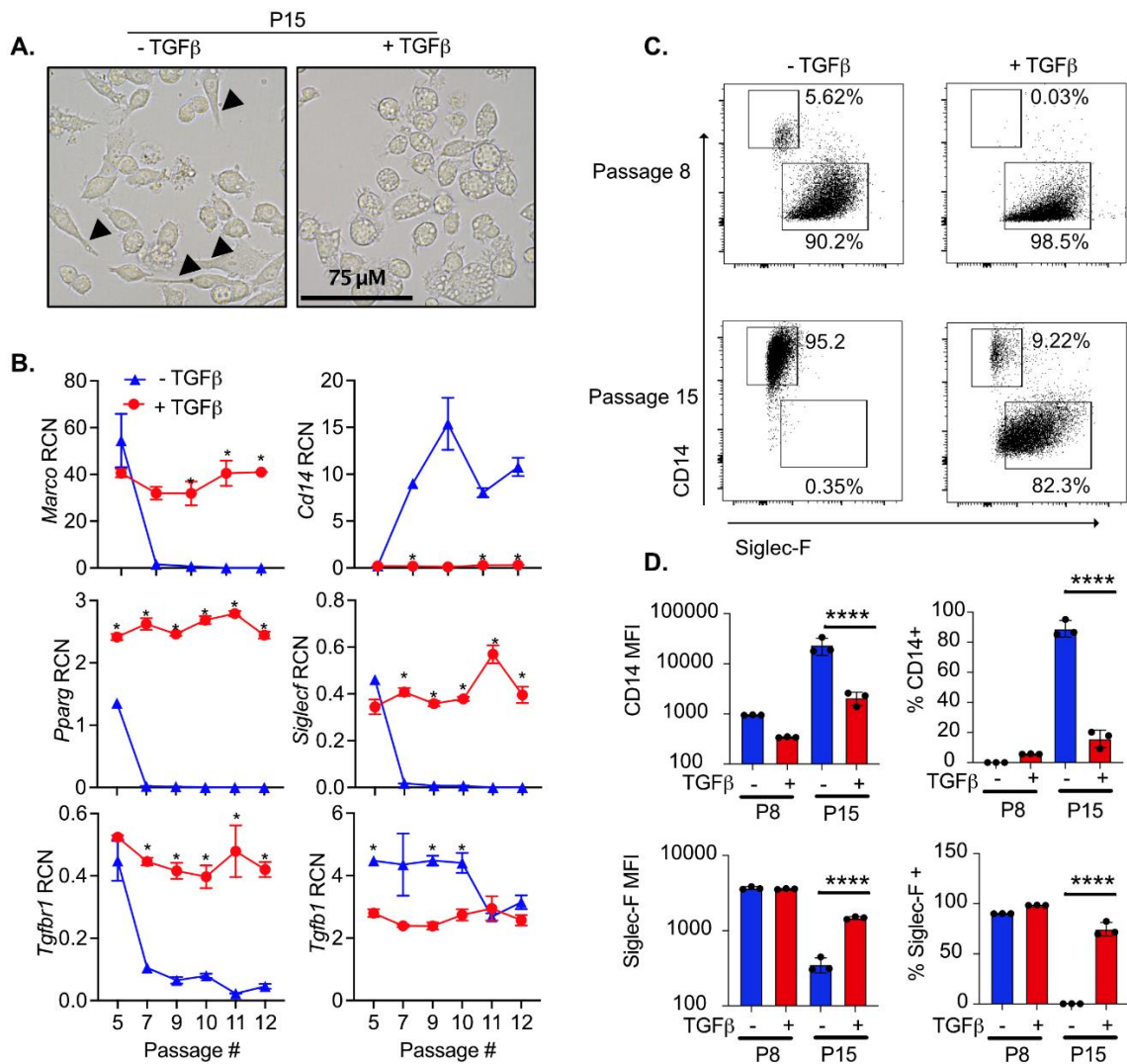


Figure 2.3 The kinetics of cSiO₂ uptake and cSiO₂-induced cell death and IL-1 release are similar among AMs and FLAMs. AMs, bone marrow-derived macrophages (BMDMs), and fetal liver cells were seeded in 96-well plates. After 24 h, media were replaced with FluoroBrite DMEM containing 200 nM Sytox green and 10% FBS. cSiO₂ at the indicated densities was added dropwise to cells and images were taken at 0, 2, 6, and 8 h using an EVOS FL2 fluorescence microscope. **(A)** The percentages of cSiO₂-filled and Sytox⁺ cells were quantified using CellProfiler software. **(B)** Representative images of Sytox⁺ and cSiO₂-filled cells (white arrows in AM panel, top right) treated with 50 μg/cm² silica for 8 h; original magnification, ×20. **(C)** In a separate experiment, the supernatant was collected after an 8-h treatment with 25 μg/cm² to assess release of the cytokines IL-1α (top) and IL-1β (bottom) by ELISA. ***p* < 0.01, ****p* < 0.001, as assessed by Student *t* tests between relevant groups. ND, not detected. Results are representative of at least two independent experiments.

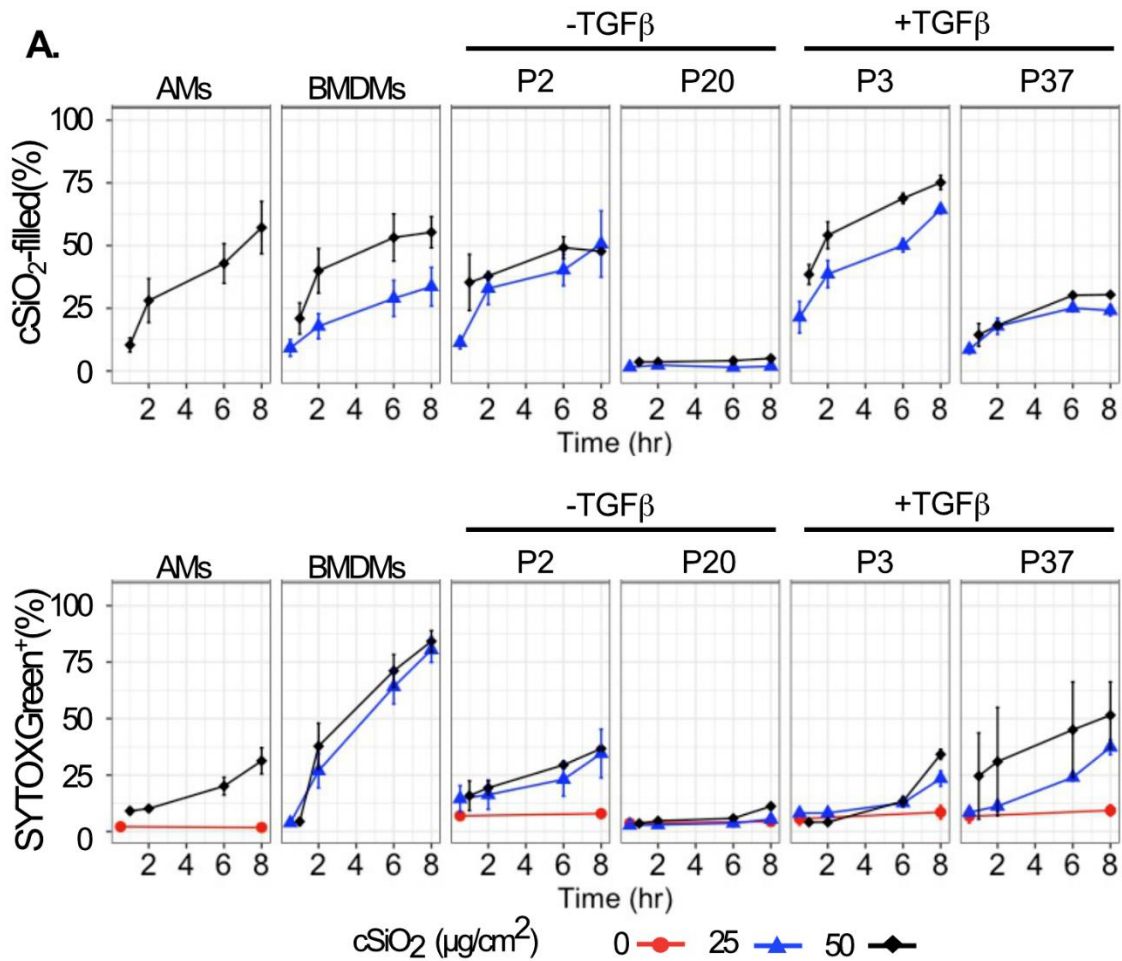


Figure 2.3 (cont'd)

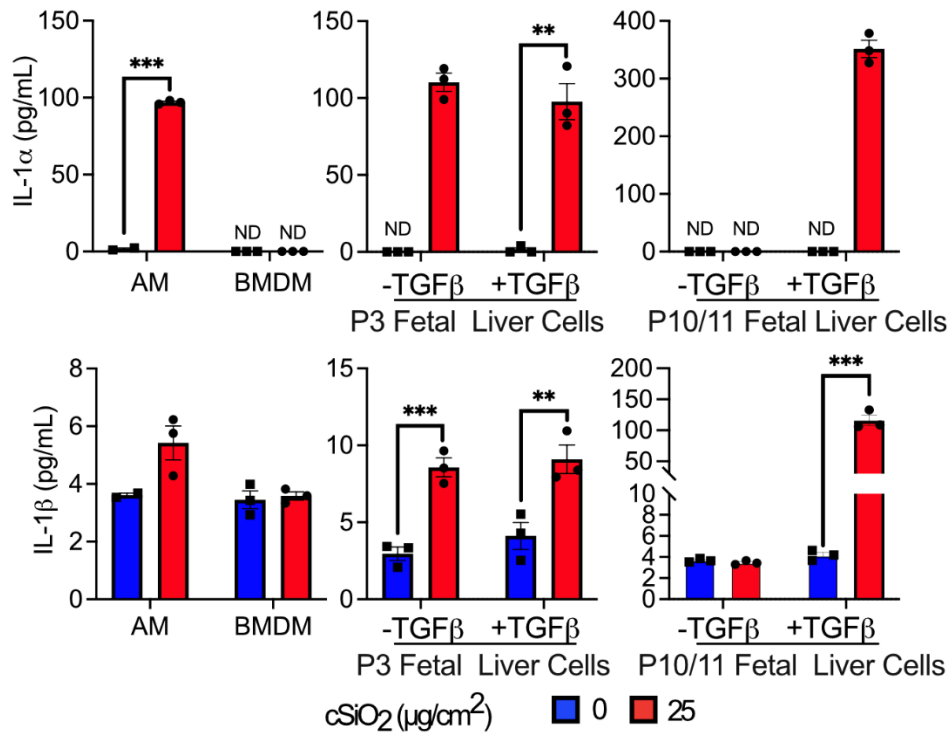
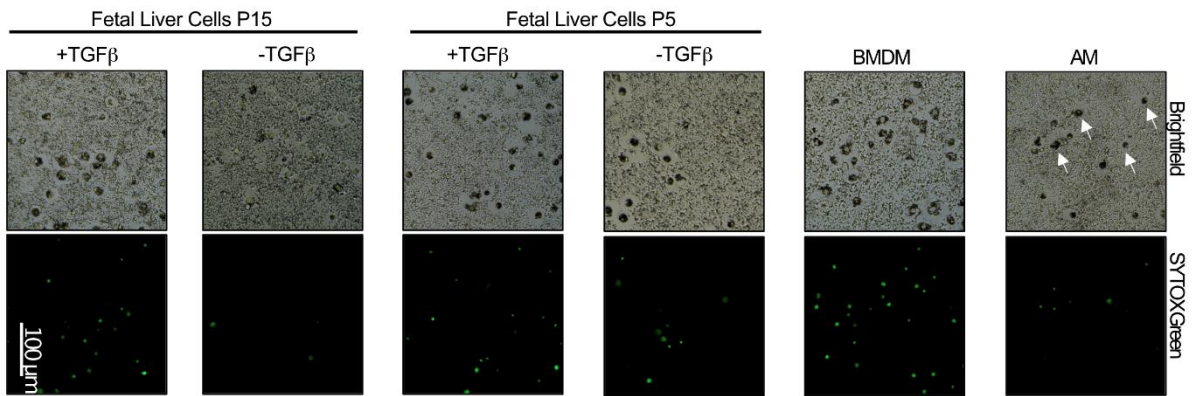


Figure 2.4 The loss of *Marco* and *Il1r1* modulate the response of FLAMs to cSiO₂ treatment. Wild-type, *Marco* knockout (KO), and *Il1r1* KO FLAMs were treated with cSiO₂ at the indicated concentrations for 8 h. (A) Cell viability was determined using the MTS assay, with 100% viability determined as the mean absorbance of the formazan dye product in the untreated wild-type cells. (B and C) Supernatant was collected to measure release of (B) IL-1 α and (C) IL-1 β . Results are representative of at least two independent experiments with biological triplicates. * $p < 0.05$, *** $p < 0.001$, between cell types within treatment groups, as determined by one-way ANOVA followed by a Tukey multiple comparison test.

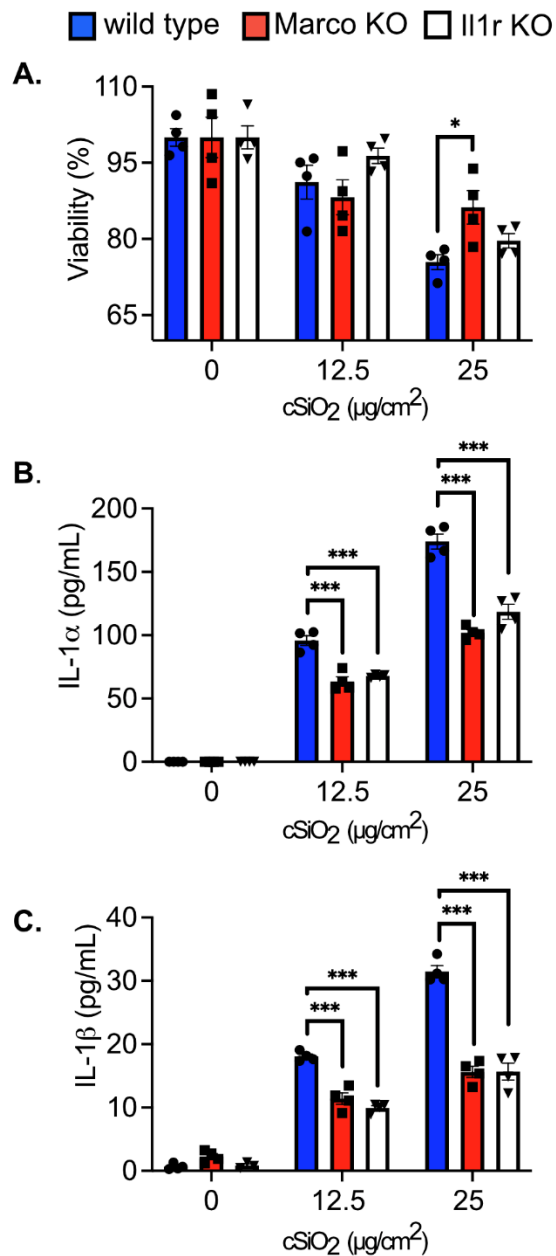


Figure 2.5 A loss-of-function forward genetic screen identifies regulators of Siglec-F surface expression on FLAMs. iBMDMs or FLAMs targeted for *I11r1* or *SiglecF* were analyzed by flow cytometry for Siglec-F surface expression. **(A)** Shown are representative histograms of surface expression. **(B)** The MFI of Siglec-F surface expression was quantified on cells of the indicated genotypes. **** $p < 0.0001$, between samples by one-way ANOVA with a Tukey correction. These data are representative of two independent experiments. **(C)** Shown is a schematic of the generation of the FLAM knockout library and screen to identify Siglec-F regulators. Transduction of Cas9⁺ FLAMs with the genome-wide library of sgRNAs results in variable Siglec-F surface expression. When parallel control FLAMs grown in the absence of TGF β lost Siglec-F expression, the top and bottom 5% of Siglec-F expression cells were isolated from the knockout FLAM library by FACS. Sorted cells were then used for downstream sequencing and analysis. **(D)** Siglec-F surface expression of library control cells grown in the absence of TGF β was monitored over time and compared with the transduced FLAM library prior to sorting. Shown is the MFI for Siglec-F expression of the indicated cells and passage numbers. **** $p < 0.0001$ by one-way ANOVA with Tukey test. **(E)** Shown is the α -RRA score of each gene in CRISPR library that passed filtering metrics in MAGeCK. Genes of interest are noted. **(F)** Normalized sg*SiglecF* counts for each sgRNA found in both the Siglec-F^{low}- and Siglec-F^{high}-sorted populations is shown.

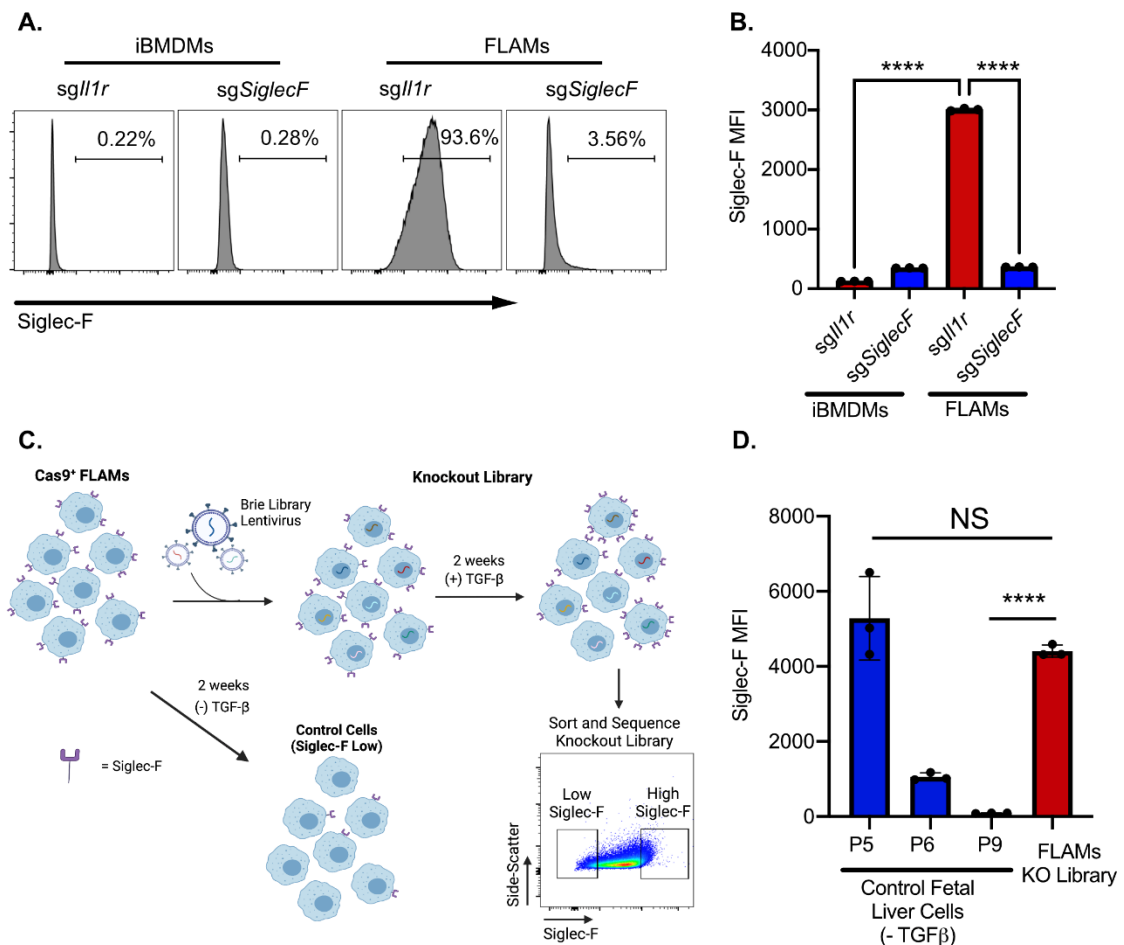
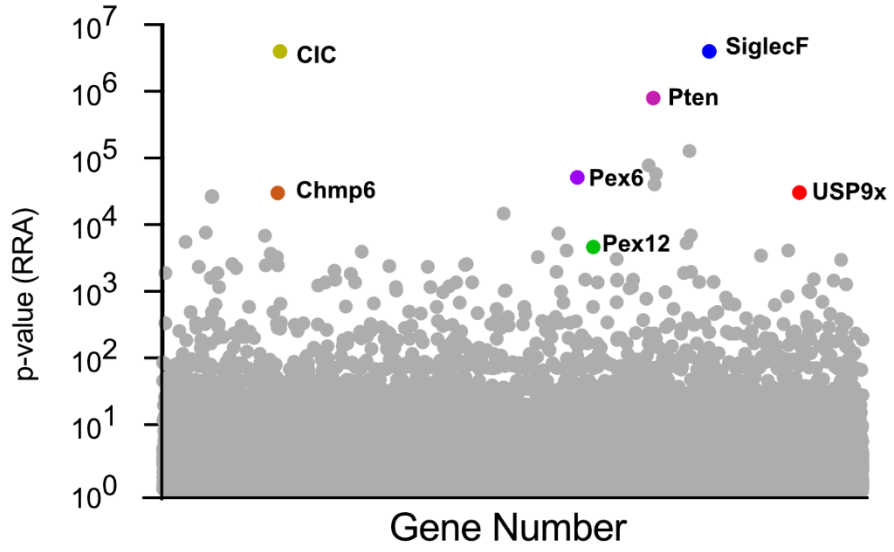


Figure 2.5 (cont'd)

E.



F.

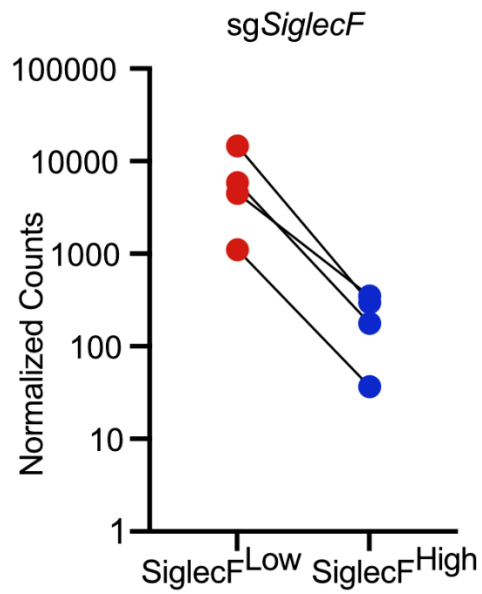


Figure 2.6 Bioinformatics analysis identifies FLAM metabolic networks as critical regulators of Siglec-F expression. (A) The TGF β response regulator USP9x was a significant hit in the screen. Shown are the normalized counts for each of the four sgRNAs targeting USP9x in each sorted population. (B) Using DAVID analysis, peroxisome biogenesis was identified as the most significantly enriched KEGG pathway. Shown is an adaptation of the KEGG peroxisome biogenesis pathway highlighting the 10 peroxisome regulators identified in the screen in pink. (C) The sgRNA distribution and mean log fold change for each peroxisome regulator (Pex) identified in the genetic screen are shown. The dashed line indicates a log₂ fold change of -1. (D) DAVID analysis identified surface proteins associated with phagocytosis. Shown are the normalized counts for each of the four sgRNAs targeting the indicated surface protein from each sorted population. (E) GSEA was used to identify enriched pathways from the entire forward genetic screen. Shown are four leading-edge analysis plots that are representative of this analysis for a subset of enriched pathways. These pathways include the peroxisome, oxidative phosphorylation, GPI anchor biosynthesis, and mTORC1 signaling.

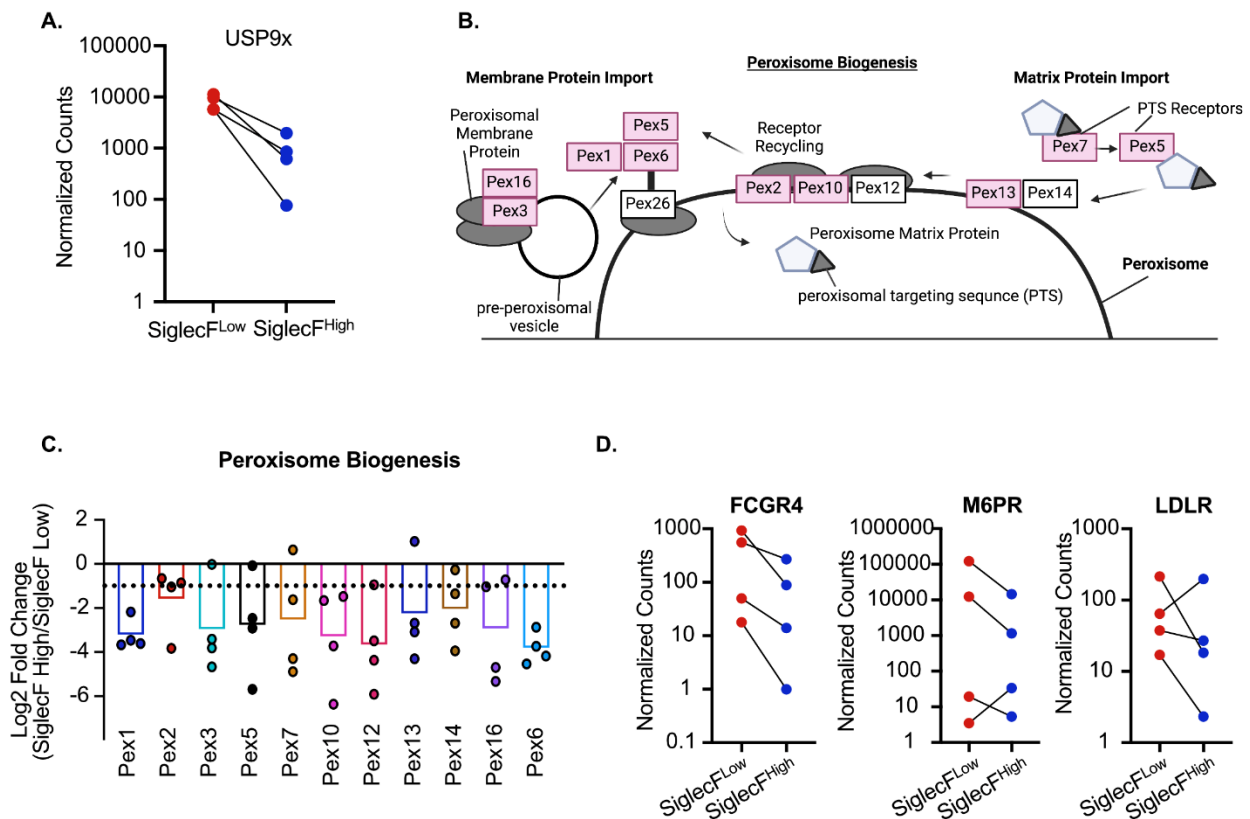
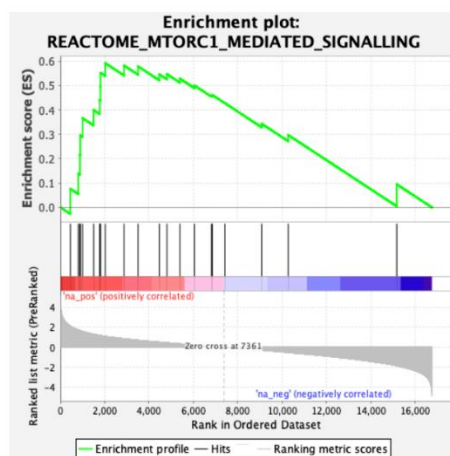
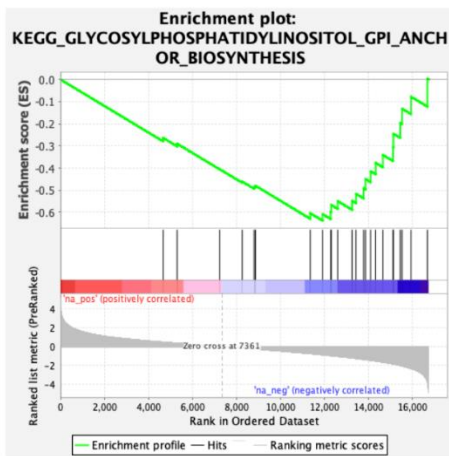
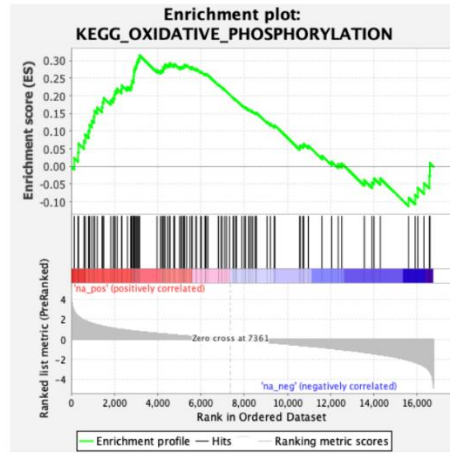
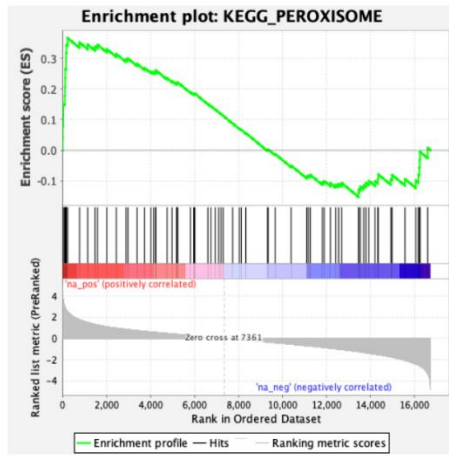


Figure 2.6 (cont'd)

E.



DECLARATIONS

Competing interests

The authors declare that they have no competing interests.

Funding

This work was supported by startup funding to AJO provided by Michigan State University, the Rackham Endowment Award (to AJO), the Dr Robert and Carol Deibel Family Endowment (to JJP), as well as by National Institutes of Health Grants AI148961 (to AJO), F31ES030593 (to KAW), ES027353 (to JJP), and T32ES030593 (to KAW), US Department of Defense Grant W81XWH2010147 (to AJO), and the US Department of Agriculture (National Institute of Food and Agriculture HATCH Grant 1019371 [to AJO])

Contributions

Conceptualization: SMT, KAW, JPP, AJO. *Methodology:* SMT, KAW, JPP, AJO.

Software: JPP, AJO. *Validation:* SMT, KAW, JPP, AJO. *Formal Analysis:* SMT, KAW, JPP, AJO. *Investigation:* SMT, KAW, JPP, AJO. *Resources:* JPP, AJO. *Data Curation:* SMT, KAW, JPP, AJO. *Writing:* SMT, KAW, JPP, AJO. *Visualization:* SMT, KAW, JPP, AJO. *Supervision:* JPP, AJO. *Project Administration:* JPP, AJO. *Funding:* KAW, JPP, AJO

BIBLIOGRAPHY

1. Davies LC, Jenkins SJ, Allen JE, Taylor PR. 2013. Tissue-resident macrophages. *Nat Immunol*2013/09/21. 14:986–995.
2. Mass E, Ballesteros I, Farlik M, Halbritter F, Gunther P, Crozet L, Jacome-Galarza CE, Handler K, Klughammer J, Kobayashi Y, Gomez-Perdiguero E, Schultze JL, Beyer M, Bock C, Geissmann F. 2016. Specification of tissue-resident macrophages during organogenesis. *Science* (1979)2016/08/06. 353.
3. Lavin Y, Winter D, Blecher-Gonen R, David E, Keren-Shaul H, Merad M, Jung S, Amit I. 2014. Tissue-resident macrophage enhancer landscapes are shaped by the local microenvironment. *Cell*2014/12/07. 159:1312–1326.
4. Hetzel M, Ackermann M, Lachmann N. 2021. Beyond “Big Eaters”: The Versatile Role of Alveolar Macrophages in Health and Disease. *Int J Mol Sci*2021/04/04. 22.
5. Reddy RC, Keshamouni VG, Jaigirdar SH, Zeng X, Leff T, Thannickal VJ, Standiford TJ. 2004. Deactivation of murine alveolar macrophages by peroxisome proliferator-activated receptor-gamma ligands. *Am J Physiol Lung Cell Mol Physiol* 286.
6. Misharin A v, Morales-Nebreda L, Mutlu GM, Budinger GR, Perlman H. 2013. Flow cytometric analysis of macrophages and dendritic cell subsets in the mouse lung. *Am J Respir Cell Mol Biol*2013/05/16. 49:503–510.
7. Guilliams M, de Kleer I, Henri S, Post S, Vanhoutte L, de Prijck S, Deswarte K, Malissen B, Hammad H, Lambrecht BN. 2013. Alveolar macrophages develop from fetal monocytes that differentiate into long-lived cells in the first week of life via GM-CSF. *J Exp Med*2013/09/18. 210:1977–1992.
8. Kopf M, Schneider C, Nobs SP. 2015. The development and function of lung-resident macrophages and dendritic cells. *Nat Immunol*2014/12/19. 16:36–44.
9. Ginhoux F, Guilliams M. 2016. Tissue-Resident Macrophage Ontogeny and Homeostasis. *Immunity*2016/03/18. 44:439–449.
10. Yu X, Buttgereit A, Lelios I, Utz SG, Cansever D, Becher B, Greter M. 2017. The Cytokine Tgfβ Promotes the Development and Homeostasis of Alveolar Macrophages. *Immunity*2017/11/12. 47:903-912 e4.
11. Schneider C, Nobs SP, Kurrer M, Rehrauer H, Thiele C, Kopf M. 2014. Induction of the nuclear receptor PPAR-gamma by the cytokine GM-CSF is critical for the differentiation of fetal monocytes into alveolar macrophages. *Nat Immunol*2014/09/30. 15:1026–1037.

12. Reddy RC. 2008. Immunomodulatory role of PPAR-gamma in alveolar macrophages. *J Investig Med*2008/03/05. 56:522–527.
13. Bonfield TL, Farver CF, Barna BP, Malur A, Abraham S, Raychaudhuri B, Kavuru MS, Thomassen MJ. 2003. Peroxisome proliferator-activated receptor-gamma is deficient in alveolar macrophages from patients with alveolar proteinosis. *Am J Respir Cell Mol Biol*2003/06/14. 29:677–682.
14. Trapnell BC, Nakata K, Bonella F, Campo I, Griese M, Hamilton J, Wang T, Morgan C, Cottin V, McCarthy C. 2019. Pulmonary alveolar proteinosis. *Nature Reviews Disease Primers* 2019 5:1 5:1–17.
15. CS B, RL K, E E, S S. 2013. Phagocytic dysfunction of human alveolar macrophages and severity of chronic obstructive pulmonary disease. *J Infect Dis* 208:2036–2045.
16. Berenson CS, Kruzel RL, Eberhardt E, Dolnick R, Minderman H, Wallace PK, Sethi S. 2014. Impaired innate immune alveolar macrophage response and the predilection for COPD exacerbations. *Thorax* <https://doi.org/10.1136/thoraxjnl-2013-203669>.
17. Liang Z, Zhang Q, Thomas CM, Chana KK, Gibeon D, Barnes PJ, Chung KF, Bhavsar PK, Donnelly LE. 2014. Impaired macrophage phagocytosis of bacteria in severe asthma. *Respiratory Research* 2014 15:1 15:1–11.
18. Lévêque M, le Trionnaire S, del Porto P, Martin-Chouly C. 2017. The impact of impaired macrophage functions in cystic fibrosis disease progression. *Journal of Cystic Fibrosis* 16:443–453.
19. AL M, JL C. 2013. Efferocytosis and lung disease. *Chest* 143:1750–1757.
20. Busch CJ, Favret J, Geirsdottir L, Molawi K, Sieweke MH. 2019. Isolation and Long-term Cultivation of Mouse Alveolar Macrophages. *Bio Protoc*2020/01/08. 9.
21. Chen YW, Huang MZ, Chen CL, Kuo CY, Yang CY, Chiang-Ni C, Chen YM, Hsieh CM, Wu HY, Kuo ML, Chiu CH, Lai CH. 2020. PM2.5 impairs macrophage functions to exacerbate pneumococcus-induced pulmonary pathogenesis. *Part Fibre Toxicol*2020/08/06. 17:37.
22. Dostert C, Petrilli V, van Bruggen R, Steele C, Mossman BT, Tschopp J. 2008. Innate immune activation through Nalp3 inflammasome sensing of asbestos and silica. *Science* (1979)2008/04/12. 320:674–677.
23. Hornung V, Bauernfeind F, Halle A, Samstad EO, Kono H, Rock KL, Fitzgerald KA, Latz E. 2008. Silica crystals and aluminum salts activate the NALP3 inflammasome through phagosomal destabilization. *Nat Immunol* 9:847–856.

24. Brenner TA, Rice TA, Anderson ED, Percopo CM, Rosenberg HF. 2016. Immortalized MH-S cells lack defining features of primary alveolar macrophages and do not support mouse pneumovirus replication. *Immunol Lett* 2016/02/27. 172:106–112.
25. Fejer G, Wegner MD, Gyory I, Cohen I, Engelhard P, Voronov E, Manke T, Ruzsics Z, Dolken L, Prazeres da Costa O, Branzk N, Huber M, Prasse A, Schneider R, Apte RN, Galanos C, Freudenberg MA. 2013. Nontransformed, GM-CSF-dependent macrophage lines are a unique model to study tissue macrophage functions. *Proc Natl Acad Sci U S A* 2013/05/28. 110:E2191-8.
26. Wierenga KA, Wee J, Gilley KN, Rajasinghe LD, Bates MA, Gavrilin MA, Holian A, Pestka JJ. 2019. Docosahexaenoic Acid Suppresses Silica-Induced Inflammasome Activation and IL-1 Cytokine Release by Interfering With Priming Signal. *Front Immunol* 10.
27. Gorki A, Symmank D, Zahalka S, Lakovits K, Hladik A, Langer B, Maurer B, Sexl V, Kain R, Knapp S. 2021. Murine ex vivo Cultured Alveolar Macrophages Provide a Novel Tool to Study Tissue-Resident Macrophage Behavior and Function. *Am J Respir Cell Mol Biol* <https://doi.org/10.1165/RCMB.2021-0190OC>.
28. Maler MD, Nielsen PJ, Stichling N, Cohen I, Ruzsics Z, Wood C, Engelhard P, Suomalainen M, Gyory I, Huber M, Muller-Quernheim J, Schamel WWA, Gordon S, Jakob T, Martin SF, Jahnke-Dechent W, Greber UF, Freudenberg MA, Fejer G. 2017. Key Role of the Scavenger Receptor MARCO in Mediating Adenovirus Infection and Subsequent Innate Responses of Macrophages. *mBio* 2017/08/03. 8.
29. Woo M, Wood C, Kwon D, Park KP, Fejer G, Delorme V. 2018. Mycobacterium tuberculosis Infection and Innate Responses in a New Model of Lung Alveolar Macrophages. *Front Immunol* 2018/03/30. 9:438.
30. Mould KJ, Jackson ND, Henson PM, Seibold M, Janssen WJ. 2019. Single cell RNA sequencing identifies unique inflammatory airspace macrophage subsets. *JCI Insight* 2019/02/06. 4.
31. Pollard KM. 2016. Silica, silicosis, and autoimmunity. *Front Immunol* 7.
32. Parks CG, Miller FW, Pollard KM, Selmi C, Germolec D, Joyce K, Rose NR, Humble MC. 2014. Expert panel workshop consensus statement on the role of the environment in the development of autoimmune disease. *Int J Mol Sci* 2014/09/10. 15:14269–14297.
33. Kuroda E, Ozasa K, Temizoz B, Ohata K, Koo CX, Kanuma T, Kusakabe T, Kobari S, Horie M, Morimoto Y, Nakajima S, Kabashima K, Ziegler SF, Iwakura Y, Ise W, Kurosaki T, Nagatake T, Kunisawa J, Takemura N, Uematsu S, Hayashi M, Aoshi T, Kobiyama K, Coban C, Ishii KJ. 2016. Inhaled Fine Particles Induce Alveolar Macrophage Death and Interleukin-1alpha Release to Promote

Inducible Bronchus-Associated Lymphoid Tissue Formation.
*Immunity*2016/12/22. 45:1299–1310.

34. Rabolli V, Badissi AA, Devosse R, Uwambayinema F, Yakoub Y, Palmai-Pallag M, Lebrun A, de Gussem V, Couillin I, Ryffel B, Marbaix E, Lison D, Huaux F. 2014. The alarmin IL-1 α is a master cytokine in acute lung inflammation induced by silica micro- and nanoparticles. *Part Fibre Toxicol*2014/12/17. 11:69.
35. Fejer G, Wegner MD, Gyory I, Cohen I, Engelhard P, Voronov E, Manke T, Ruzsics Z, Dolken L, Prazeres da Costa O, Branzk N, Huber M, Prasse A, Schneider R, Apte RN, Galanos C, Freudenberg MA. 2013. Nontransformed, GM-CSF-dependent macrophage lines are a unique model to study tissue macrophage functions. *Proc Natl Acad Sci U S A*2013/05/28. 110:E2191-8.
36. Platt RJ, Chen S, Zhou Y, Yim MJ, Swiech L, Kempton HR, Dahlman JE, Parnas O, Eisenhaure TM, Jovanovic M, Graham DB, Jhunjhunwala S, Heidenreich M, Xavier RJ, Langer R, Anderson DG, Hacohen N, Regev A, Feng G, Sharp PA, Zhang F. 2014. CRISPR-Cas9 knockin mice for genome editing and cancer modeling. *Cell* 159:440–455.
37. Cortez JT, Montauti E, Shifrut E, Gatchalian J, Zhang Y, Shaked O, Xu Y, Roth TL, Simeonov DR, Zhang Y, Chen S, Li Z, Woo JM, Ho J, Vogel IA, Prator GY, Zhang B, Lee Y, Sun Z, Ifergan I, van Gool F, Hargreaves DC, Bluestone JA, Marson A, Fang D. 2020. CRISPR screen in regulatory T cells reveals modulators of Foxp3. *Nature* 582:416–420.
38. Thakur SA, Beamer CA, Migliaccio CT, Holian A. 2009. Critical role of MARCO in crystalline silica-induced pulmonary inflammation. *Toxicol Sci*2009/01/20. 108:462–471.
39. Hornung V, Bauernfeind F, Halle A, Samstad EO, Kono H, Rock KL, Fitzgerald KA, Latz E. 2008. Silica crystals and aluminum salts activate the NALP3 inflammasome through phagosomal destabilization. *Nat Immunol*2008/07/08. 9:847–856.
40. Hamilton Jr. RF, Thakur SA, Mayfair JK, Holian A. 2006. MARCO mediates silica uptake and toxicity in alveolar macrophages from C57BL/6 mice. *J Biol Chem*2006/09/21. 281:34218–34226.
41. Kiritsy MC, Ankley LM, Trombley J, Huizinga GP, Lord AE, Orning P, Elling R, Fitzgerald KA, Olive AJ. 2021. A genetic screen in macrophages identifies new regulators of IFN γ -inducible MHCII that contribute to T cell activation. *Elife* 10.
42. Sanson KR, Hanna RE, Hegde M, Donovan KF, Strand C, Sullender ME, Vaimberg EW, Goodale A, Root DE, Piccioni F, Doench JG. 2018. Optimized libraries for CRISPR-Cas9 genetic screens with multiple modalities. *Nature Communications* 2018 9:1 9:1–15.

43. Li W, Xu H, Xiao T, Cong L, Love MI, Zhang F, Irizarry RA, Liu JS, Brown M, Liu XS. 2014. MAGECK enables robust identification of essential genes from genome-scale CRISPR/Cas9 knockout screens. *Genome Biol* 15:554.
44. Dupont S, Mamidi A, Cordenonsi M, Montagner M, Zacchigna L, Adorno M, Martello G, Stinchfield MJ, Soligo S, Morsut L, Inui M, Moro S, Modena N, Argenton F, Newfeld SJ, Piccolo S. 2009. FAM/USP9x, a deubiquitinating enzyme essential for Tgf β signaling, controls Smad4 monoubiquitination. *Cell* 136:123–135.
45. Esteves F, Rueff J, Kranendonk M. 2021. The Central Role of Cytochrome P450 in Xenobiotic Metabolism-A Brief Review on a Fascinating Enzyme Family. *J Xenobiot* 11:94–114.
46. Woods PS, Kimmig LM, Meliton AY, Sun KA, Tian Y, O'Leary EM, Gökalp GA, Hamanaka RB, Mutlu GM. 2020. Tissue-resident alveolar macrophages do not rely on glycolysis for LPS-induced inflammation. *Am J Respir Cell Mol Biol* 62:243–255.
47. Sinclair C, Bommakanti G, Gardinassi L, Loebbermann J, Johnson MJ, Hakimpour P, Hagan T, Benitez L, Todor A, Machiah D, Oriss T, Ray A, Bosinger S, Ravindran R, Li S, Pulendran B. 2017. mTOR regulates metabolic adaptation of APCs in the lung and controls the outcome of allergic inflammation. *Science* 357:1014–1021.
48. Bissonnette EY, Lauzon-Joset JF, Debley JS, Ziegler SF. 2020. Cross-Talk Between Alveolar Macrophages and Lung Epithelial Cells is Essential to Maintain Lung Homeostasis. *Front Immunol* 2020/11/13. 11:583042.
49. Fejer G, Sharma S, Gyory I. 2015. Self-renewing macrophages--a new line of enquiries in mononuclear phagocytes. *Immunobiology* 2014/12/04. 220:169–174.
50. Luo M, Lai W, He Z, Wu L. 2021. Development of an Optimized Culture System for Generating Mouse Alveolar Macrophage-like Cells. *The Journal of Immunology* 207:1683–1693.
51. Gorki AD, Zymmank D, Zahalka S, Lakovits A, Hladik A, Langer B, Maurer B, Sexl V, Kain R, Knapp S. 2021. Murine ex vivo cultured alveolar macrophages provide a novel tool to study tissue-resident macrophage behavior and function. *bioRxiv* 2021/02/11. <https://doi.org/10.1101/2021.02.11.430791>.
52. Kawasaki H. 2015. A mechanistic review of silica-induced inhalation toxicity. *Inhal Toxicol* 27:363–377.
53. Arredouani MS, Palecanda A, Koziel H, Huang YC, Imrich A, Sulahian TH, Ning YY, Yang Z, Pikkarainen T, Sankala M, Vargas SO, Takeya M, Tryggvason K, Kobzik L. 2005. MARCO is the major binding receptor for unopsonized particles

- and bacteria on human alveolar macrophages. *J Immunol* 2005/10/21. 175:6058–6064.
54. Mao H, Kano G, Hudson SA, Brummet M, Zimmermann N, Zhu Z, Bochner BS. 2013. Mechanisms of Siglec-F-Induced Eosinophil Apoptosis: A Role for Caspases but Not for SHP-1, Src Kinases, NADPH Oxidase or Reactive Oxygen. *PLoS One* 8:e68143.
 55. Feng YH, Mao H. 2012. Expression and preliminary functional analysis of Siglec-F on mouse macrophages. *J Zhejiang Univ Sci B* 13:386.
 56. Ginhoux F. 2014. Fate PPAR-titoning: PPAR-gamma “instructs” alveolar macrophage development. *Nat Immunol* 2014/10/21. 15:1005–1007.
 57. Coleman MM, Ruane D, Moran B, Dunne PJ, Keane J, Mills KHG. 2013. Alveolar macrophages contribute to respiratory tolerance by inducing FoxP3 expression in naive T cells. *Am J Respir Cell Mol Biol* 48:773–780.
 58. Li S, Lei Y, Lei J, Li H. 2021. All-trans retinoic acid promotes macrophage phagocytosis and decreases inflammation via inhibiting CD14/TLR4 in acute lung injury. *Mol Med Rep* 24.
 59. Munger JS, Huang X, Kawakatsu H, Griffiths MJD, Dalton SL, Wu J, Pittet JF, Kaminski N, Garat C, Matthay MA, Rifkin DB, Sheppard D. 1999. A Mechanism for Regulating Pulmonary Inflammation and Fibrosis: The Integrin $\alpha\beta 6$ Binds and Activates Latent TGF $\beta 1$. *Cell* 96:319–328.
 60. Kannan S, Huang H, Seeger D, Audet A, Chen Y, Huang C, Gao H, Li S, Wu M. 2009. Alveolar epithelial type II cells activate alveolar macrophages and mitigate *P. Aeruginosa* infection. *PLoS One* 4.
 61. Bates MA, Brandenberger C, Langohr I, Kumagai K, Harkema JR, Holian A, Pestka JJ. 2015. Silica triggers inflammation and ectopic lymphoid neogenesis in the lungs in parallel with accelerated onset of systemic autoimmunity and glomerulonephritis in the lupus-prone NZBWF1 mouse. *PLoS One* 10.
 62. Bates MA, Akbari P, Gilley KN, Wagner JG, Li N, Kopec AK, Wierenga KA, Jackson-Humbles D, Brandenberger C, Holian A, Benninghoff AD, Harkema JR, Pestka JJ. 2018. Dietary docosahexaenoic acid prevents silica-induced development of pulmonary ectopic germinal centers and glomerulonephritis in the lupus-prone NZBWF1 mouse. *Front Immunol* 2018/09/28. 9:2002.
 63. Weischenfeldt J, Porse B. 2008. Bone marrow-derived macrophages (BMM): Isolation and applications. *Cold Spring Harb Protoc* 3.
 64. Fahy RJ, Exline MC, Gavrillin MA, Bhatt NY, Besecker BY, Sarkar A, Hollyfield JL, Duncan MD, Nagaraja HN, Knatz NL, Hall M, Wewers MD. 2008.

- Inflammasome mRNA expression in human monocytes during early septic shock. *Am J Respir Crit Care Med* 2008/02/12. 177:983–988.
65. Carpenter AE, Jones TR, Lamprecht MR, Clarke C, Kang IH, Friman O, Guertin DA, Chang JH, Lindquist RA, Moffat J, Golland P, Sabatini DM. 2006. CellProfiler: image analysis software for identifying and quantifying cell phenotypes. *Genome Biol* 2006/11/02. 7:R100.
 66. Fulco CP, Munschauer M, Anyoha R, Munson G, Grossman SR, Perez EM, Kane M, Cleary B, Lander ES, Engreitz JM. 2016. Systematic mapping of functional enhancer-promoter connections with CRISPR interference. *Science* (1979) 354:769–773.
 67. Shalem O, Sanjana NE, Hartenian E, Shi X, Scott DA, Mikkelsen TS, Heckl D, Ebert BL, Root DE, Doench JG, Zhang F. 2014. Genome-scale CRISPR-Cas9 knockout screening in human cells. *Science* 343:84–87.
 68. Doench JG, Fusi N, Sullender M, Hegde M, Vaimberg EW, Donovan KF, Smith I, Tothova Z, Wilen C, Orchard R, Virgin HW, Listgarten J, Root DE. 2016. Optimized sgRNA design to maximize activity and minimize off-target effects of CRISPR-Cas9. *Nat Biotechnol* 2016/01/19. 34:184–191.
 69. Chen S, Sanjana NE, Zheng K, Shalem O, Lee K, Shi X, Scott DA, Song J, Pan JQ, Weissleder R, Lee H, Zhang F, Sharp PA. 2015. Genome-wide CRISPR screen in a mouse model of tumor growth and metastasis. *Cell* 160:1246.
 70. Huang DW, Sherman BT, Lempicki RA. 2009. Systematic and integrative analysis of large gene lists using DAVID bioinformatics resources. *Nat Protoc* 4:44–57.

CHAPTER 3: TGF β PRIMES ALVEOLAR-LIKE
MACROPHAGES TO INDUCE TYPE I IFN FOLLOWING
TLR2 ACTIVATION

PUBLICATION NOTICE

The following chapter contains work done in collaboration with Joshua Obar at Dartmouth College and is currently in preparation for publication. Authors of this work are: Sean Thomas^{1*}, Laurisa Ankley^{1*}, Kayla Conner¹, Alex Rapp², Chris Tanner², Abigail McGee², Joshua Obar², Andrew Olive¹. * indicates that these authors contributed equally to this work. ¹ Indicates contributors from the Department of Microbiology and Molecular Genetics, College of Osteopathic Medicine, Michigan State University. ² indicates contributors from the Department of Microbiology and Immunology, Geisel School of Medicine at Dartmouth.

In this work, data from Figures 3.1 and 3.2 were collected and analyzed by LA and KC. Figure 3.3 was completed by ST, LA, and KC. Figure 3.4 was completed by ST. Figure 3.5 was completed by ST, AR, CT, and AM.

ABSTRACT

Alveolar macrophages (AMs) are key mediators of lung function and are potential targets for therapies during respiratory infections. The cytokine TGF β is an important regulator of AM maintenance but, how TGF β directly modulates the innate immune responses of AMs remains unclear. This shortcoming prevents effective targeting of AMs to improve lung function in health and disease. Here we leveraged an optimized *ex vivo* AM model system, fetal-liver derived alveolar-like macrophages (FLAMs), to dissect the role of TGF β in AMs. Using transcriptional analysis, we globally defined how TGF β regulates gene expression of resting FLAMs. We found that TGF β maintains the baseline metabolic state of AMs by driving lipid metabolism and restricting inflammation. To better understand inflammatory regulation in FLAMs, we directly tested how TGF β alters the response to the TLR2 agonist PAM3CSK4. While both TGF β (+) and TGF β (-) FLAMs robustly responded to TLR2 activation we found an unexpected activation of type I interferon (IFN) responses only in TGF β (+) FLAMs. Follow up studies found that several TLR2 activators, including *Mycobacterium tuberculosis* infection, drive robust type I IFN responses in FLAMs and primary AMs in a TGF β dependent manner. Further examination of the pathways driving this IFN response determined that the mitochondrial antiviral signaling protein and the interferon regulator factors 3 and 7 were required for IFN production. In contrast, we observed a limited role for aerobic glycolysis in driving IFNs. Together, these data suggest that TGF β modulates AM metabolic networks and innate immune signaling cascades to control inflammatory pathways in AMs.

INTRODUCTION

The pulmonary space is a specialized environment evolved to facilitate gas exchange and maintain lung function (1, 2). To protect against exposures to airborne microorganisms and particulates, lung alveoli contain a specialized phagocyte population, alveolar macrophages (AMs) (2, 3). These AMs, like many other tissue-resident macrophages, seed the lungs from the fetal liver and serve two primary purposes: to preserve lung homeostasis by maintaining optimal surfactant levels in the lungs and to patrol the alveolar space for inhaled debris, initiating an inflammatory response when necessary (4-6). Given the importance of maintaining pulmonary function, AMs must strictly regulate their inflammatory responses to prevent unnecessary inflammation and tissue damage (7, 8). Compared to other inflammatory macrophages, including bone marrow-derived macrophages (BMDMs), AMs are more hypo-inflammatory against many pathogenic stimuli, a characteristic that is mediated by their distinct ontogeny and the lung environment (8-10). In fact, circulating monocytes that are recruited to the lungs following infection have been shown to adapt to the local environment and take on AM-like phenotypes (11). Two key cytokines, GM-CSF and TGF β , are known to mediate AM functions in the lung environment (6, 12, 13). While the role of GM-CSF is better understood due to its importance in preventing pulmonary alveolar proteinosis, how TGF β directly modulates the AM state and function remains unclear, limiting our ability to target AMs and improve lung function in health and disease.

TGF β exists as three separate isoforms (TGF β 1-3) that all bind to the same TGF β coreceptors (TGF β RI, TGF β RII) (14). TGF β -1 is primarily produced by

macrophages, but in an inactive form, conjugated with a latency-associated peptide (LAP) (15-17). Inactive TGF β 1 (referred to as TGF β from here on) is activated following enzymatic, acidic, or receptor-mediated cleavage of the LAP from TGF β (17, 18). In the lungs, inactive TGF β is primarily produced by AMs which is then activated by the alveolar epithelial type II cells (AECII) through the activity of the α v β 6 integrin on alveolar epithelial cells (6, 17). Thus, maintaining AMs requires unique interactions between the lung epithelium and disruptions of this environment results in dysregulated pulmonary responses.

In its active form, TGF β is a versatile cytokine that triggers Smad complex translocation to the nucleus to drive a multitude of processes, including stem cell differentiation, chemotaxis, and immune regulation, depending on the context in which it is acting (19, 20). Much of this heterogeneity in cellular responses to TGF β is thought to be due to crosstalk between other transcriptional regulators and epigenetic regulation (21). In the lungs, TGF β plays critical roles both in lung development and disease. Mice lacking any of the three isoforms of TGF β or either of the two receptors have varying degrees of deformed lung structure and alveologenesis due to dysregulated interactions between the lung epithelium and mesenchyme during development (22-25). TGF β is also implicated in the development of idiopathic pulmonary fibrosis (IPF) through its induction of myofibroblast differentiation from lung fibroblasts and suppression of anti-fibrotic factors prostaglandin E2 and hepatocyte growth factor production (26-28). Given the importance of TGF β to maintain AMs in the lungs it is essential to better understand how TGF β modulates the inflammatory potential of AMs.

Fully dissecting the role of TGF β in AM regulation requires *ex vivo* models that faithfully recapitulate key aspects of the lung environment. Recent work by several groups showed that growth of macrophages in both GM-CSF and TGF β stabilizes the AM-like state for cells grown in culture (29-31). We recently optimized the fetal liver-derived alveolar-like macrophages (FLAMs) model which propagates fetal liver cells in both GM-CSF and TGF β allowing for long-term propagation and genetic manipulation of cells that recapitulate many aspects of AM functions (31). Removing TGF β from these cells results in a loss of the AM-like state such as decreased expression of the key AM transcription factor peroxisome-proliferating activating receptor gamma (PPAR γ) and increased expression of the LPS co-receptor CD14. These data suggest that TGF β not only maintains the AM state but plays an important role in modulating the inflammatory response of AMs.

In this report we directly examine how TGF β shapes AM function and inflammatory responses. Using transcriptional analysis, we globally defined how TGF β regulates the gene expression of resting FLAMs, identifying a key role of TGF β in maintaining the metabolic state of AMs. In parallel, we characterized how TGF β shapes the inflammatory response of AMs following the activation of toll-like receptor 2 (TLR2), uncovering an unexpected link between TGF β , TLR2, and type I interferon (IFN). We found that a range of TLR2 agonists, including *Mycobacterium tuberculosis*, drive exacerbated IFN responses in a TGF β -dependent manner. Further mechanistic studies found this IFN response was not dependent on glycolysis and required the mitochondrial antiviral signaling adaptor (MAVS) as well as the transcription factors interferon regulatory factor 3 and 7 (IRF3/7). These data suggest that TGF β rewires the

metabolic networks in AMs and this activates unique innate immune signaling not observed in other macrophage populations.

RESULTS

TGF β drives lipid metabolism, restrains cytokine expression, and maintains FLAMs in the AM-like state.

We previously developed FLAMs as an *ex vivo* model of AMs to understand the mechanistic signals and regulatory networks that maintain cells in the AM-like state (31). TGF β is a key cytokine needed to maintain AMs *in vivo* and to maintain FLAMs in the AM-like state, yet how TGF β modulates AM functions and transcriptional networks remains unclear. As a first step, we confirmed that TGF β is required to broadly maintain the AM-like state in FLAMs. Since PPAR γ is a key transcription factor in AMs, and is expressed in AMs and FLAMs, we measured the effect of TGF β on PPAR γ expression (**Figure 3.1A**) (31). FLAMs were grown in GM-CSF in the presence or absence of TGF β for two-weeks and the mRNA expression of the transcription factor PPAR γ was quantified by quantitative RT-PCR. As expected, FLAMs with TGF β maintained higher expression of PPAR γ , while cells grown in the absence of TGF β significantly decreased PPAR γ expression (6, 31). These data confirm that TGF β helps maintain FLAMs in an AM-like state long-term.

To better understand how TGF β globally regulates FLAMs, we next conducted whole-transcriptome RNA sequencing analysis on FLAMs grown in the presence and absence of TGF β . Differential expression analysis identified hundreds of genes that were significantly changed between FLAMs grown with or without TGF β (**Figure 3.1B**).

To globally identify pathways that were uniquely enriched in TGF β (+) FLAMs, we employed gene set enrichment analysis (GSEA), using a ranked gene list generated from the differential expression analysis. Among the top KEGG pathways enriched in TGF β (+) FLAMs were PPAR signaling, fatty acid synthesis, lipid metabolism, and lysosome pathways (**Figure 3.1C**). Given that AMs are known to drive PPAR γ -dependent lipid metabolism, these data suggest the FLAM transcriptional profile is similar to primary AMs (32, 33). In contrast, pathways enriched in TGF β (-) FLAMs were related to cytokine and chemokine expression and cell proliferation. We directly compared the expression of a subset of genes related to these pathways and AM signature genes (**Figure 3.1C**). We found high expression of PPAR γ , MARCO, SiglecF in TGF β (+) FLAMs in addition to lipid metabolism genes including Acat2, Acat3, and FadS2 (Figure 1D). In TGF β (-) FLAMs, we observed a significant increase in chemokines including CCL2, CCL3, CCL4 and CXCL3 (Figure 1D). Taken together these data show that TGF β maintains metabolic functions of AMs while restraining inflammation in line with previous reports suggesting AMs are hypo-inflammatory (8).

TGF β mediates a type 1 IFN in AMs following Pam3 Activation.

Since TGF β (+) FLAMs did not express inflammatory genes as highly as TGF β (-) FLAMs, we next directly tested the response of these cells to inflammatory stimuli. Many bacterial respiratory infections, including *Mycobacterium tuberculosis*, activate TLR2 signaling during infection (34, 35). Thus, we examined how the activation of TLR2 with the purified agonist Pam3CSK4 (referred to as Pam3) differentially alters the transcriptome of FLAMs in a TGF β -dependent manner. TGF β (+) and TGF β (-) FLAMs

were stimulated with Pam3 for 18 hours, then, RNA sequencing and differential expression analysis was used to identify changes in the transcriptional landscape. We identified hundreds of genes that were significantly altered following Pam3 activation of TGF β (+) FLAMs compared to untreated TGF β (+) FLAMs (**Figure 3.2A**) and Pam3 activated TGF β (-) FLAMs (**Figure 3.2B**). We were curious as to what pathways were enriched in TGF β (+) FLAMs compared to following PAM activation to identify TGF β - dependent and perhaps, AM-specific immune signaling (**Figure 3.2A**). Using GSEA we found an unexpected enrichment in pathways related to IFN signaling (**Figure 3.2C**). When we examined the entire IFN hallmark pathway across all conditions we only observed robust induction of IFN-related genes in Pam3 activated TGF β (+) FLAMs (**Figure 3.2D**). This finding suggests that while TGF β restrains several inflammatory cytokines following Pam3 stimulation, TGF β skews the macrophages response to drive the activation of IFN pathways.

To further understand the role of nucleotide sensing in the TLR2 response of TGF β (+) FLAMs, we next directly examined the normalized reads of IFN β and two other interferon-stimulated genes (ISGs) (**Figure 3.3A**). While we observed similar baseline expression of IFN β 1, CXCL10 and Rsad2 between conditions, TGF β (+) FLAMs induced significantly higher expression of all three genes following Pam3 activation. To corroborate the RNA sequencing results, we compared the secretion of cytokines in resting and Pam3-activated TGF β (+) and TGF β (-) FLAMs using a multiplex Luminex assay (**Figure 3.3B**). In agreement with our transcriptional results, we observed a significant increase in IFN β 1 and CXCL10 in Pam3-activated TGF β (+) FLAMs compared to TGF β (-) FLAMs. We next confirmed this phenotype occurs in

primary AMs by isolating cells from the lungs and activating them with Pam3 and examining the production of IFN β by ELISA (**Figure 3.3C**). In line with our results in FLAMs, we observed a significant increase in IFN β in AMs following activation with Pam3. These data confirm that TGF β signaling in AMs drives the production of type I IFN following Pam3 stimulation.

TGF β mediates TLR2-dependent type 1 IFN activation in AMs.

Pam3 is a potent TLR2 agonist, so we hypothesized that other TLR2 activators would similarly drive the production of type I IFNs in TGF β (+) FLAMs. To test this, we stimulated TGF β (-) and TGF β (+) cells with the known TLR2 activators Peptidoglycan and Zymosan. Since Zymosan can activate cells through both TLR2 and Dectin1, we also tested depleted Zymosan and curdlan that will only activate cells through Dectin1. 18 hours after activation with each agonist, we measured the CXCL10 by ELISA as a marker for IFN production (**Figure 3.4A**). We observed that both Peptidoglycan and Zymosan stimulations of TGF β (+) FLAMs resulted in a significant increase in CXCL10 production compared to TGF β (-) FLAMs. However, we observed no significant induction of CXCL10 following activation with depleted Zymosan or curdlan. We next infected TGF β (-) and TGF β (+) FLAMs with *Mycobacterium tuberculosis*, a known activator of TLR2, and quantified the production of IFN β (**Figure 3.4B**) and CXCL10 (**Figure 3.4C**) using a multiplex Luminex assay the following day (35). We found that infection of TGF β (+) FLAMs resulted in a significant increase in both IFN β and CXCL10 compared to TGF β (-) FLAMs.

Since our results suggested that TLR2-dependent activation drives the increased IFN response in TGF β (+) FLAMs, we next directly tested this using TLR2^{-/-} FLAMs. Wild type and TLR2^{-/-} TGF β (+) FLAMs were stimulated with Pam3 and the following day IFN β was quantified in the supernatants by ELISA. While wild type TGF β (+) FLAMs robustly induced IFN β , this was lost in TLR2^{-/-} FLAMs. Taken together these results suggest that TGF β signaling in FLAMs drives a unique response to TLR2 activation that results in the production of type I IFN.

MAVS and IRF3/7 but not aerobic glycolysis contribute to TGF β -dependent Type I IFN responses.

We next wanted to better understand the pathways driving the TGF β -dependent type I IFN response. One key type I IFN production pathway is mediated by the mitochondrial antiviral-signaling protein (MAVS) which triggers the activation of the transcription factors interferon regulatory factors 3 and 7 (Irf3/Irf7) to mediate the transcription of IFN β (36, 37). To test the role of these genes in controlling TGF β -dependent IFN responses, we used our previously described CRISPR-Cas9 editing approaches in FLAMs to target *Mavs*, *Irf3* and *Irf7* with individual sgRNAs (**Figure 5A**) (31). We then left cells untreated or stimulated TGF β (+) wild type, TLR2^{-/-}, sgMAVs, sgIrf3, and sgIrf7 FLAMs with zymosan, depleted zymosan, or LyoVec-complexed Poly I:C and quantified secreted IFN β the following day. We observed that wildtype FLAMs induced IFN β in all conditions, except following depleted zymosan stimulation. In contrast, for all stimulations, we found significantly reduced IFN β from sgMAVs, sgIrf3,

and sglrf7 FLAMs. These data suggest that TGF β -dependent, TLR2-mediated type I IFN responses are controlled by MAVS and Irf3/Irf7.

A previous report showed that MAVS signaling is regulated by lactate produced through glycolysis (38). Given the expression differences in key metabolic pathways we observed between TGF β - and TGF β (+) FLAMs, we wondered whether differential metabolic regulation of MAVS may explain differences in the type I IFN response. As a first step, we tested whether direct activation of the MAVS pathway with poly I:C would result in differential type I IFN between TGF β (+) and TGF β (-) FLAMs (**Figure 3.5B**). We observed that TGF β (+) FLAMs induced significantly more CXCL10 compared to TGF β (-) FLAMs, suggesting increased activity of the RIG-I/MAVS signaling pathway. We next tested whether inhibiting lactate dehydrogenase and thus, reducing intracellular lactate levels would alter the TGF β -dependent type I IFN response in FLAMs. FLAMs grown with and without TGF β were transfected with poly I:C with increasing levels of Oxamate and the following day we quantified CXCL10 in the supernatants (**Figure 3.5C**). We observed a dose-dependent decrease in CXCL10 production in TGF β (-) FLAMs suggesting the IFN response in these cells is dependent on aerobic glycolysis. In contrast, we observed no significant effect of oxamate on the high CXCL10 production found in TGF β (+) FLAMs. Taken together these data suggest that TGF β -dependent type I IFN responses in FLAMs is independent of changes in aerobic glycolysis.

DISCUSSION

TGF β signaling is essential for alveolar macrophage (AM) development and homeostasis in the lung environment (6). How TGF β regulates distinct functions of AMs and their response to external stimuli remains unclear. Here, we leveraged an *ex vivo* model of AMs, known as FLAMs, to dissect transcriptional changes in AM-like cells that are mediated by TGF β . We found that while TGF β restrains a subset of inflammatory pathways, TGF β also primes AMs for a type I IFN (IFN) response following TLR2 activation. These results suggest that distinct innate immune signaling networks in AMs are regulated by the tissue environment and directly alter the inflammatory response following the activation of TLR2.

While our findings suggest an unexpected link between TLR2 and IFN in AMs, how TLR2 activates IFN remains an open question. Several pattern recognition receptors (PRRs), including TLR3, TLR7 and TLR9 activate IFNs through the activation of IRF3 or IRF7, but these PRRs are localized to the endosome and generally respond to viral ligands (39, 40). In contrast, TLR2 is present on both the surface and in the endosome, similar to TLR4. Previous studies showed that TLR4 signaling through the plasma membrane drives Myd88-dependent NF κ B activation while signaling through the endosome activates a TRIF dependent IFN response (41). Whether the localization of TLR2 drives the IFN response in TGF β cultured AMs and the contribution of the adaptors, Myd88 and TRIF, to the response will need to be determined. While several previous studies suggest TLR2 can activate IFNs, the ligands and cell types capable of this response remain controversial (42-45). For example, Barbalat et al showed BMDMs can make IFN in response to viral ligands but not bacterial ligands, while Dietrich et al.

showed BMDMs can make IFN following activation with bacterial ligands (43, 44). Our data support the role of bacterial and fungal TLR2 ligands in activating an IFN response in AMs that is dependent on TGF β signaling. FLAMs grown in the absence of TGF β did not robustly induce IFNs following TLR2 activation. Our genetic studies found that IRF3, IRF7, and MAVS were all required for the TLR2-activated IFN response. This suggests TLR2-mediated IFN may activate parallel pathways, one dependent on direct signaling through MyD88/TRIF, and a second dependent on the cytosolic nucleotide sensing pathways dependent on MAVS. Given that we observed exacerbated IFN responses in TGF β (+) FLAMs following direct activation of MAVS by poly I:C treatment, our data support a model where TGF β primes AMs to enhance the activation of MAVS-dependent IFN production.

The mechanisms underlying TGF β priming IFN responses remain unknown. TGF β is known to activate PPAR γ and fatty acid oxidation, which we confirmed through our transcriptional analysis (6). Previous studies have linked cellular metabolism and type I IFN production. Both cholesterol biosynthesis and glycolysis byproducts such as lactate are known to regulate the magnitude of the type I IFN response in BMDMs (38, 46). However, when lactate levels were modulated with the pyruvate dehydrogenase inhibitor oxamate, we observed no changes in the TGF β -dependent IFN response. Thus, lactate is not directly modulating the IFN response in our model. Given the increased fatty acid oxidation and mitochondrial function in TGF β cultured FLAMs, it is possible that TGF β -dependent changes in lipid metabolism and mitochondrial function directly drive subsequent IFN responses following TLR2 activation. Since we observed increased activation of MAVS-dependent IFN production following TLR2 stimulation in

the absence of exogenous cytosolic nucleotides, this suggests the possibility of endogenous cellular ligands such as mitochondrial DNA amplifying the TLR2 response in AMs (47). How changes in mitochondrial dynamics or possibly mitochondrial ROS generation contribute to the production of IFN β remains unknown. Future studies will be needed to dissect the role of fatty acid oxidation, oxidative respiration, and mitochondrial damage in driving TLR2-mediated TGF β -dependent IFN responses in AMs.

Our finding that AMs are uniquely programmed by TGF β to drive an IFN response suggests that these specialized resident macrophages differentially activate their inflammatory profiles in the lung environment compared to other macrophages. Understanding the consequences of an IFN-skewed response in the lungs is an important line of research for future studies. Type I IFNs are known to be potent regulators of antiviral immunity, suggesting the host response in the lungs is particularly tuned to respond to invading viral pathogens (37). However, IFNs also play a key role in controlling fungal pathogens like *Aspergillus fumigatus* in humans and in mice (48). In several disease states however, including Systemic Lupus Erythematosus (SLE) and tuberculosis, elevated type I IFNs are associated with worse disease, and blocking type I IFN has been shown to improve clinical outcomes (49-51). Our data support the role of type I IFNs as a key initial response to invading pathogens in the lungs and more broadly suggests the balance of type I IFNs can mediate protective or pathologic host responses.

Interestingly, TGF β is produced in an inactive form by AMs in the lungs and it is processed into an active form by integrins on lung epithelial cells which then signal back

to AMs to maintain their function (6, 17, 18). This interconnected signaling ensures that AMs are properly tuned to the airspace and suggests the lung environment is an important mediator of the enhanced type I response observed in AMs. Better understanding the underlying mechanisms driving TGF β -dependent type I IFN may enable the development of therapeutics that modulate the balance of type I IFNs more effectively in the lungs to control infections and prevent autoinflammatory diseases.

METHODS

Animals

Experimental protocols were approved by the Institutional Animal Care and Use Committee at Michigan State University (animal use form [AUF] no.

PROTO202200127). All protocols were strictly adhered to throughout the entire study.

Six- to 8-wk-old C57BL/6 mice (catalog no. 000664), TLR2^{-/-} mice (catalog no. 004650) and Cas9⁽⁺⁾ mice (catalog no. 026179) were obtained from The Jackson Laboratory (Bar Harbor, ME). Mice were given free access to food and water under controlled conditions (humidity, 40–55%; lighting, 12-hour light/12-hour dark cycles; and temperature, 24 \pm 2°C), as described previously (Bates 2002, 2015). Pregnant dams at 8–10 week of age and 14–18 gestational days were euthanized to obtain murine fetuses. AMs were isolated from male and female mice >10 week of age.

FLAM cell culture

Wild type and TLR2^{-/-} FLAMs were isolated as previously described (31) cultured in complete RPMI (Thermo Fisher Scientific) containing 10% FBS (R&D Systems), 1%

penicillin-streptomycin (Thermo Fisher Scientific), 30 ng/ml recombinant mouse GM-CSF (PeproTech), and 20 ng/ml recombinant human TGF β 1 (PeproTech) included where indicated. Media were refreshed every 2–3 d. When cells reached 70–90% confluency, they were lifted by incubating for 10 min with 37°C PBS containing 10 mM EDTA, followed by gentle scraping.

AM isolation and culture

Mice were euthanized by CO₂ exposure followed by exsanguination via the inferior vena cava. Lungs were lavaged as previously described (Busch, 2019). Cells were then resuspended in RPMI 1640 media containing 30 ng/ml GM-CSF and 20 ng/ml recombinant human TGF β 1 (PeproTech) and plated in untreated 48- or 24-well plates. AMs were lifted from plates using Accutase (BioLegend) and seeded for experiments.

TLR2 activation

Cells were seeded in 24-well treated culture plates at a density of 150,000 cells/well and allowed to settle overnight. Cells were treated with Pam3CSK4 25ng/ml (Invivogen, Cat no. tlr1-pms), peptidoglycan from *S. aureus* at 50ug/ml (Invivogen, cat no. tlr1-pgns2), zymosan at 50ug/ml (Invivogen, Cat no. tlr1-zyn), Zymosan Depleted at 50ug/ml (Invivogen, Cat no. tlr1-zyd), Curdlan at 50ug/ml (Invivogen, Cat no. tlr1-curd) or poly I:C at 20ug/mL (Invivogen, Cat no. tlr1-pic-5). Poly I:C was complexed with Lyovec for transfection prior to stimulation.

Cytokine analysis

Where indicated, supernatants were analyzed by a Luminex multiplex assay (Eve Technology). In addition, secreted CXCL10 was quantified using the R&D Duoset kit (R&D Sciences) per manufacturer's instructions. Secreted IFN β was quantified with the LumiKine Xpress mIFN-B 2.0 kit (Invivogen, catalog no luex-mIFN β v2) per manufacturer's instructions. Luminescent signal was detected on a Spark $\text{\textcircled{R}}$ multimode microplate reader (Tecan).

Mtb culture and infection

FLAMs were seeded at 200,000 cells/well in a 6 well plate prior to infection. PDIM-positive H36Rv was grown in 7H9 medium containing 10% oleic albumin dextrose catalase growth supplement and 0.05% Tween 80 as done previously (52). To obtain a single cell suspension, samples were centrifuged at 200xg for 5 minutes to remove clumps. Culture density was determined by taking the supernatant from this centrifugation and determining the OD₆₀₀, with the assumption that OD₆₀₀ = 1.0 is equivalent to 3x10⁸ bacteria per ml. Bacteria were added to macrophages for 4 hours then cells were washed with PBS and fresh media was added. 24 hours later, supernatant was removed and sterile filtered for analysis.

qRT PCR

RNA from FLAMs was extracted using the Directzol RNA Extraction Kit (Zymo Research, Cat no. R2072) according to the manufacturer's protocol. Quality was assessed using NANODROP. The One-step Syber Green RT-PCR Kit (Qiagen, Cat no.

210215) reagents were used to amplify the RNA and amplifications were monitored using the QuantStudio3 (ThermoFisher, Cat no. A28567).

PPAR γ FWD: 5'-CTC CAA GAA TAC CAA AGT GCG A -3'

PPAR γ REV: 5'-GTA ATC AGC AAC CAT TGG GTC A -3'

GAPDH FWD: 5'-AGG TCG GTG TGA ACG GAT TTG-3'

GAPDH REV: 5'-TGT AGA CCA TGT AGT TGA GGT CA- 3'

CRISPR-targeted knockouts

Single-guide RNA (sgRNA) cloning sgOpti was a gift from Eric Lander and David Sabatini (Addgene plasmid no. 85681) (53). Individual sgRNAs were cloned as previously described (54). In short, sgRNA targeting sequences were annealed and phosphorylated, then cloned into a dephosphorylated and BsmBI (New England Biolabs) digested sgOpti. sgRNA constructs were then packaged into lentivirus as previously described and used to transduce early passage Cas9⁺ FLAMs. Two days later, transductants were selected with puromycin. After 1 week of selection, cells were validated for SiglecF/CD14 expression and used for experimentation.

sgIRF3-Fwd: CACCGGGCTGGACGAGAGCCGAACG

sgIRF3-Rev: AAACCGTTCGGCTCTCGTCCAGCCC

sgIRF7-Fwd: CACCGCTTGCGCCAAGACAATTCAG

sgIRF7-Rev: AAACCTGAATTGTCTTGGCGCAAGC

sgMAVS-Fwd: CACCGGAGGACAAACCTCTTGTCTG

sgMAVS-Rev: AAACCAGACAAGAGGTTTGTCTCC

RNAseq

FLAMs grown with and without the presence of TGF β were seeded in 6-well plates at 1×10^6 cells/well and treated with Poly(I:C) or PAM as described above for 6 hours. RNA was extracted from three replicates of each treatment and control group. We used the Direct-zol RNA Extraction Kit (Zymo Research, Cat no. R2072] to extract RNA according to the manufacturer's protocol. Quality was assessed by the MSU Genomics Core using an Agilent 4200 TapeStation System. Samples with an RNA Integrity Number >9 as calculated by TapeStation were selected for RNA sequencing. The Illumina Stranded mRNA Library Prep kit (Illumina, Cat no. 20040534) with IDT for Illumina RNA Unique Dual Index adapters was used for library preparation following the manufacturer's recommendations but using half-volume reactions. Qubit™ dsDNA HS (ThermoFischer Scientific, Cat no. Q32851) and Agilent 4200 TapeStation HS DNA1000 assays (Agilent, Cat no. 5067-5584) were used to ensure quality and quantity of the generated libraries. The libraries were pooled in equimolar amounts, and the Invitrogen Collibri Quantification qPCR kit (Invitrogen, Cat no. A38524100) was used to quantify the pooled library. The pooled library was divided equally and loaded on 2 lanes of a NovaSeq S4 flow cell, and sequencing was performed in a 2x150 bp paired-end format using the NovaSeq 6000 v1.5 100-cycle reagent kit (Illumina, Cat no. 20028316). Base calling was performed with Illumina Real Time Analysis (RTA; Version 3.4.4), and the output of RTA was demultiplexed and converted to the FastQ format with Illumina Bcl2fastq (Version 2.20.0). RNAseq analysis was completed using the MSU High Performance Computing Cluster (HPCC). FastQC (Version 0.11.7) was used to assess read quality prior to downstream analysis. Bowtie2 (Version 2.4.1) (55) with

default settings was used to map reads with the GRCm39 mouse reference genome. Aligned reads counts were assessed using FeatureCounts from the Subread package (Version 2.0.0) (56), producing raw counts tables for each sample. Differential gene expression analysis was conducted using the DESeq2 package (Version 1.36.0) (57) in R (Version 4.2.1).

FIGURES

Figure 3.1. TGF β drives lipid metabolism, restrains cytokine expression, and maintains FLAMs in the AM-like state. **(A)** PPAR γ transcription was quantified by qRT-PCR using $2^{-(DDCT)}$ relative to GAPDH in untreated (+) and (-) TGF β FLAMs. Each point represents a technical replicate from one representative experiment of 3. ** $p < .01$ by unpaired students t-test. **(B)** Differentially expressed genes were identified between untreated (+) and (-) TGF β FLAMs. Red points represent significantly underexpressed genes and blue points represent significantly overexpressed genes between (+) and (-) TGF β FLAMs. Each point represents the mean of three biological replicates from one experiment. DeSeq2 was used to determine significance using the adjusted p-value to account for multiple hypothesis testing. **(C)** Expression of genes from three pathways that are enriched between untreated (+) and (-) TGF β FLAMs and a subset of AM-signature genes. Each column is representative of one technical replicate. **(D)** Gene expression was quantified from normalized counts for key genes important in lipid metabolism, inflammation, and TGF β signaling. Each point represents a technical replicate from one experiment. *** adjusted p-value $< .001$ using DeSeq2 analysis.

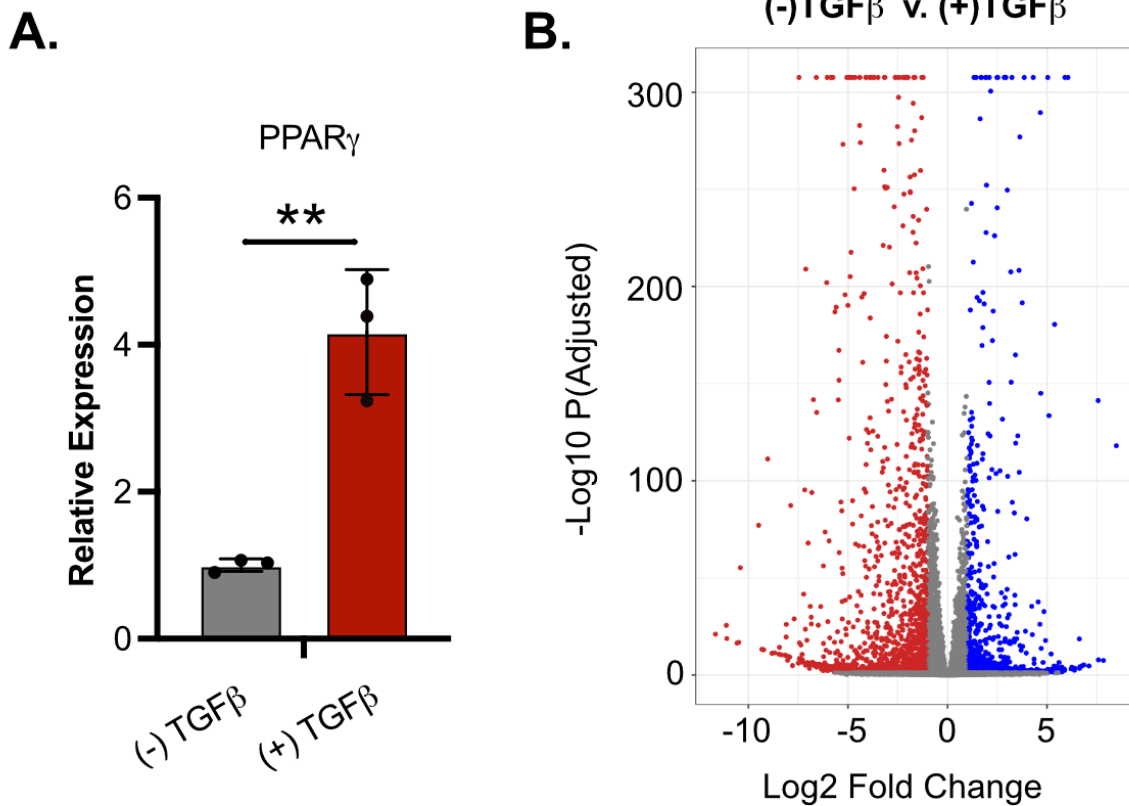


Figure 3.1 (cont'd)

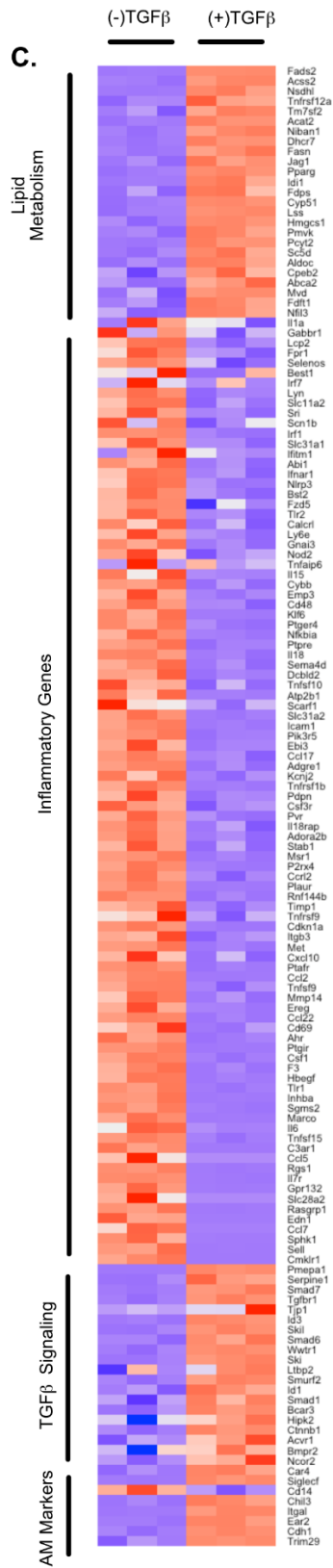


Figure 3.1 (cont'd)

D.

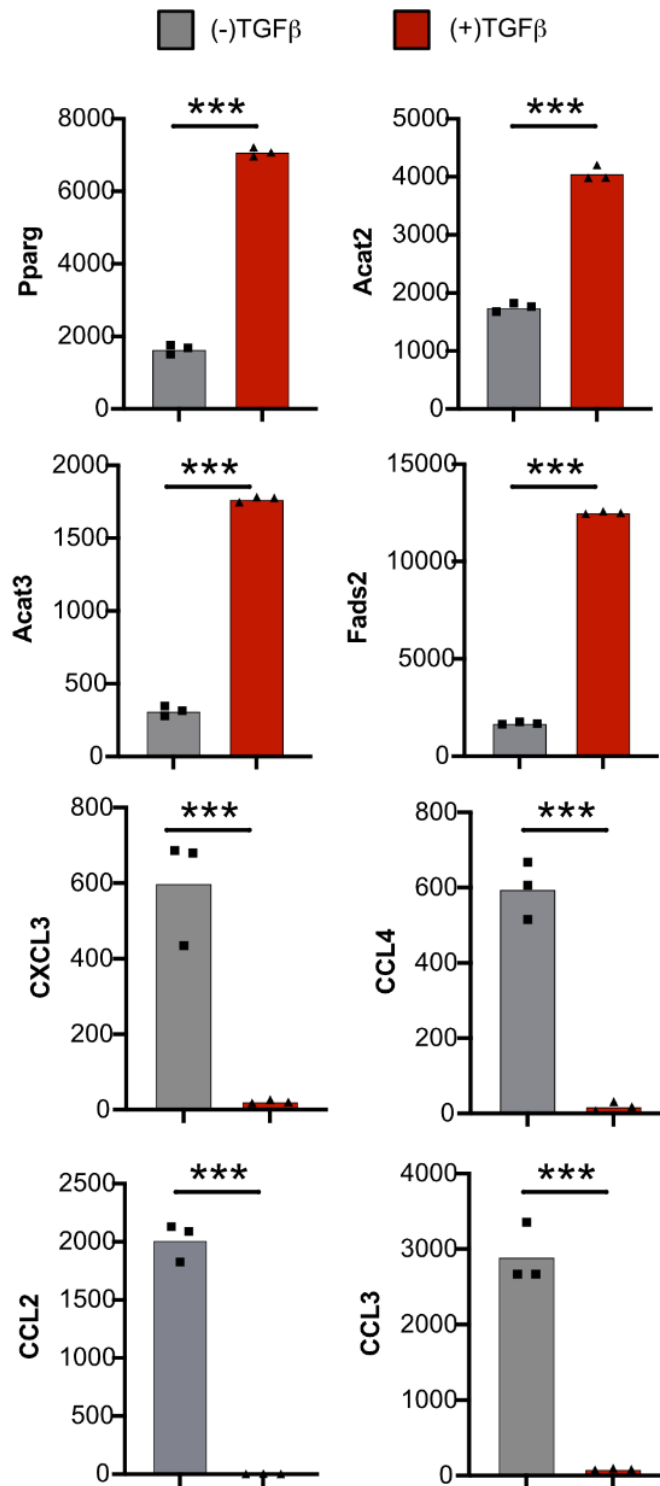


Figure 3.2. TGF β mediates cytosolic DNA sensing and type 1 IFN responses during TLR2 activation. (A) Differentially expressed genes were identified between +TGF β FLAMs (+) and (-) Pam3 treated for 6 hours. Red points represent underexpressed genes and blue points represent overexpressed genes between (+) and (-) TGF β FLAMs. Each point represents the mean of three biological replicates from one experiment. **(B)** Differentially expressed genes were identified between (+) and (-) TGF β FLAMs treated with Pam3 for 6 hours. Red points represent underexpressed genes and blue points represent overexpressed genes between (+) and (-) TGF β FLAMs. Each point represents the mean of three technical replicates from one experiment. **(C)** Leading edge analysis of the IFN hallmark Pathway comparing Pam3 activation in (+) and (-) TGF β FLAMs **(D)** Expression of genes representing the IFN hallmark pathway between (+) and (-)TGF β FLAMs that have or have not been treated with Pam3. Each column represents a biological replicate from one experiment.

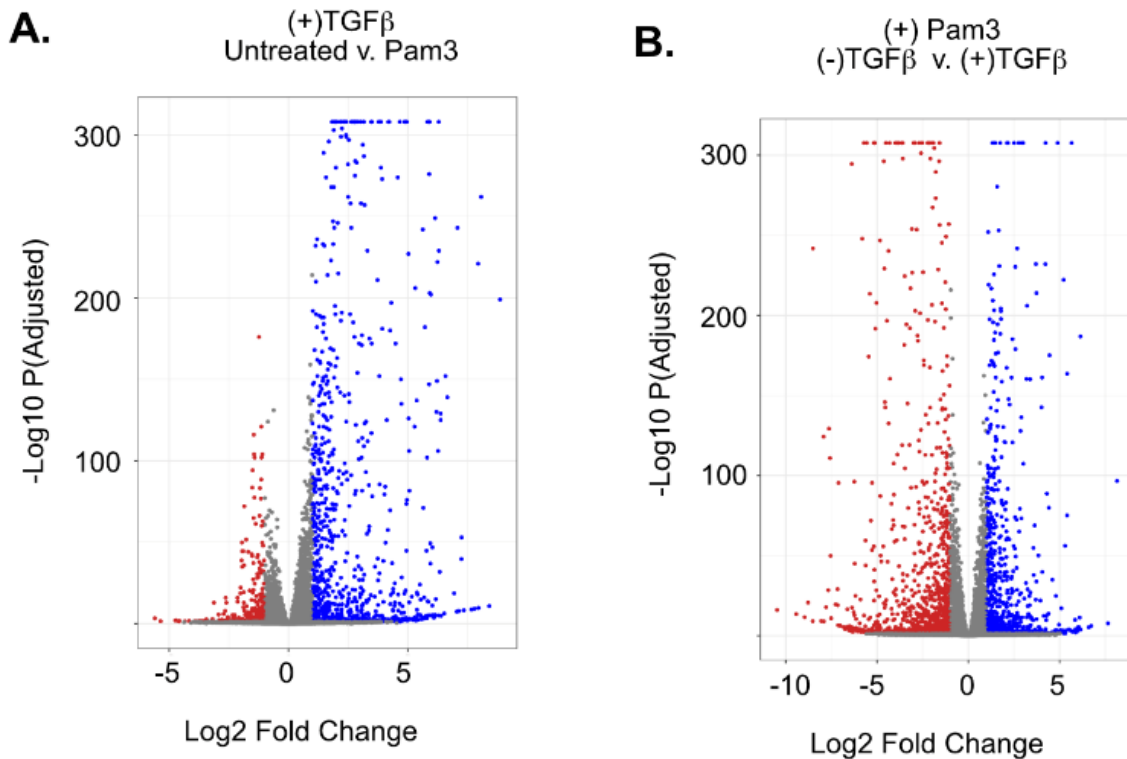


Figure 3.2 (cont'd)

C.

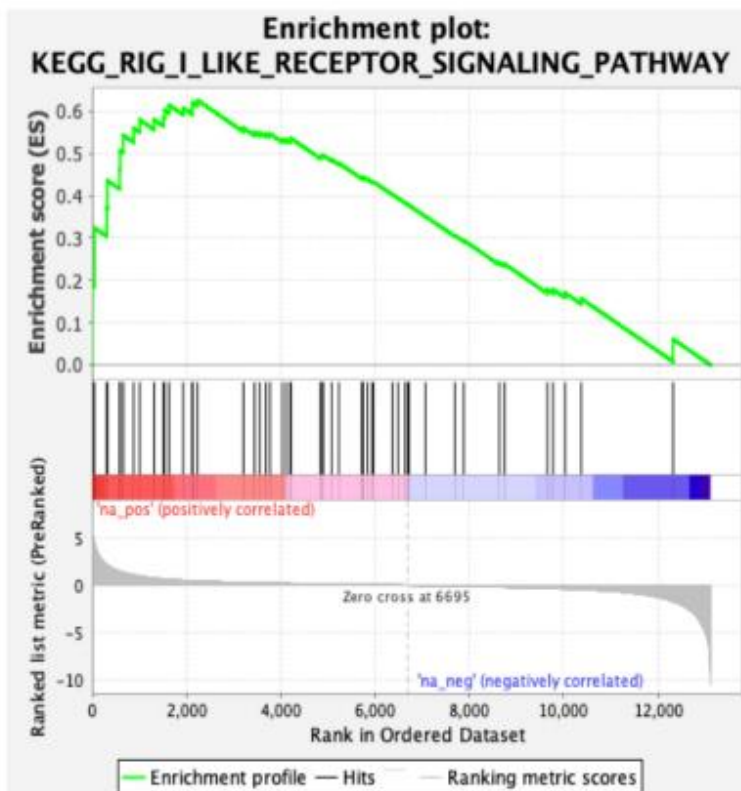


Figure 3.2 (cont'd)

D.

Type I IFN Hallmark Pathway

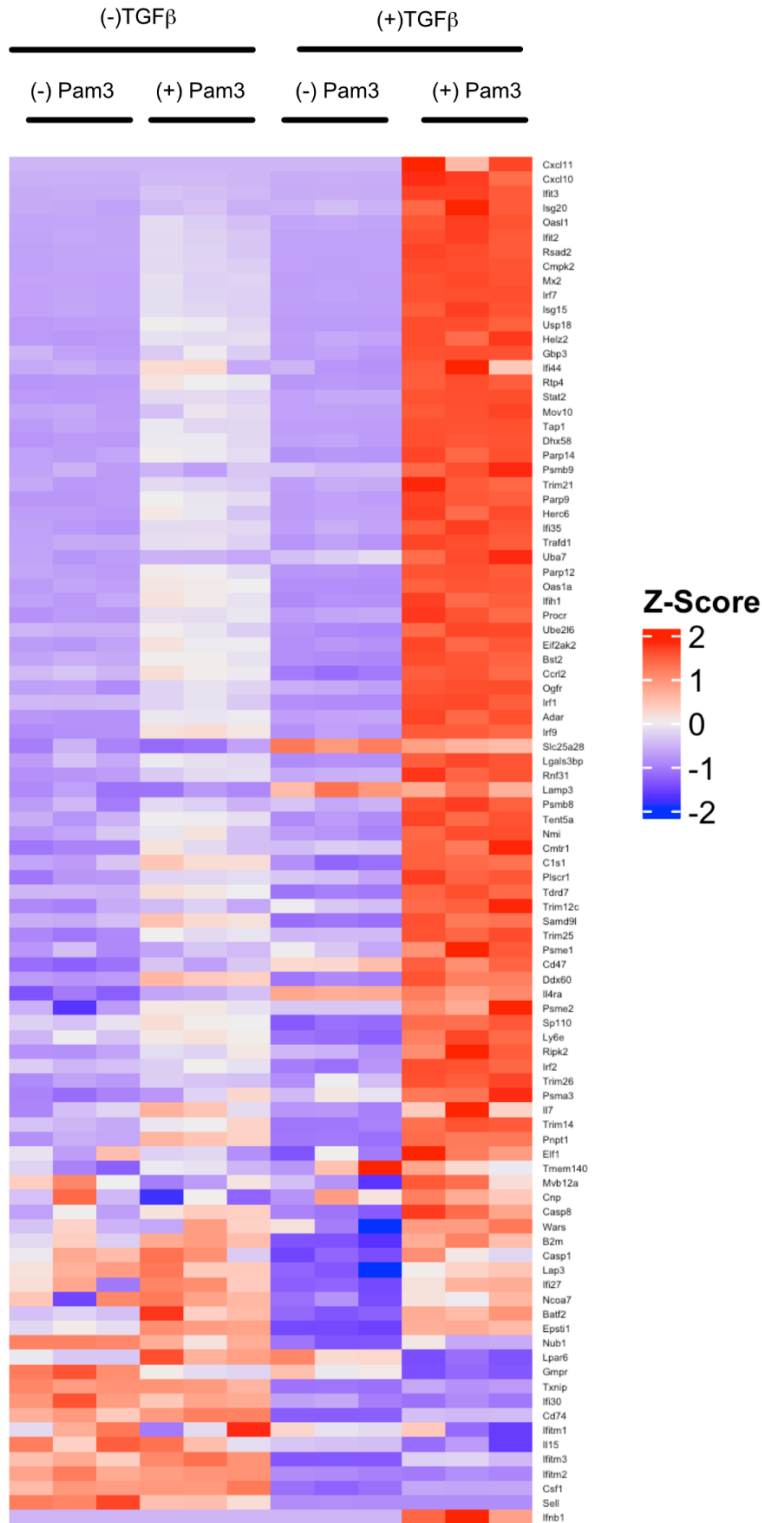


Figure 3.3. IFN β and ISG transcription and secretion is heightened in Pam3-activated AMs and FLAMs cultured with TGF β . (A) Normalized read counts from IFN β , Rsad2 and CXCL10 from Pam3 RNA sequencing experiment. *** adjusted p-value <.001 using DeSeq2 analysis. (B) (+) and (-) TGF β FLAMs were stimulated with Pam3 for 24hrs. Supernatants were collected and IFN β , CXCL10 were quantified by Luminex cytokine assay. (C) Primary AMs were stimulated with Pam3 and IFN β was quantified by bioluminescent ELISA the following day. Shown is one representative experiment of two with 3 replicates per experiment. **p<.01 by unpaired students t-test.

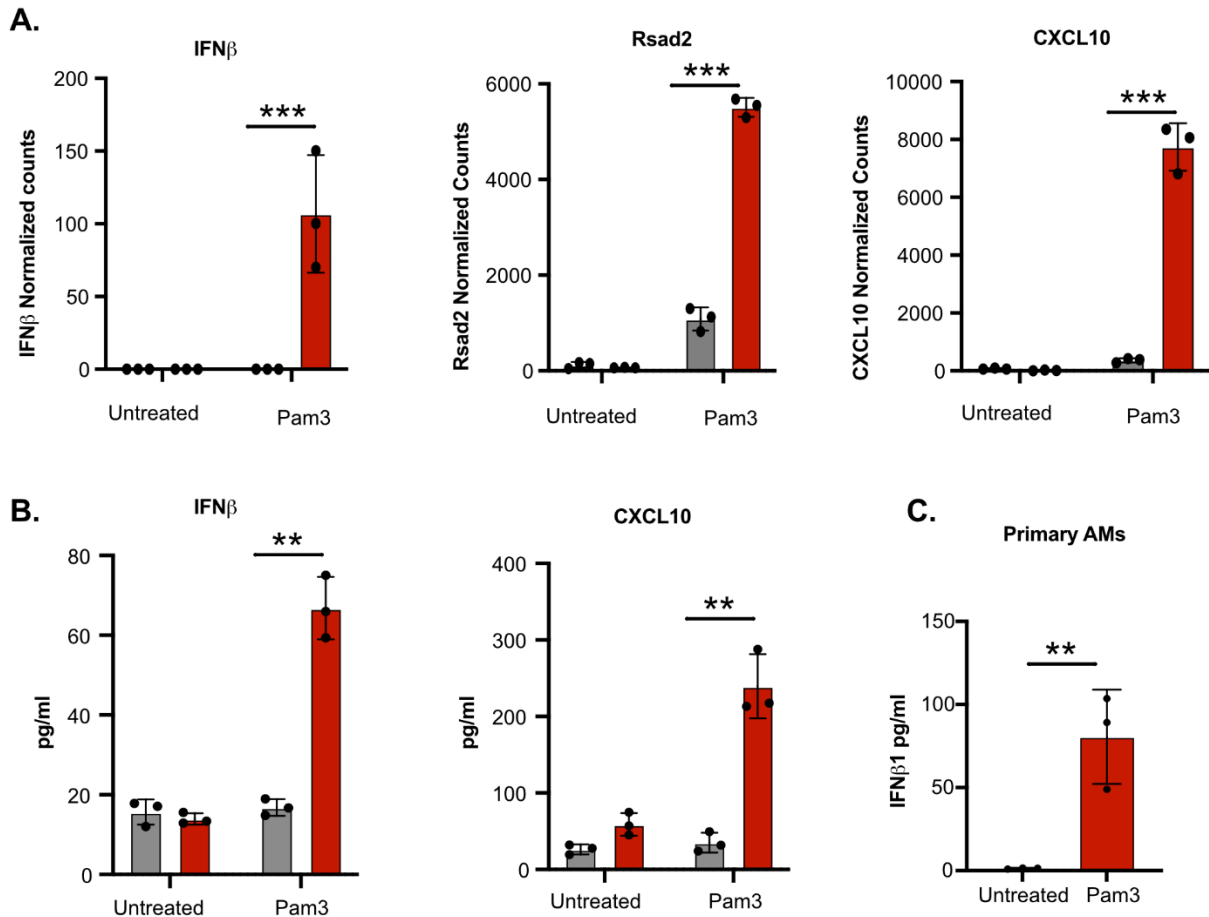


Figure 3.4. TLR2-dependent activation of type 1 IFN pathways in (+) TGFβ FLAMs is conserved among physiologically relevant TLR2 agonists. (A) (+) and (-) TGFβ FLAMs were stimulated with 50ug/ml Peptidoglycan, Zymosan, Zymosan Depleted, or Curdlan for 24hrs. CXCL10 was quantified by ELISA. **(B and C)** (+) and (-) TGFβ FLAMs were left uninfected or infected with Mtb H37Rv at an MOI of 5 for 24hrs. **(B)** IFNβ and **(C)** CXCL10 were quantified by Luminex multiplex assay. **(D)** WT FLAMs, TLR2-/- FLAMs, and Primary AMs were stimulated with Pam3 for 24hrs. Secreted IFNβ was quantified by bioluminescent ELISA. Each point represents data from a single well from one representative experiment of three. ****p<.0001 ** p<.01 by one-way ANOVA with a tukey test for multiple comparisons.

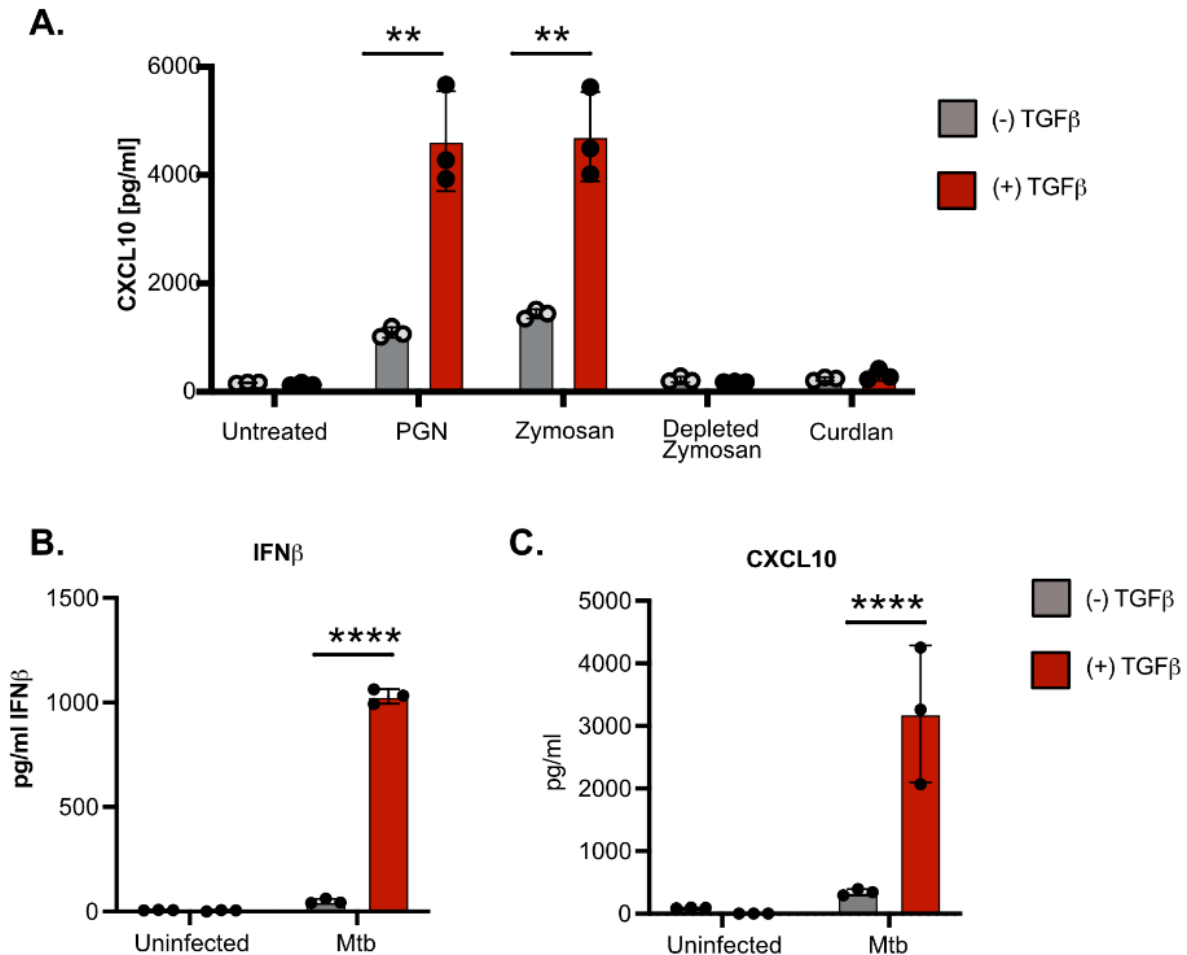


Figure 3.4 (cont'd)

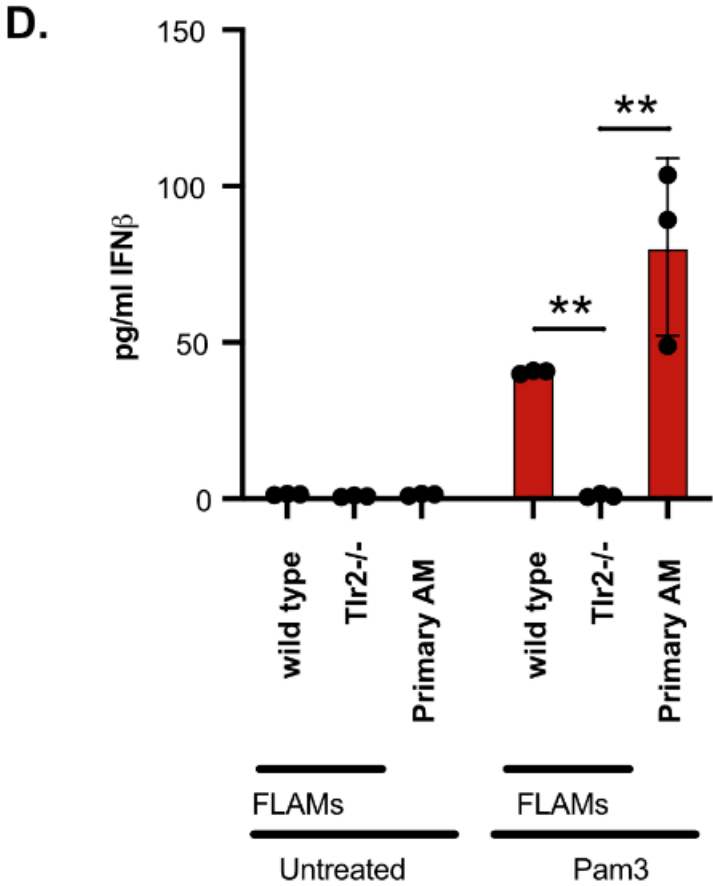


Figure 3.5. MAVS and IRF3/7, but not aerobic glycolysis, contribute to TGF β -dependent Type I IFN responses. (A) Wild type, sgMAVS, sgIRF3, and sgIRF7 FLAMs were stimulated with Zymosan, Zymosan Depleted, and poly I:C for 24hrs. Secreted IFN β was quantified by bioluminescent ELISA. **(B)** (+) and (-) TGF β FLAMs were treated with poly I:C for 24hrs. Secreted CXCL10 was quantified by ELISA. **(C)** (+) and (-) TGF β FLAMs were stimulated with complexed poly I:C and left untreated or treated with Oxamate. Secreted CXCL10 was quantified by ELISA. Each point represents data from a single well from one representative experiment of three. *** $p < .001$, ** $p < .01$ by one-way ANOVA with a tukey test for multiple comparisons.

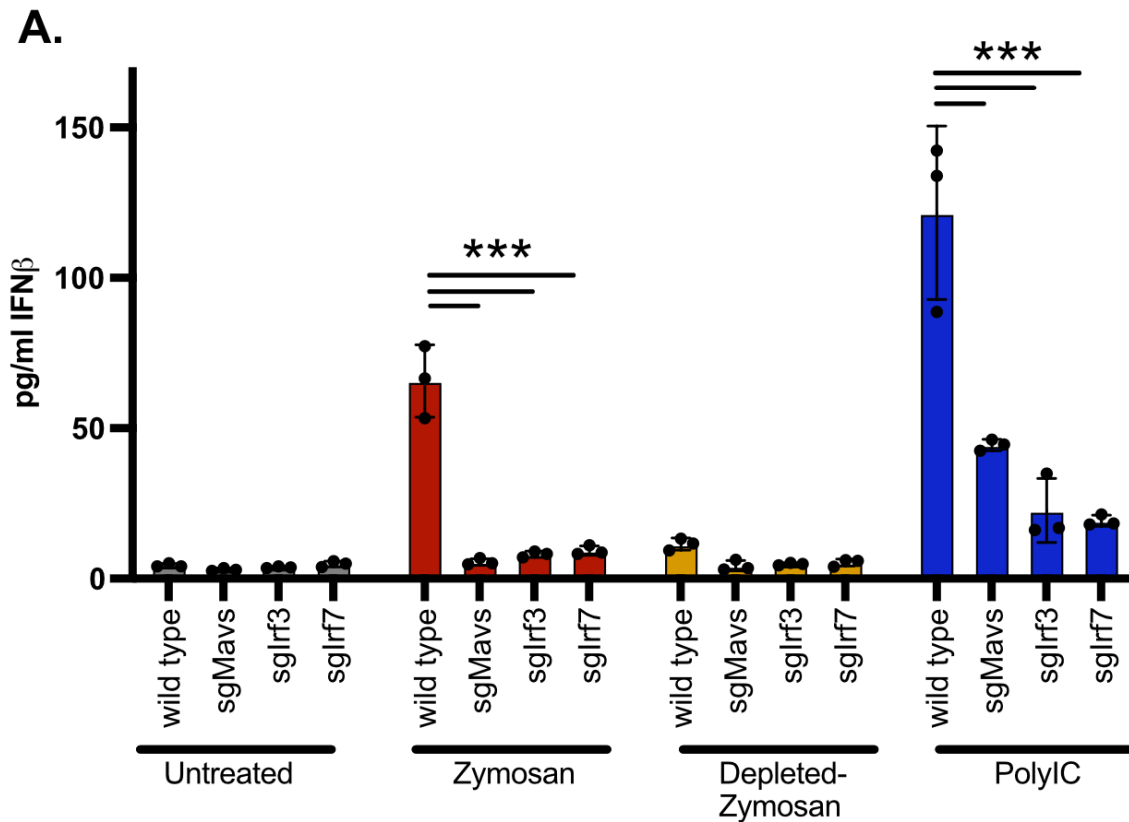
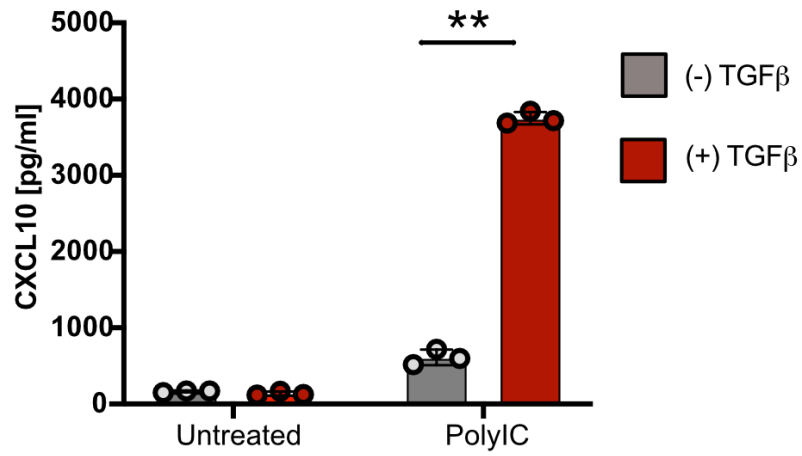
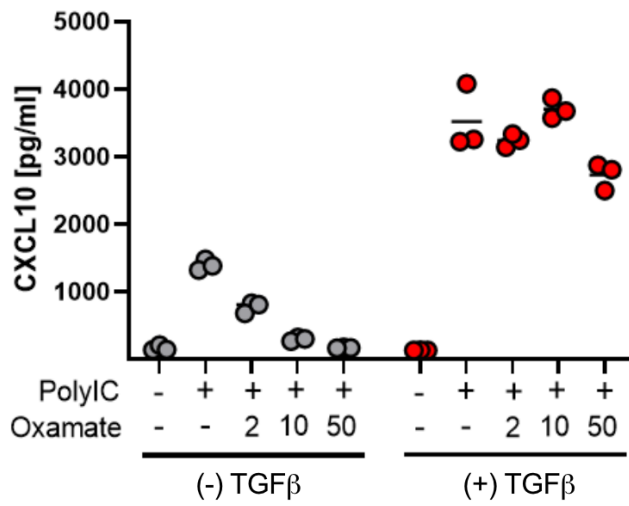


Figure 3.5 (cont'd)

B.



C.



DECLARATIONS

Competing interests

The authors declare that they have no competing interests.

Funding

This work was supported by the National Institutes of Health Grant AI139133 (to JO) and the National Institute of General Medical Sciences Grant GM146795 (to AO).

Contributions

Conceptualization: ST, LA, AR, CT, AM, JO, AO. *Methodology:* ST, LA, KC, AR, CT, AM, JO, AO. *Software:* KC, JO, AO. *Validation:* SMT, KAW, JPP, AJO. *Formal Analysis:* ST, LA, KC, AR, CT, AM, JO, AO. *Investigation:* ST, LA, AR, CT, AM, JO, AO. *Resources:* JO, AO. *Data Curation:* ST, LA, KC, AR, CT, AM, JO, AO. *Writing:* SMT, KAW, JPP, AJO. *Visualization:* ST, LA, KC, AR, CT, AM, JO, AO. *Supervision:* JO, AO. *Project Administration:* JO, AO. *Funding:* JO, AO.

BIBLIOGRAPHY

1. Hsia CC, Hyde DM, Weibel ER. 2016. Lung Structure and the Intrinsic Challenges of Gas Exchange. *Compr Physiol* 6:827-95.
2. Kopf M, Schneider C, Nobs SP. 2015. The development and function of lung-resident macrophages and dendritic cells. *Nat Immunol* 16:36-44.
3. Branchett WJ, Lloyd CM. 2019. Regulatory cytokine function in the respiratory tract. *Mucosal Immunol* 12:589-600.
4. Wu Y, Hirschi KK. 2020. Tissue-Resident Macrophage Development and Function. *Front Cell Dev Biol* 8:617879.
5. van de Laar L, Saelens W, De Prijck S, Martens L, Scott CL, Van Isterdael G, Hoffmann E, Beyaert R, Saeys Y, Lambrecht BN, Guilliams M. 2016. Yolk Sac Macrophages, Fetal Liver, and Adult Monocytes Can Colonize an Empty Niche and Develop into Functional Tissue-Resident Macrophages. *Immunity* 44:755-68.
6. Yu X, Buttgereit A, Lelios I, Utz SG, Cansever D, Becher B, Greter M. 2017. The Cytokine TGF-beta Promotes the Development and Homeostasis of Alveolar Macrophages. *Immunity* 47:903-912 e4.
7. Ardain A, Marakalala MJ, Leslie A. 2020. Tissue-resident innate immunity in the lung. *Immunology* 159:245-256.
8. Rothchild AC, Olson GS, Nemeth J, Amon LM, Mai D, Gold ES, Diercks AH, Aderem A. 2019. Alveolar macrophages generate a noncanonical NRF2-driven transcriptional response to *Mycobacterium tuberculosis* in vivo. *Sci Immunol* 4.
9. Pisu D, Huang L, Grenier JK, Russell DG. 2020. Dual RNA-Seq of *Mtb*-Infected Macrophages In Vivo Reveals Ontologically Distinct Host-Pathogen Interactions. *Cell Rep* 30:335-350 e4.
10. Huang L, Nazarova EV, Tan S, Liu Y, Russell DG. 2018. Growth of *Mycobacterium tuberculosis* in vivo segregates with host macrophage metabolism and ontogeny. *J Exp Med* 215:1135-1152.
11. Aegerter H, Kulikauskaite J, Crotta S, Patel H, Kelly G, Hessel EM, Mack M, Beinke S, Wack A. 2020. Influenza-induced monocyte-derived alveolar macrophages confer prolonged antibacterial protection. *Nat Immunol* 21:145-157.
12. Suzuki T, Sakagami T, Rubin BK, Nogee LM, Wood RE, Zimmerman SL, Smolarek T, Dishop MK, Wert SE, Whitsett JA, Grabowski G, Carey BC, Stevens C, van der Loo JC, Trapnell BC. 2008. Familial pulmonary alveolar proteinosis caused by mutations in *CSF2RA*. *J Exp Med* 205:2703-10.

13. Schneider C, Nobs SP, Kurrer M, Rehrauer H, Thiele C, Kopf M. 2014. Induction of the nuclear receptor PPAR-gamma by the cytokine GM-CSF is critical for the differentiation of fetal monocytes into alveolar macrophages. *Nat Immunol* 15:1026-37.
14. Tzavlaki K, Moustakas A. 2020. TGF-beta Signaling. *Biomolecules* 10.
15. Nunes I, Shapiro RL, Rifkin DB. 1995. Characterization of latent TGF-beta activation by murine peritoneal macrophages. *J Immunol* 155:1450-9.
16. Dennis PA, Rifkin DB. 1991. Cellular activation of latent transforming growth factor beta requires binding to the cation-independent mannose 6-phosphate/insulin-like growth factor type II receptor. *Proc Natl Acad Sci U S A* 88:580-4.
17. Annes JP, Rifkin DB, Munger JS. 2002. The integrin alphaVbeta6 binds and activates latent TGFbeta3. *FEBS Lett* 511:65-8.
18. Gleizes PE, Munger JS, Nunes I, Harpel JG, Mazzieri R, Noguera I, Rifkin DB. 1997. TGF-beta latency: biological significance and mechanisms of activation. *Stem Cells* 15:190-7.
19. Gong D, Shi W, Yi SJ, Chen H, Groffen J, Heisterkamp N. 2012. TGFbeta signaling plays a critical role in promoting alternative macrophage activation. *BMC Immunol* 13:31.
20. Gratchev A. 2017. TGF-beta signalling in tumour associated macrophages. *Immunobiology* 222:75-81.
21. Chung JY, Chan MK, Li JS, Chan AS, Tang PC, Leung KT, To KF, Lan HY, Tang PM. 2021. TGF-beta Signaling: From Tissue Fibrosis to Tumor Microenvironment. *Int J Mol Sci* 22.
22. Chen H, Zhuang F, Liu YH, Xu B, Del Moral P, Deng W, Chai Y, Kolb M, Gauldie J, Warburton D, Moses HL, Shi W. 2008. TGF-beta receptor II in epithelia versus mesenchyme plays distinct roles in the developing lung. *Eur Respir J* 32:285-95.
23. Sanford LP, Ormsby I, Gittenberger-de Groot AC, Sariola H, Friedman R, Boivin GP, Cardell EL, Doetschman T. 1997. TGFbeta2 knockout mice have multiple developmental defects that are non-overlapping with other TGFbeta knockout phenotypes. *Development* 124:2659-70.
24. Kulkarni AB, Huh CG, Becker D, Geiser A, Lyght M, Flanders KC, Roberts AB, Sporn MB, Ward JM, Karlsson S. 1993. Transforming growth factor beta 1 null mutation in mice causes excessive inflammatory response and early death. *Proc Natl Acad Sci U S A* 90:770-4.

25. Shull MM, Ormsby I, Kier AB, Pawlowski S, Diebold RJ, Yin M, Allen R, Sidman C, Proetzel G, Calvin D, et al. 1992. Targeted disruption of the mouse transforming growth factor-beta 1 gene results in multifocal inflammatory disease. *Nature* 359:693-9.
26. Willis BC, Liebler JM, Luby-Phelps K, Nicholson AG, Crandall ED, du Bois RM, Borok Z. 2005. Induction of epithelial-mesenchymal transition in alveolar epithelial cells by transforming growth factor-beta1: potential role in idiopathic pulmonary fibrosis. *Am J Pathol* 166:1321-32.
27. Frangogiannis N. 2020. Transforming growth factor-beta in tissue fibrosis. *J Exp Med* 217:e20190103.
28. Garrison G, Huang SK, Okunishi K, Scott JP, Kumar Penke LR, Scruggs AM, Peters-Golden M. 2013. Reversal of myofibroblast differentiation by prostaglandin E(2). *Am J Respir Cell Mol Biol* 48:550-8.
29. Gorki AD, Symmank D, Zahalka S, Lakovits K, Hladik A, Langer B, Maurer B, Sexl V, Kain R, Knapp S. 2022. Murine Ex Vivo Cultured Alveolar Macrophages Provide a Novel Tool to Study Tissue-Resident Macrophage Behavior and Function. *Am J Respir Cell Mol Biol* 66:64-75.
30. Luo M, Lai W, He Z, Wu L. 2021. Development of an Optimized Culture System for Generating Mouse Alveolar Macrophage-like Cells. *J Immunol* 207:1683-1693.
31. Thomas ST, Wierenga KA, Pestka JJ, Olive AJ. 2022. Fetal Liver-Derived Alveolar-like Macrophages: A Self-Replicating Ex Vivo Model of Alveolar Macrophages for Functional Genetic Studies. *Immunohorizons* 6:156-169.
32. Baker AD, Malur A, Barna BP, Ghosh S, Kavuru MS, Malur AG, Thomassen MJ. 2010. Targeted PPARgamma deficiency in alveolar macrophages disrupts surfactant catabolism. *J Lipid Res* 51:1325-31.
33. Remmerie A, Scott CL. 2018. Macrophages and lipid metabolism. *Cell Immunol* 330:27-42.
34. Oliveira-Nascimento L, Massari P, Wetzler LM. 2012. The Role of TLR2 in Infection and Immunity. *Front Immunol* 3:79.
35. Gopalakrishnan A, Salgame P. 2016. Toll-like receptor 2 in host defense against *Mycobacterium tuberculosis*: to be or not to be-that is the question. *Curr Opin Immunol* 42:76-82.
36. Ivashkiv LB, Donlin LT. 2014. Regulation of type I interferon responses. *Nat Rev Immunol* 14:36-49.

37. McNab F, Mayer-Barber K, Sher A, Wack A, O'Garra A. 2015. Type I interferons in infectious disease. *Nat Rev Immunol* 15:87-103.
38. Zhang W, Wang G, Xu ZG, Tu H, Hu F, Dai J, Chang Y, Chen Y, Lu Y, Zeng H, Cai Z, Han F, Xu C, Jin G, Sun L, Pan BS, Lai SW, Hsu CC, Xu J, Chen ZZ, Li HY, Seth P, Hu J, Zhang X, Li H, Lin HK. 2019. Lactate Is a Natural Suppressor of RLR Signaling by Targeting MAVS. *Cell* 178:176-189 e15.
39. Thompson MR, Kaminski JJ, Kurt-Jones EA, Fitzgerald KA. 2011. Pattern recognition receptors and the innate immune response to viral infection. *Viruses* 3:920-40.
40. Li D, Wu M. 2021. Pattern recognition receptors in health and diseases. *Signal Transduct Target Ther* 6:291.
41. Toshchakov V, Jones BW, Perera PY, Thomas K, Cody MJ, Zhang S, Williams BR, Major J, Hamilton TA, Fenton MJ, Vogel SN. 2002. TLR4, but not TLR2, mediates IFN-beta-induced STAT1alpha/beta-dependent gene expression in macrophages. *Nat Immunol* 3:392-8.
42. Stack J, Doyle SL, Connolly DJ, Reinert LS, O'Keeffe KM, McLoughlin RM, Paludan SR, Bowie AG. 2014. TRAM is required for TLR2 endosomal signaling to type I IFN induction. *J Immunol* 193:6090-102.
43. Dietrich N, Lienenklaus S, Weiss S, Gekara NO. 2010. Murine toll-like receptor 2 activation induces type I interferon responses from endolysosomal compartments. *PLoS One* 5:e10250.
44. Barbalat R, Lau L, Locksley RM, Barton GM. 2009. Toll-like receptor 2 on inflammatory monocytes induces type I interferon in response to viral but not bacterial ligands. *Nat Immunol* 10:1200-7.
45. Oosenbrug T, van de Graaff MJ, Haks MC, van Kasteren S, Rensing ME. 2020. An alternative model for type I interferon induction downstream of human TLR2. *J Biol Chem* 295:14325-14342.
46. York AG, Williams KJ, Argus JP, Zhou QD, Brar G, Vergnes L, Gray EE, Zhen A, Wu NC, Yamada DH, Cunningham CR, Tarling EJ, Wilks MQ, Casero D, Gray DH, Yu AK, Wang ES, Brooks DG, Sun R, Kitchen SG, Wu TT, Reue K, Stetson DB, Bensinger SJ. 2015. Limiting Cholesterol Biosynthetic Flux Spontaneously Engages Type I IFN Signaling. *Cell* 163:1716-29.
47. West AP, Shadel GS. 2017. Mitochondrial DNA in innate immune responses and inflammatory pathology. *Nat Rev Immunol* 17:363-375.
48. Wang X, Cunha C, Grau MS, Robertson SJ, Lacerda JF, Campos A, Jr., Lagrou K, Maertens J, Best SM, Carvalho A, Obar JJ. 2022. MAVS Expression in

- Alveolar Macrophages Is Essential for Host Resistance against *Aspergillus fumigatus*. *J Immunol* 209:346-353.
49. Mayer-Barber KD, Andrade BB, Oland SD, Amaral EP, Barber DL, Gonzales J, Derrick SC, Shi R, Kumar NP, Wei W, Yuan X, Zhang G, Cai Y, Babu S, Catalfamo M, Salazar AM, Via LE, Barry CE, 3rd, Sher A. 2014. Host-directed therapy of tuberculosis based on interleukin-1 and type I interferon crosstalk. *Nature* 511:99-103.
 50. Ji DX, Witt KC, Kotov DI, Margolis SR, Louie A, Chevee V, Chen KJ, Gaidt MM, Dhaliwal HS, Lee AY, Nishimura SL, Zamboni DS, Kramnik I, Portnoy DA, Darwin KH, Vance RE. 2021. Role of the transcriptional regulator SP140 in resistance to bacterial infections via repression of type I interferons. *Elife* 10.
 51. Postal M, Vivaldo JF, Fernandez-Ruiz R, Paredes JL, Appenzeller S, Niewold TB. 2020. Type I interferon in the pathogenesis of systemic lupus erythematosus. *Curr Opin Immunol* 67:87-94.
 52. Olive AJ, Smith CM, Kiritsy MC, Sasseti CM. 2018. The Phagocyte Oxidase Controls Tolerance to *Mycobacterium tuberculosis* Infection. *J Immunol* doi:10.4049/jimmunol.1800202.
 53. Fulco CP, Munschauer M, Anyoha R, Munson G, Grossman SR, Perez EM, Kane M, Cleary B, Lander ES, Engreitz JM. 2016. Systematic mapping of functional enhancer-promoter connections with CRISPR interference. *Science* 354:769-773.
 54. Shalem O, Sanjana NE, Hartenian E, Shi X, Scott DA, Mikkelsen T, Heckl D, Ebert BL, Root DE, Doench JG, Zhang F. 2014. Genome-scale CRISPR-Cas9 knockout screening in human cells. *Science* 343:84-87.
 55. Langmead B, Salzberg SL. 2012. Fast gapped-read alignment with Bowtie 2. *Nat Methods* 9:357-9.
 56. Liao Y, Smyth GK, Shi W. 2014. featureCounts: an efficient general purpose program for assigning sequence reads to genomic features. *Bioinformatics* 30:923-30.
 57. Love MI, Huber W, Anders S. 2014. Moderated estimation of fold change and dispersion for RNA-seq data with DESeq2. *Genome Biol* 15:550.

CHAPTER 4: RAPID LETHALITY OF MICE LACKING
PHAGOCYTE OXIDASE AND CASPASE1/11
FOLLOWING *MYCOBACTERIUM TUBERCULOSIS*
INFECTION.

PUBLICATION NOTICE

The following chapter has been submitted for publication to *Infection and Immunity* and is currently In Revision. It is available as a preprint through BioRxiv: “S.M. Thomas, A.J. Olive, Rapid lethality of mice lacking the phagocyte oxidase and Caspase1/11 following *Mycobacterium tuberculosis* infection, bioRxiv. <https://doi.org/10.1101/2023.02.08.527787>.”

ABSTRACT

Immune networks that control antimicrobial and inflammatory mechanisms have overlapping regulation and functions to ensure effective host responses. Genetic interaction studies of immune pathways that compare host responses in single and combined knockout backgrounds are a useful tool to identify new mechanisms of immune control during infection. For disease caused by pulmonary *Mycobacterium tuberculosis* infections, which currently lacks an effective vaccine, understanding genetic interactions between protective immune pathways may identify new therapeutic targets or disease-associated genes. Previous studies suggested a direct link between the activation of NLRP3-Caspase1 inflammasome and the NADPH-dependent phagocyte oxidase complex during Mtb infection. Loss of the phagocyte oxidase complex alone resulted in increased activation of Caspase1 and IL1 β production during Mtb infection, resulting in failed disease tolerance during the chronic stages of disease. To better understand this interaction, we generated mice lacking both *Cybb*, a key subunit of the phagocyte oxidase, and *Caspase1/11*. We found that *ex vivo* Mtb infection of *Cybb*^{-/-}*Caspase1/11*^{-/-} macrophages resulted in the expected loss of IL1 β secretion but an unexpected change in other inflammatory cytokines and bacterial control. Mtb infected *Cybb*^{-/-}*Caspase1/11*^{-/-} mice rapidly progressed to severe TB, succumbing within four weeks to disease characterized by high bacterial burden, increased inflammatory cytokines, and the recruitment of granulocytes that associated with Mtb in the lungs. These results uncover a key genetic interaction between the phagocyte oxidase complex and Caspase1/11 that controls protection against TB and

highlight the need for a better understanding of the regulation of fundamental immune networks during Mtb infection.

INTRODUCTION

Defense against infection requires the regulated activation of immune networks that determine the magnitude and duration of the host response (1, 2). Dysregulation of these immune networks contributes to increased susceptibility to infection and reduced disease tolerance (3-5). During lung infections with *Mycobacterium tuberculosis*, pro-inflammatory responses mediated by cytokines such as interleukin 1-beta (IL1 β), tumor necrosis factor (TNF) and interferon-gamma (IFN γ) must be strong enough to restrict infection, while maintaining respiratory function and controlling tissue damage (5-9). This balance is controlled by the tight regulation of cytokine and chemokine secretion to effectively direct the inflammatory process and immune cell recruitment (10, 11). Disruption of this balance contributes to progressive inflammatory tuberculosis (TB) disease which results in over 1.5 million deaths each year (12). Understanding the factors contributing to protection or susceptibility during Mtb infection is essential to devise more effective therapies and immunization strategies.

TB susceptibility is controlled by a combination of bacterial, host and environmental factors (13, 14). Many defined protective host genes comprise the mendelian susceptibility to mycobacterial diseases (MSMD) (15). Patients with these conditions have loss-of-function alleles in genes that are essential for protective host responses such as IFN γ signaling. Additional genes related to autophagy, reactive oxygen and nitrogen species (ROS/RNS) production, and cytokine production are also

protective in the mouse model of Mtb (16-19). However, while many genes are now identified as protective against Mtb, the precise mechanisms by which they control disease remains unclear.

One such protective mechanism is the ROS produced by the NADPH Phagocyte Oxidase (20). In humans, Chronic Granulomatous Disease (CGD) in patients with dysfunctional phagocyte oxidase complexes is associated with increased susceptibility to mycobacterial infections (21). Mice deficient in the phagocyte oxidase subunit *Cybb* control Mtb replication yet show defects in disease tolerance that result in a modest reduction in survival following high dose Mtb infection (18, 22-24). The loss of *Cybb* results in the hyperactivation of the NLRP3 inflammasome and exacerbated IL1 β production by bone marrow-derived macrophages (BMDMs) and *in vivo* during murine Mtb infection (18). This exacerbated IL1 β can be reversed in BMDMs with chemical inhibitors of NLRP3 or Caspase1. Caspase1 is a critical component of the NLRP3 inflammasome and is responsible for the activation of mature IL1 β , IL18, and Gasdermin D (25, 26). However, while Mtb infection of Caspase1-deficient macrophages results in loss of mature IL1 β production, mice lacking Caspase1/11 have no defects in IL1 β and minimal changes in susceptibility to TB *in vivo* (27, 28). Even though previous studies found clear links between phagocyte oxidase and the NLRP3 inflammasome that contribute to protection during Mtb infection, how these pathways interact and regulate each other's function remains unclear.

Here, we used a genetic approach to understand interactions between the phagocyte oxidase and the inflammasome by generating *Cybb*^{-/-}*Caspase1/11*^{-/-} animals. Mtb infection of macrophages and dendritic cells from these animals reversed the

exacerbated IL1 β production that was responsible for failed tolerance in *Cybb*^{-/-} cells. However, we found dysregulation of other pro-inflammatory mediators and reduced bacterial control during infection of *Cybb*^{-/-}*Caspase1/11*^{-/-} BMDMs. *In vivo*, we uncovered a synthetic susceptibility with *Cybb*^{-/-}*Caspase1/11*^{-/-} animals succumbing rapidly to TB disease within 4 weeks. We observed the loss of bacterial control and the recruitment of permissive granulocytes in *Cybb*^{-/-}*Caspase1/11*^{-/-} that were not seen in wild type, *Cybb*^{-/-} or *Caspase1/11*^{-/-} animals. Thus, our results uncovered a previously unknown genetic interaction between the phagocyte oxidase and the Caspase1 inflammasome that contributes to TB protection. Furthermore, our results highlight the complexity of the interactions between immune networks that control Mtb susceptibility and the importance of the regulation of inflammatory cytokines in the lung environment.

RESULTS

Loss of Caspase 1/11 results in decreased IL1 β production in *Cybb*^{-/-} phagocytes

Macrophages deficient in the phagocyte oxidase subunit *Cybb* hyperactivate the NLRP3 inflammasome and produce damaging levels of IL1 β during Mtb infection (18). We developed a genetic model to understand the interaction between these genes by generating mice deficient in both *Cybb* and *Caspase1/11* in the C57BL6/J background. We first examined the regulation of IL1 β during Mtb infection in cells lacking *Cybb*^{-/-} *Caspase1/11*^{-/-}. Bone marrow-derived macrophages (BMDMs) from wild type, *Cybb*^{-/-}, *Caspase1/11*^{-/-}, and *Cybb*^{-/-}*Caspase1/11*^{-/-} mice were infected with Mtb H37Rv. 14 hours later, the supernatants were removed from infected and uninfected control cells and the levels of IL1 β were quantified by ELISA. As previously shown, Mtb infected *Cybb*^{-/-}

phagocytes secreted significantly more IL1 β compared to wild type cells while *Caspase1/11*^{-/-} cells released nearly undetectable levels of IL1 β (**Figure 4.1A**) (18). Loss of *Caspase1/11* in combination with *Cybb* resulted in no IL1 β release, similar to what was observed in *Caspase1/11*^{-/-} macrophages. The experiment was repeated using bone marrow-derived dendritic cells (BMDCs) and the results were consistent with BMDMs. *Cybb*^{-/-} cells produce high levels of IL1 β which is reversed in the absence of *Caspase1/11* (**Figure 4.1B**). These data show that loss of *Caspase1/11* reverses the elevated IL1 β production observed in *Cybb*^{-/-} deficient phagocytes infected with *Mtb*.

***Cybb*^{-/-}*Caspase1/11*^{-/-} BMDMs dysregulate cytokines and *Mtb* control during infection.**

Both the ROS produced by the phagocyte oxidase and the immune pathways regulated by the inflammasome can modulate the inflammatory state of macrophages (29, 30). To better understand how the functions of *Cybb* and *Caspase1/11* interact to regulate inflammation, we infected BMDMs from each genotype with *Mtb* and we quantified cell death and cytokine release via multiplex cytokine analysis. Over the 14-hour infection, we observed no significant differences in cell death between any genotype (**Figure 4.2A**). Similar to the ELISA above, we observed increased IL1 β production by *Cybb*^{-/-} macrophages which was reversed in macrophages from *Cybb*^{-/-} *Caspase1/11*^{-/-} mice (**Figure 4.2B**). While IL1a production was also increased by *Cybb*^{-/-} cells, this was not reversed and was, in contrast to IL1 β , exacerbated in *Cybb*^{-/-} *Caspase1/11*^{-/-} macrophages. The increased IL1a production was not due to loss of *Caspase1/11* alone, since *Caspase1/11*^{-/-} BMDMs produced nearly undetectable levels

of IL1a following Mtb infection. Thus, IL1a production by BMDMs is exacerbated in the absence of both *Cybb* and *Caspase1/11*.

The multiplex cytokine panel included a range of other inflammatory cytokines that were compared between each macrophage genotype (**Figure 4.2C**). Most cytokines, including TNF, RANTES and CXCL1 showed no significant difference between any of the genotypes. However, IL6 and IL10 production were both significantly increased by *Cybb*^{-/-} BMDMs which was further exacerbated by *Cybb*^{-/-} *Caspase1/11*^{-/-} cells. Finally, CXCL2 was significantly increased only in *Cybb*^{-/-} *Caspase1/11*^{-/-} macrophages. Taken together, *Cybb*^{-/-} *Caspase1/11*^{-/-} macrophages dysregulate a range of inflammatory cytokines in response to Mtb infection.

Since the inflammatory milieu was altered during infection of *Cybb*^{-/-} *Caspase1/11*^{-/-} BMDMs, we next tested if intracellular control of Mtb growth was compromised. BMDMs from each genotype were infected with Mtb and growth was monitored using a CFU assay. We observed no significant difference between genotypes in bacterial uptake 4 hours following infection (**Figure 4.2D**). 5 days later we observed no change in bacterial control in *Cybb*^{-/-} or *Caspase1/11*^{-/-} BMDMs but found significantly more Mtb growth in *Cybb*^{-/-} *Caspase1/11*^{-/-} BMDMs. These data suggest that the loss of *Cybb* and *Caspase1/11* together does not compromise cell survival but does result in less effective Mtb control and dysregulated cytokine production that does not occur in either knockout mouse genotype alone.

***Cybb*^{-/-}*Caspase1/11*^{-/-} mice are hyper-susceptible to *Mtb* infection**

Our experiments in BMDMs showed that the loss of *Cybb* and *Caspase1/11* together results in dysregulated host responses during *Mtb* infection. We hypothesized that this dysregulation would result in changes to *in vivo* TB disease progression. To test this hypothesis, wild type, *Cybb*^{-/-}, *Caspase1/11*^{-/-}, and *Cybb*^{-/-}*Caspase1/11*^{-/-} mice were infected with *Mtb* by low dose aerosol. As mice were monitored during the infection, we observed dramatic weight loss of *Cybb*^{-/-}*Caspase1/11*^{-/-} animals that required almost all animals to be euthanized prior to 30 days post-infection (**Figure 4.3A**). In contrast, all other genotypes had gained weight over the same time of infection. Survival analysis during these infections found that *Cybb*^{-/-}*Caspase1/11*^{-/-} mice are highly susceptible to *Mtb* infection, with all animals requiring euthanasia earlier than 5 weeks post infection (**Figure 4.3B**). In contrast, wild type, *Cybb*^{-/-} and *Caspase1/11*^{-/-} animals all survived beyond day 75 similar to previous studies (18, 27, 28). This observation suggests a strong genetic interaction between *Cybb* and *Caspase1/11* that results in the synthetic hyper-susceptibility of animals to *Mtb* infection.

***Mtb* infection of *Cybb*^{-/-}*Caspase1/11*^{-/-} mice results in increased bacterial growth and inflammatory cytokine production.**

We next sought to determine the mechanisms driving the susceptibility of *Cybb*^{-/-}*Caspase1/11*^{-/-} animals. Wild type, *Cybb*^{-/-}, *Caspase1/11*^{-/-}, and *Cybb*^{-/-}*Caspase1/11*^{-/-} mice were infected with H37Rv YFP by low dose aerosol, and 25 days later, viable *Mtb* in the lungs and spleen were quantified by CFU plating (31). We observed similar numbers of *Mtb* in wild type, *Cybb*^{-/-}, and *Caspase1/11*^{-/-} animals in both organs and in

line with previous reports (18, 27, 28). In contrast, over 10-fold more Mtb were present in the lungs and ~5-fold more Mtb were present in the spleens of infected *Cybb*^{-/-} *Caspase1/11*^{-/-} mice (**Figure 4.4A and 4B**). We further characterized the cytokine profile from infected lung homogenates using a Luminex multiplex assay. We found that *Cybb*^{-/-} *Caspase1/11*^{-/-} mice express high levels of inflammatory cytokines including IL1a, IL1β, TNF, and IL6 but not IL10 (**Figure 4.4C**). We observed no significant differences between *Caspase1/11*^{-/-} and wild type mice, while in *Cybb*^{-/-} mice we found increased levels of IL1β but no other cytokines in line with previous studies (18, 27, 28). Thus, mice deficient in both *Cybb* and *Caspase 1/11* are unable to effectively control Mtb replication and display hyperinflammatory cytokine responses.

Permissive granulocytes are recruited to the lungs of *Cybb*^{-/-} *Caspase1/11*^{-/-} mice during Mtb infection.

The extreme susceptibility and increased Mtb growth observed in *Cybb*^{-/-} *Caspase1/11*^{-/-} mice is similar to mice lacking *IFN*γ or *Nos2* (7, 31-33). Recent work showed that the susceptibility of *Nos2*^{-/-} animals is driven by dysregulated inflammation that recruits permissive granulocytes to the lungs which then allow for amplified Mtb replication (33, 34). We hypothesized that similar responses may be associated with the susceptibility of *Cybb*^{-/-} *Caspase1/11*^{-/-} mice during Mtb infection. To test this hypothesis, we first analyzed the myeloid-derived populations of cells in the lungs and spleen of wild type, *Caspase1/11*^{-/-} *Cybb*^{-/-} and *Cybb*^{-/-} *Caspase1/11*^{-/-} animals infected with Mtb H37Rv YFP by low dose aerosol for 25 days. While wild type and *Caspase1/11*^{-/-} animals showed indistinguishable distributions of cells, *Cybb*^{-/-} mice recruited more GR1^{hi}

CD11b⁺ neutrophils in agreement with our previous findings (**Figure 4.5A and 5B**) (18). However, we observed a significant increase in the total number of GR1^{int} CD11b⁺ cells in the lungs of *Cybb*^{-/-}*Caspase1/11*^{-/-} mice. This population is consistent with the permissive myeloid cells seen in mice that are highly susceptible to Mtb infection (33, 34).

If the recruited GR1^{int} CD11b⁺ granulocytes in the lungs of *Cybb*^{-/-}*Caspase1/11*^{-/-} mice are permissive for Mtb growth, we predicted these cells would harbor a disproportionate fraction of intracellular Mtb in the lungs. To test this prediction, we quantified the total YFP⁺ infected cells from each genotype. We found an increase in the total number YFP⁺ cells only in *Cybb*^{-/-}*Caspase1/11*^{-/-} mice (**Figure 4.5D**). These data show that the lungs of *Cybb*^{-/-}*Caspase1/11*^{-/-} mice harbor more infected cells than wild type or single knockout controls. We next examined the distinct cellular populations that were infected with Mtb in each genotype. We found that over 40% of infected cells in *Cybb*^{-/-}*Caspase1/11*^{-/-} mice were found to be CD11b⁺GR1^{int} granulocytes a significant increase compared to wild type, *Cybb*^{-/-} and *Caspase1/11*^{-/-} animals (**Figure 4.5E and 5F**). This represents a shift in the *in vivo* intracellular distribution of Mtb in *Cybb*^{-/-}*Caspase1/11*^{-/-} mice. Altogether these experiments show that the susceptibility of *Cybb*^{-/-}*Caspase1/11*^{-/-} mice is associated with the recruitment of permissive granulocytes to the lungs that harbor high levels of Mtb.

DISCUSSION

While the phagocyte oxidase is undoubtedly important for protection against Mtb, the precise mechanisms by which it protects remain unclear (18, 21, 35, 36). In animal

models, the loss of *Cybb* alone results in a loss of disease tolerance through increased Caspase1 activation (18). Our results show that phagocyte oxidase also contributes to protection through a mechanism that is revealed only in the absence of Caspase1/11. While loss of either *Cybb* or *Caspase1/11* results in minor changes in survival, combining the mutations resulted in a dramatic increase in susceptibility, similar to mice lacking *IFNg*, *Nos2* or *Atg5* (7, 16, 17, 31). The synthetic susceptibility phenotype was characterized by increased granulocyte influx and Mtb replication in the lungs. Whether this susceptibility is a result of failed antimicrobial resistance, failed tolerance or both remains to be fully understood. However, based on the genetic interaction, it is likely that *Cybb* and *Caspase1/11* control parallel pathways that regulate cytokine and chemokine production and contribute to protection against TB.

While Mtb infection of both *Cybb*^{-/-} and *Cybb*^{-/-}*Casp1/11*^{-/-} mice drives increased granulocyte trafficking to the lungs, the properties of these cells are distinct. In *Cybb*^{-/-} mice the granulocytes express high levels of GR1 and the distribution of Mtb infected cells is unchanged compared to wild type mice. In contrast, granulocytes recruited to the lungs of *Cybb*^{-/-}*Caspase1/11*^{-/-} mice express intermediate levels of GR1 and are associated with high levels of Mtb. A recent report characterizing the susceptibility of mice deficient in *Nos2* found that GR1^{int} granulocytes were long-lived, unable to control bacterial growth, and were not suppressive even with increased IL10 production (33). In humans, low density granulocyte populations are associated with severe susceptibility to TB and may be analogous to these permissive GR1^{int} cells seen in susceptible mice (37). It is possible that these granulocytes are not directly driving the susceptibility but rather are associated with uncontrolled TB disease caused by other defects in the host

response. Future work using depletion and conditional knockouts will be required to understand how these changes in the cellular dynamics in *Cybb*^{-/-}*Caspase1/11*^{-/-} mice contribute to susceptibility.

Our current model predicts that the phagocyte oxidase and Caspase1/11 control the inflammatory state of myeloid cells during Mtb infection. When this control is lost, the result is a failure of disease tolerance, which drives progressive disease and recruits permissive granulocytes that modulate a feedforward loop of inflammation, Mtb growth, and tissue damage. While the exact signals that recruit granulocytes to the lungs of *Cybb*^{-/-}*Caspase1/11*^{-/-} mice remain unclear, we observed dysregulation of IL6, CXCL2 and IL1a in Mtb infected *Cybb*^{-/-}*Caspase1/11*^{-/-} macrophages. While the importance of each cytokine to *Cybb*^{-/-}*Caspase1/11*^{-/-} susceptibility will need to be examined extensively, IL1a was the most significantly changed cytokine in *Cybb*^{-/-}*Caspase1/11*^{-/-} macrophages and *in vivo*. IL1a is known to be required for protection against Mtb, as knockout mice are highly susceptible to disease (19, 38). Whether exacerbated IL1a directly contributes to TB susceptibility remains to be fully understood. Several non-mutually exclusive mechanisms could explain the dysregulation of IL1a and possibly other cytokines. For example, there is evidence that changes in calcium influx and mitochondrial stability directly control the expression and processing of IL1a (39). Thus, *Cybb* or Caspase1/11 may modulate calcium flux and mitochondrial function during Mtb infection that activate excessive IL1a production. Recent studies also suggest that metabolic pathways control ROS production that is directly required for processing of GSDMD which may link cellular metabolism to ROS signaling and inflammasome function (40). There is also evidence of a direct interaction between the phagocyte

oxidase subunits and Caspase1 that modulates phagosome dynamics during *Staphylococcus aureus* infection, but if this mechanism plays a role during Mtb infection remains unknown (41). Ongoing work is focused on examining the contribution of each potential mechanism to the susceptibility of *Cybb*^{-/-}*Caspase1/11*^{-/-} animals to better understand the regulatory networks that control inflammatory TB disease.

One outstanding line of questions from our findings is the specificity of the genetic interaction between *Cybb* and *Caspase1/11*. Both Caspase1- and Caspase11-dependent pathways are activated during Mtb infection, yet the direct contribution of either Caspase1 or Caspase11 to our observed susceptibility remains to be investigated by individually generating either *Cybb*^{-/-}*Caspase1*^{-/-} or *Cybb*^{-/-}*Caspase11*^{-/-} animals (18, 42-44). Given the recent availability of clean *Caspase1* and *Caspase11* knockout mice, we are in the process of developing these models for the future (45-47). In addition, whether mutations in the inflammasome sensor NLRP3 or the adaptor ASC and other subunits of the phagocyte oxidase recapitulate the susceptibility of *Cybb*^{-/-}*Caspase1/11*^{-/-} remain unknown. Further dissecting these specific genetic interactions between other phagocyte oxidase and inflammasome components will help to elucidate the underlying mechanisms controlling the susceptibility observed in *Cybb*^{-/-}*Caspase1/11*^{-/-} animals. Our discovery of a synthetic susceptibility to Mtb in *Cybb*^{-/-}*Caspase1/11*^{-/-} mice was serendipitous. As the susceptibility observed in *Cybb*^{-/-} mice was found to be due to dysregulated Caspase1 activation and IL1 β production, we initially hypothesized that the combined loss of *Cybb* and *Caspase1* would reverse the tolerance defects found in mice lacking the phagocyte oxidase and were surprised to uncover a synthetic susceptibility. Since the phagocyte oxidase and inflammasomes are among the most

studied pathways in immunology, our findings highlight a fundamental lack of understanding of interactions between immune signaling networks that control inflammation and immunity. To develop new host-directed therapeutics that could shorten treatment times and improve disease control, it is critical to understand how these interconnected networks function to protect against TB. A major obstacle in identifying protective networks against *Mtb* is the redundancy among host pathways, which mask important functions in single-knockout animals. A global understanding of genetic interactions that impact key inflammatory networks during TB would significantly inform the development of effective host-directed therapies or immunization strategies. Large-scale genetic interaction studies are common in cancer biology and should be applied to immune signaling networks during *Mtb* infection to better define these critical but currently unknown mechanisms that control protection against TB (48). Altogether, these findings suggest genetic interactions are key regulators of protection against *Mtb* with *Cybb* and *Caspase1/11* contributing together to protect against TB.

MATERIALS AND METHODS

Mice and Ethics Statement

Mouse studies were performed in accordance using the recommendations from the Guide for the Care and Use of Laboratory Animals of the National Institutes of Health and the Office of Laboratory Animal Welfare. Mouse studies were performed using protocols approved by the Institutional Animal Care and Use Committee (IACUC) in a manner designed to minimize pain and suffering in *Mtb*-infected animals. All mice were monitored and weighed regularly. Mice were euthanized following an evaluation of

clinical signs with a score of 14 or higher. C57BL6/J mice (# 000664) and *Cybb*^{-/-} mice (# 002365) were purchased from Jackson labs. *Caspase1/11*^{-/-} were a kind gift from Katharine Fitzgerald and *Cybb*^{-/-}*Caspase1/11*^{-/-} were generated in-house. All mice were housed and bred under specific pathogen-free conditions and in accordance with the University of Massachusetts Medical School (Sasseti Lab A221-20-11) and Michigan State University (PROTO202200127) IACUC guidelines. All animals used for experiments were 6-12 weeks old.

Macrophage and dendritic cell generation

Bone marrow-derived macrophages and dendritic cells were obtained from the femurs and tibias of sex- and age-matched mice. For BMDMs, cells were cultured in 10cm² non-tissue culture treated petri dishes with 10 mls DMEM with 10% FBS and 20% L929 supernatant for 1 week. On day 3, the old media was decanted, and fresh differentiation media was added. After 7 days of differentiation, cells were lifted in PBS with 10mM EDTA and seeded in tissue-culture treated dishes in DMEM with 10% FBS with no antibiotics then used the following day for experiments.

For BMDCs, cells were cultured in 10cm² non-tissue culture treated petri dishes with 10 ml DMEM with 10% FBS, L-Glutamine, 2 mM 2-mercaptoethanol and 10% supernatant from B16-GM-CSF cells as described previously. After 7 days of differentiation, BMDCs were further enriched by isolating loosely adherent cells removing F4/80⁺ cells then isolating CD11c⁺ cells by bead purification following manufacturer's instructions (Stem Cell Tech). Cells were then plated in tissue culture treated dishes in DMEM with 10% FBS then used the following day for experiments.

Bone marrow-derived macrophage and dendritic cell infections and analysis.

PDIM positive H37Rv was grown in 7H9 medium containing 10% oleic albumin dextrose catalase growth supplement and 0.05% Tween 80 as done previously (18). Prior to infection, cultures were washed in a PBS- 0.05% Tween solution and resuspended in DMEM with 10% FBS. To obtain a single cell suspension, samples were centrifuged at 200xg for 5 minutes to remove clumps. Culture density was determined by taking the supernatant from this centrifugation and determining the OD₆₀₀, with the assumption that OD₆₀₀ = 1.0 is equivalent to 3x10⁸ bacteria per ml. Bacteria were added to macrophages for 4 hours then cells were washed with PBS and fresh media was added. For cytokine analysis, at the indicated time points, supernatants were harvested and centrifuged through a 0.2-micron filter. Supernatants were then analyzed by a Luminex multiplex assay (Eve Technology) or by ELISA following manufacturer protocols (R&D). For CFU analysis, at the indicated timepoints, 1% saponin was added to each well without removing media to lyse cells while maintaining extracellular bacteria. Serial dilutions were then completed in phosphate-buffered saline containing tween 80 (PBS-T) and dilutions were plated on 7H10 agar. For cell death experiments, at the indicated time points media was removed and a CellTiter-Glo assay (Promega) was completed following manufacturer's instructions.

Mouse infections and CFU quantification

For animal infections, H37Rv or YFP⁺ H37Rv were resuspended in PBS-T. Prior to infection, bacteria were sonicated for 30 seconds, then delivered into the respiratory tract using an aerosol generation device (Glas-Col). To verify low dose aerosol delivery,

a subset of control mice was euthanized the following day. Otherwise the endpoints are designated in the figure legends. To determine total CFU in either the lung or spleen, mice were anesthetized via Carbon Dioxide asphyxiation and cervical dislocation. the organs were removed aseptically and homogenized. 10-fold serial dilutions of each organ homogenate were made in PBS-T and plated on 7H10 agar plates and incubated at 37C for 21-28 days. Viable bacteria were then counted. Both male and female mice were used throughout the study and no significant differences in phenotypes were observed between sexes.

Flow Cytometry

Analysis of infected myeloid cells in the lungs was done as previously described (13, 33). In short, lung tissue was homogenized in DMEM containing FBS using C-tubes (Miltenyi). Collagenase type IV/DNaseI (Sigma) was added, and tissues were dissociated for 10 seconds on a GentleMACS system (Miltenyi). Lung tissue was then oscillated for 30 minutes at 37C. Following incubation, tissue was further dissociated for 30 seconds on a GentleMACS. Single cell suspensions were isolated following passage through a 40-micron filter. Cell suspensions were then washed in DMEM and aliquoted into 96 well plates for flow cytometry staining. Non-specific antibody binding was first blocked using Fc-Block. Cells were then stained with anti-GR1 Pacific Blue, anti-CD11b PE, anti-CD11c APC, anti-CD45.2 PercP Cy5.5 (Biolegend). Live cells were identified using zombie aqua (Biolegend). No antibodies were used in the FITC channel to allow quantification of YFP⁺ Mtb in the tissues. All experiments contained a non-fluorescent H37Rv infection control to identify infected cells. Cells were stained for 30 minutes at

room temperature and fixed in 1% Paraformaldehyde for 60 minutes. All flow cytometry was run on a MACSQuant Analyzer 10 (Miltenyi) and was analyzed using FlowJo version 9 (Tree Star).

Statistical Analysis

Statistical analyses were performed using Prism 10 (Graph Pad) software as done previously (18, 49). Statistical tests used for each experiment are described in each figure legend along with symbols indicating significance or no significance.

FIGURES

Figure 4.1 Exacerbated IL1 β following Mtb infection of *Cybb*^{-/-} myeloid-cells is dependent on Caspase1/11. (A) BMDMs or (B) BMDCs from wild type, *Caspase1/11*^{-/-}, *Cybb*^{-/-} and *Cybb*^{-/-}*Caspase1/11*^{-/-} mice were left uninfected or infected with Mtb H37Rv at an MOI of 5. The following day IL1 β was quantified from the supernatants by ELISA. Each point represents data from a single well from one representative experiment of three. *** p<.001 by one-way ANOVA with a tukey test for multiple comparisons.

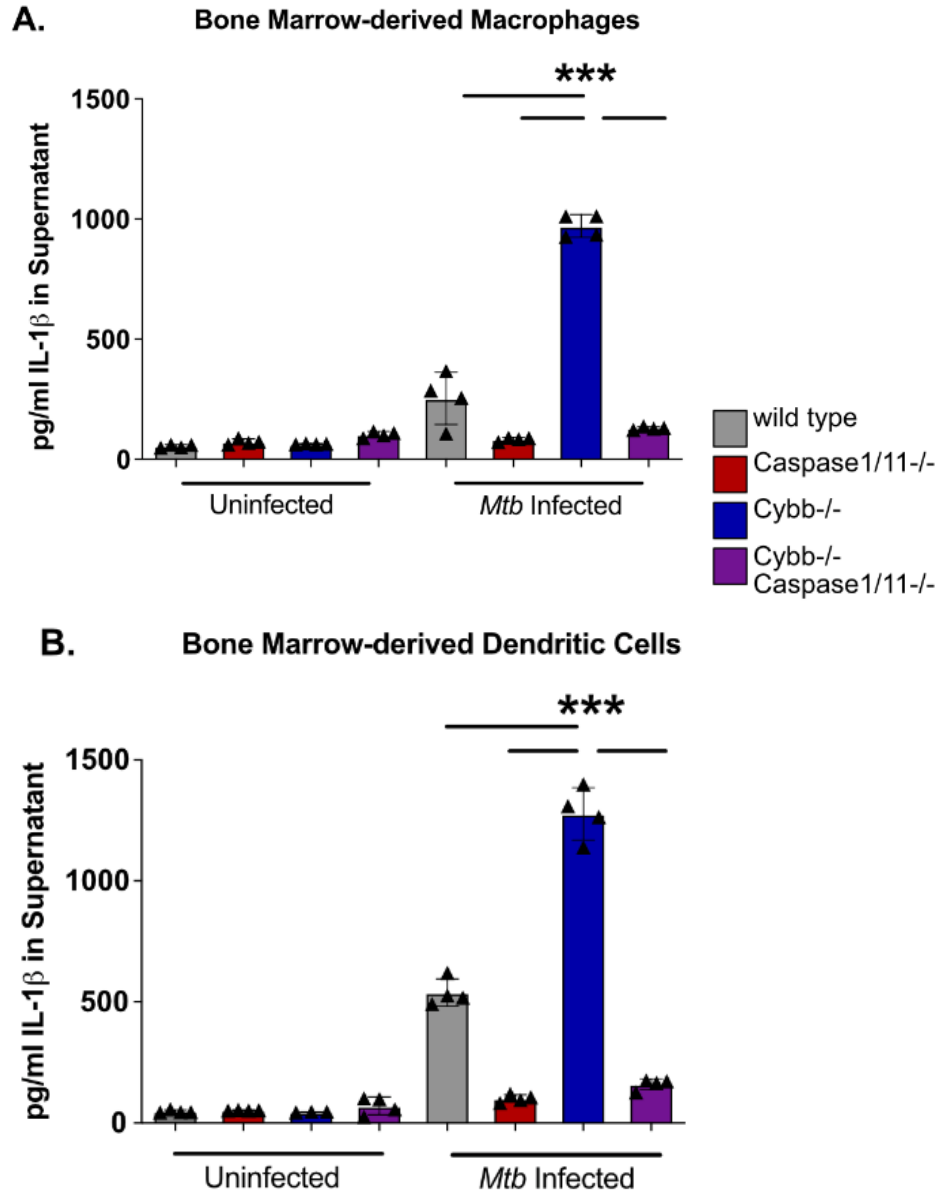


Figure 4.2 *Cybb*^{-/-}*Caspase1*/*11*^{-/-} macrophages are hyperinflammatory and permissive to bacterial growth during *Mtb* infection. (A) BMDMs from wild type, *Caspase1*/*11*^{-/-}, *Cybb*^{-/-} and *Cybb*^{-/-}*Caspase1*/*11*^{-/-} mice were left uninfected or were infected with *Mtb* H37Rv at an MOI of 5. The following day, total viable cells were quantified in each infection condition and normalized to uninfected control cells. Shown is percent viability of infected cells compared to uninfected cells of the same genotype. **(B)** BMDMs from wild type, *Caspase1*/*11*^{-/-}, *Cybb*^{-/-} and *Cybb*^{-/-}*Caspase1*/*11*^{-/-} mice were infected with *Mtb* H37Rv at an MOI of 5. The following day, cytokines from the supernatant were quantified by Luminex multiplex assay. Shown are results for IL1 β and IL1 α , and **(C)** other indicated cytokines (TNF, CXCL1, RANTES, IL6, IL10, and CXCL2). **(D)** BMDMs from wild type, *Caspase1*/*11*^{-/-}, *Cybb*^{-/-} and *Cybb*^{-/-}*Caspase1*/*11*^{-/-} mice were infected with *Mtb* H37Rv at an MOI of 1. At the indicated timepoints, cells were lysed and viable *Mtb* CFU were quantified. In all experiments, each point represents data from a single well and shown is mean \pm SD from one representative experiment of two or three similar experiments. * $p < .05$ ** $p < .01$ NS no significance, by one-way ANOVA with a tukey test for multiple comparisons.

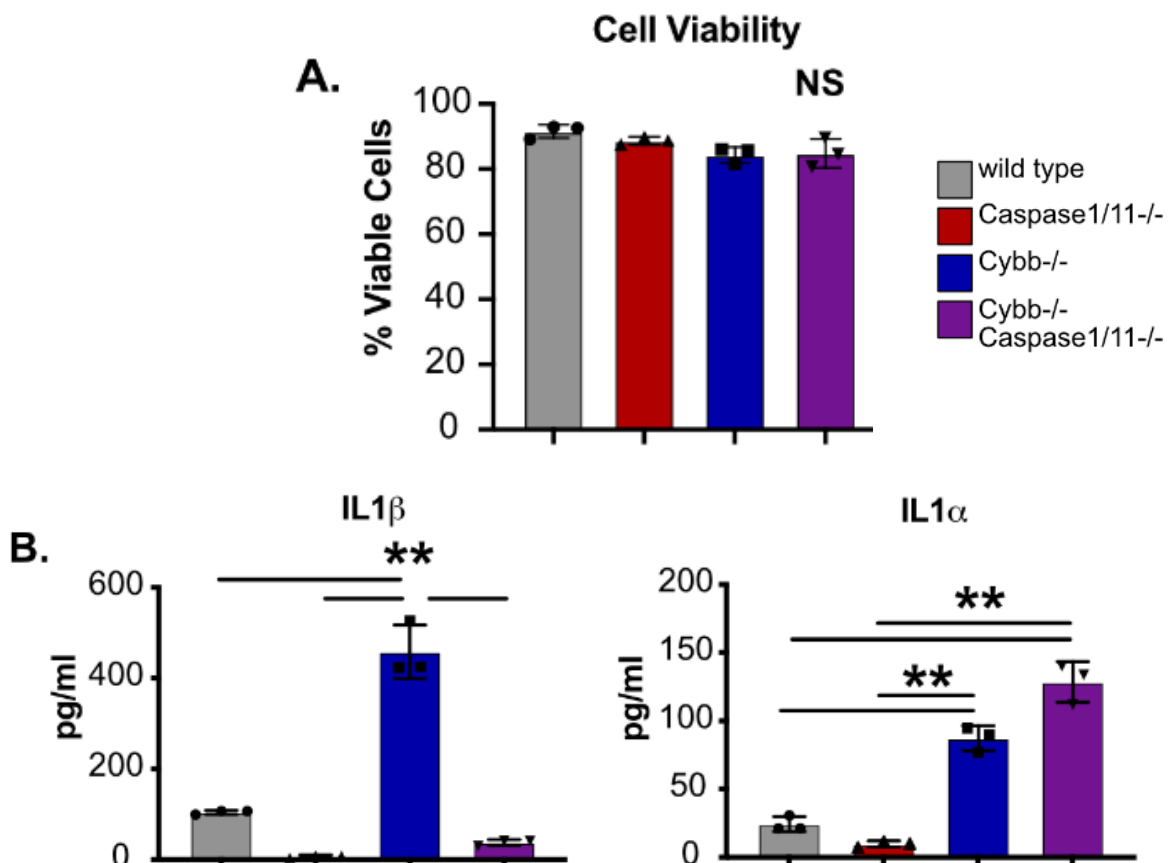


Figure 4.2 (cont'd)

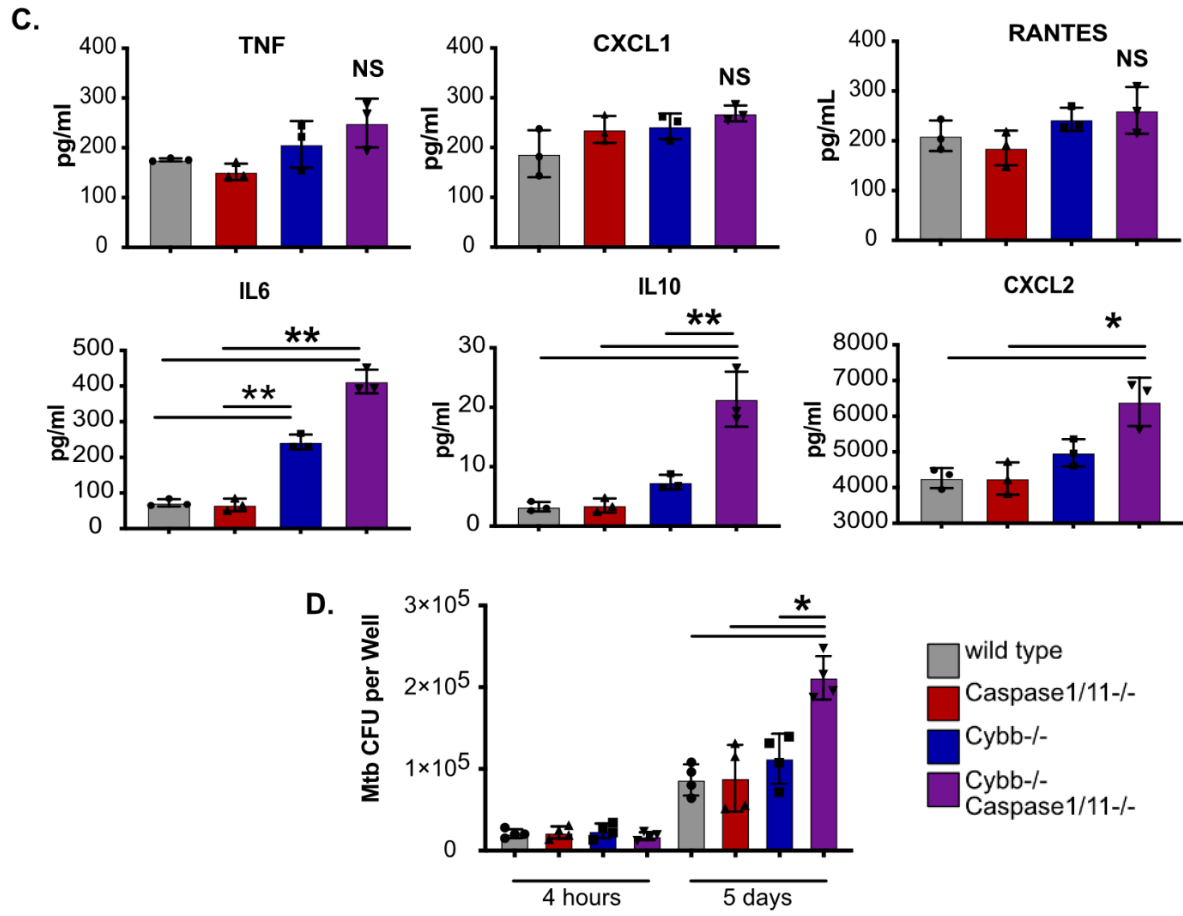


Figure 4.3 *Cybb*^{-/-}*Caspase1/11*^{-/-} mice rapidly succumb to pulmonary *Mtb* infection.

Wild type, *Caspase1/11*^{-/-}, *Cybb*^{-/-} and *Cybb*^{-/-}*Caspase1/11*^{-/-} mice were infected with *Mtb* H37Rv by the aerosol route in a single batch (Day 1 50-150 CFU). **(A)** Change in mouse weight from Day 0 to 24 days post-infection was quantified. Data are from one experiment and are representative of three similar experiments. Statistics were determined by a Mann Whitney test ***p*<.01. **(B)** The relative survival of each genotype was quantified over 75 days of infection. Data are pooled from two independent experiments. Statistics were determined by a Mantel-Cox test *** *p*<.001.

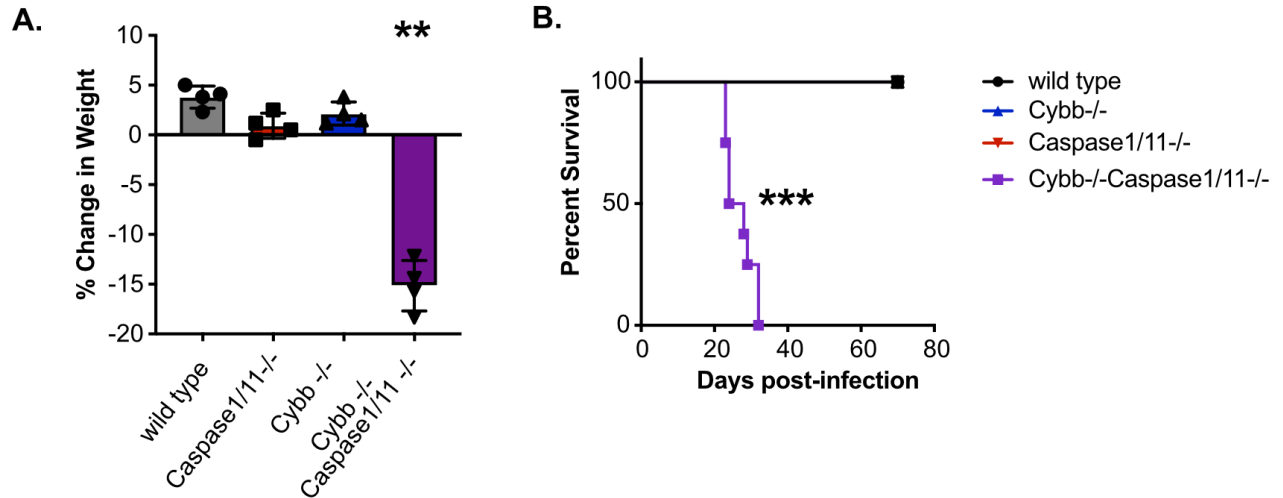


Figure 4.4 *Cybb*^{-/-}*Caspase1/11*^{-/-} mice do not control *Mtb* growth and are hyperinflammatory. Wild type, *Caspase1/11*^{-/-}, *Cybb*^{-/-} and *Cybb*^{-/-}*Caspase1/11*^{-/-} mice were infected with *Mtb* H37Rv YFP by the aerosol route in a single batch (Day 1 50-100 CFU). Lungs and spleen were collected at 25 days post-infection and used to quantify bacterial CFU. **(A)** Bacterial burden in the lungs and **(B)** spleens of mice are shown. **(C)** Concentrations of cytokines in lung homogenates from infected mice were quantified (IL1a, IL1β, IL6, TNF, IL10 and RANTES). Each point represents a single mouse, data are representative of one experiment from three similar experiments. * p<.05 ** p<.01 NS no significance, by one-way ANOVA with a tukey test for multiple comparisons.

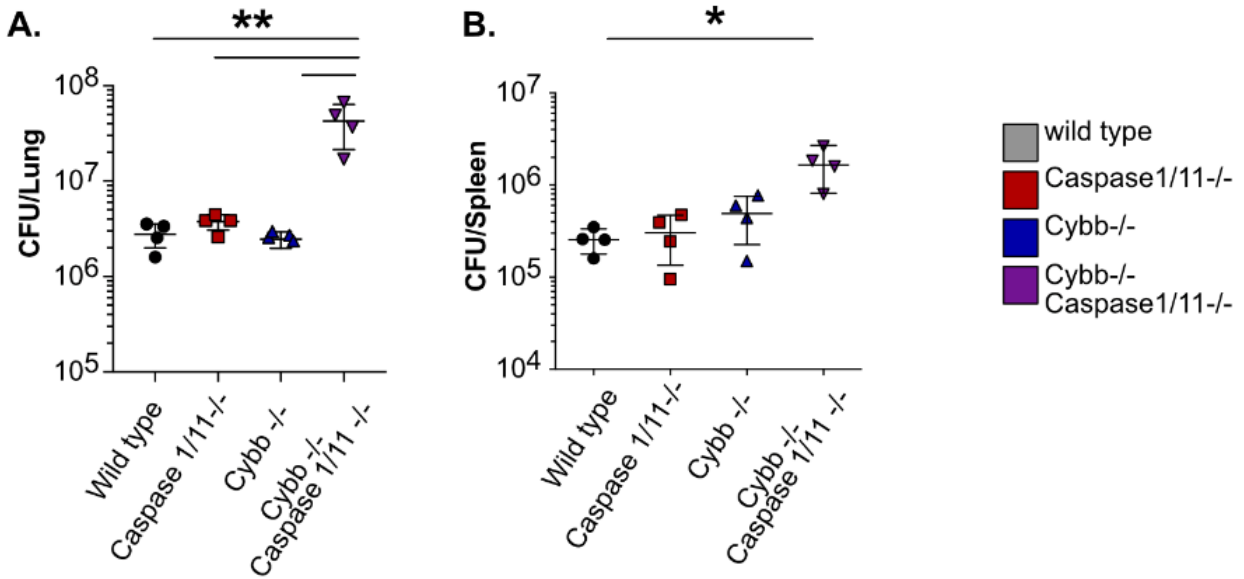


Figure 4.4 (cont'd)

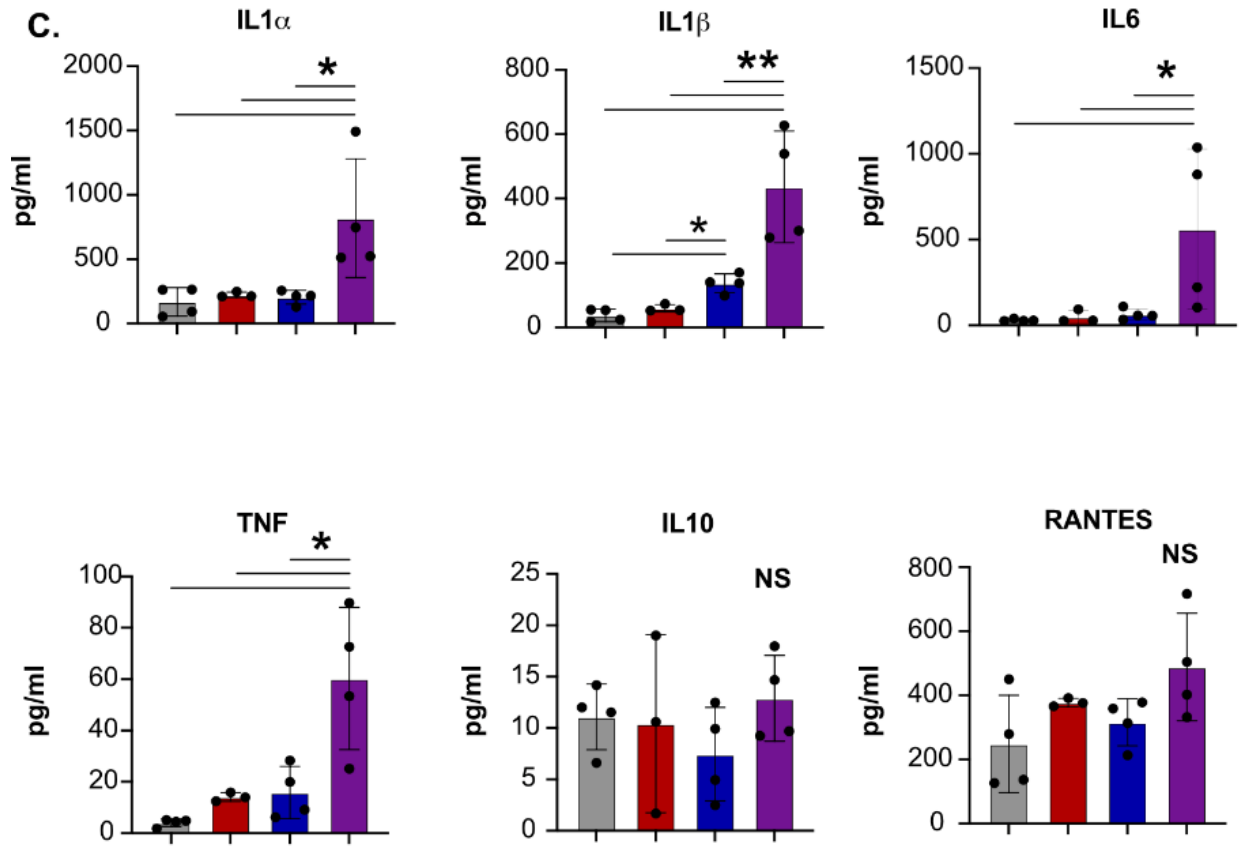


Figure 4.5 GR-1^{int} granulocytes are recruited to the lungs and are associated with Mtb during infection of *Cybb*^{-/-}*Caspase1/11*^{-/-} mice. Wild type, *Caspase1/11*^{-/-}, *Cybb*^{-/-} and *Cybb*^{-/-}*Caspase1/11*^{-/-} mice were infected with Mtb H37Rv YFP by the aerosol route in a single batch (Day 1 50-100 CFU). Lungs were collected at 25 days post-infection and single cell homogenates were made for flow cytometry analysis. **(A)** Shown is a representative flow cytometry plot of total lung granulocytes based on CD11b and GR1 staining (Gated on live CD45.2⁺ single cells). Gates indicate CD11b⁺ GR1^{hi} or CD11b⁺ GR1^{int} granulocytes present in the lungs. **(B)** The percent of gated cells (live CD45.2⁺ single cells) that were CD11b⁺ GR1^{hi} and **(C)** CD11b⁺ GR1^{int} were quantified. **(D)** The total number of H37Rv YFP⁺ cells were quantified from each mouse lung following gating on live, CD45.2⁺ single cells. **(E)** The percent of gated H37Rv YFP⁺ cells that were CD11b⁺ GR1^{int} were quantified. **(F)** Shown is a representative flow cytometry plot of H37Rv YFP⁺ infected granulocytes (Gated on live CD45.2⁺ YFP⁺ single cells). Gates indicate CD11b⁺ GR1^{hi} or CD11b⁺ GR1^{int} granulocytes present in the lungs. Each point represents a single mouse and data are representative of one experiment from three similar experiments. * p<.05 ** p<.01 by one-way ANOVA with a tukey test for multiple comparisons.

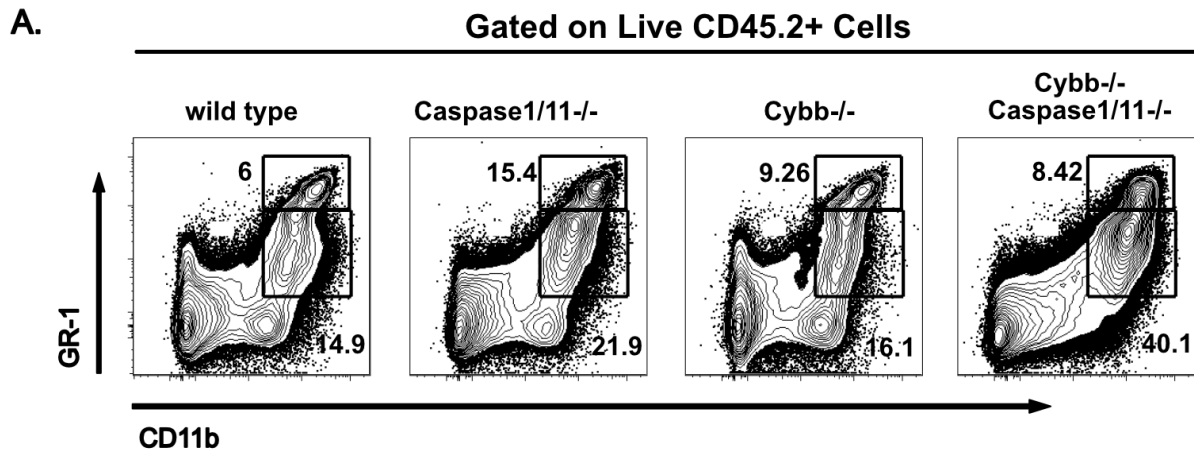
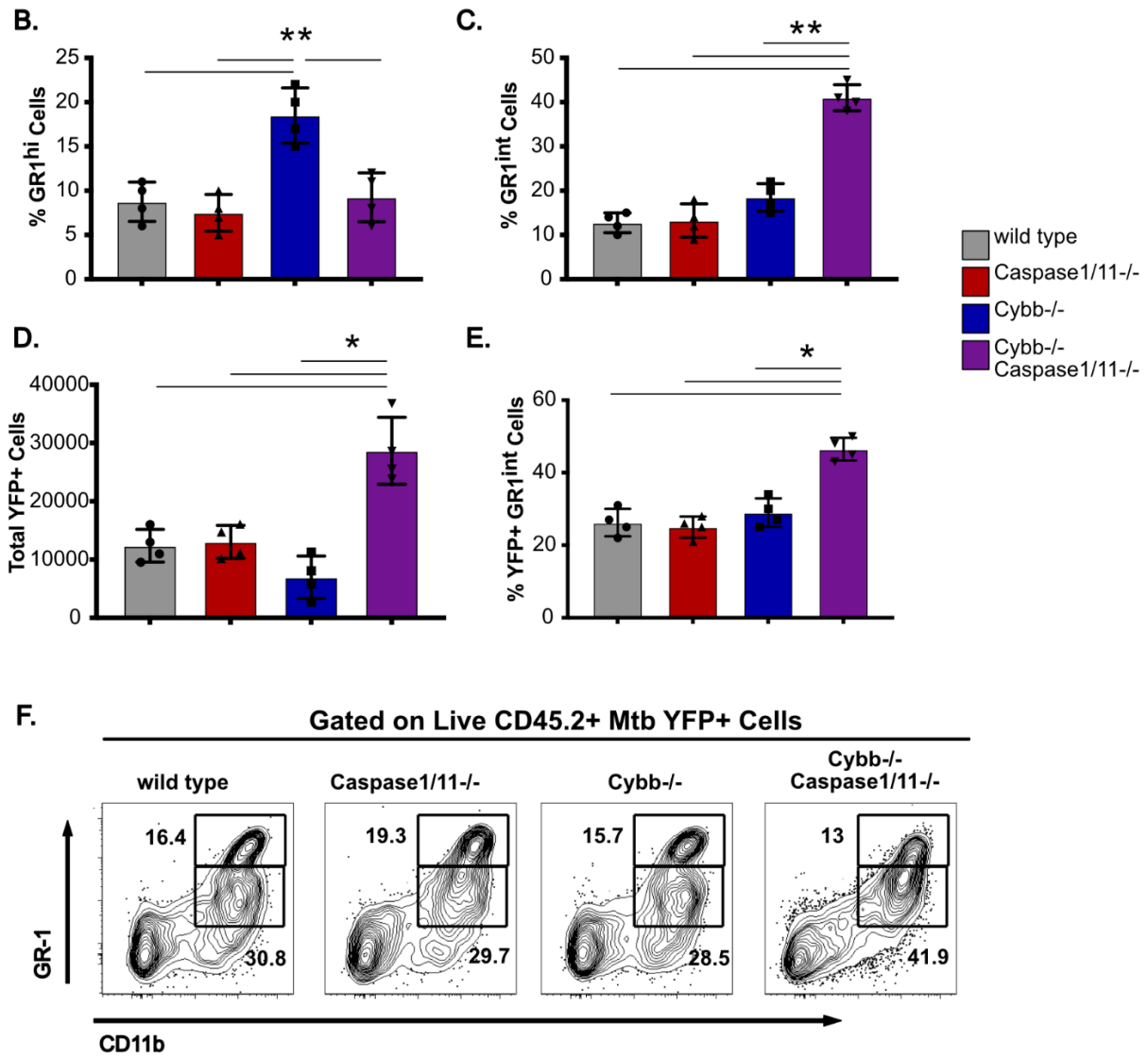


Figure 4.5 (cont'd)



DECLARATIONS

Competing interests

The authors declare that they have no competing interests.

Funding

This work was supported by the Michigan State University Rudolph Hugh Award (to SMT) and the National Institutes of Health Grant AI148961 (to AJO).

Contributions

Conceptualization: SMT, AJO. *Methodology:* SMT, AJO. *Software:* AJO. *Validation:* SMT, AJO. *Formal Analysis:* SMT, AJO. *Investigation:* SMT, AJO. *Resources:* AJO. *Data Curation:* SMT, AJO. *Writing:* SMT, AJO. *Visualization:* SMT, AJO *Supervision:* AJO. *Project Administration:* AJO. *Funding:* SMT, AJO.

BIBLIOGRAPHY

1. Mogensen TH. 2009. Pathogen recognition and inflammatory signaling in innate immune defenses. *Clin Microbiol Rev* 22:240-73, Table of Contents.
2. Ernst JD. 2012. The immunological life cycle of tuberculosis. *Nat Rev Immunol* 12:581-91.
3. Olive AJ, Sassetti CM. 2018. Tolerating the Unwelcome Guest; How the Host Withstands Persistent *Mycobacterium tuberculosis*. *Front Immunol* 9:2094.
4. Martins R, Carlos AR, Braza F, Thompson JA, Bastos-Amador P, Ramos S, Soares MP. 2019. Disease Tolerance as an Inherent Component of Immunity. *Annu Rev Immunol* 37:405-437.
5. Divangahi M, Khan N, Kaufmann E. 2018. Beyond Killing *Mycobacterium tuberculosis*: Disease Tolerance. *Front Immunol* 9:2976.
6. Nunes-Alves C, Booty MG, Carpenter SM, Jayaraman P, Rothchild AC, Behar SM. 2014. In search of a new paradigm for protective immunity to TB. *Nat Rev Microbiol* 12:289-99.
7. Nandi B, Behar SM. 2011. Regulation of neutrophils by interferon-gamma limits lung inflammation during tuberculosis infection. *J Exp Med* 208:2251-62.
8. Bohrer AC, Tocheny C, Assmann M, Ganusov VV, Mayer-Barber KD. 2018. Cutting Edge: IL-1R1 Mediates Host Resistance to *Mycobacterium tuberculosis* by Trans-Protection of Infected Cells. *J Immunol* 201:1645-1650.
9. Flynn JL, Goldstein MM, Chan J, Triebold KJ, Pfeffer K, Lowenstein CJ, Schreiber R, Mak TW, Bloom BR. 1995. Tumor necrosis factor-alpha is required in the protective immune response against *Mycobacterium tuberculosis* in mice. *Immunity* 2:561-72.
10. Algood HM, Chan J, Flynn JL. 2003. Chemokines and tuberculosis. *Cytokine Growth Factor Rev* 14:467-77.
11. Raveshloot-Chavez MM, Van Dis E, Stanley SA. 2021. The Innate Immune Response to *Mycobacterium tuberculosis* Infection. *Annu Rev Immunol* 39:611-637.
12. Chakaya J, Petersen E, Nantanda R, Mungai BN, Migliori GB, Amanullah F, Lungu P, Ntoui F, Kumarasamy N, Maeurer M, Zumla A. 2022. The WHO Global Tuberculosis 2021 Report - not so good news and turning the tide back to End TB. *Int J Infect Dis* 124 Suppl 1:S26-S29.
13. Olive AJ, Sassetti CM. 2016. Metabolic crosstalk between host and pathogen: sensing, adapting and competing. *Nat Rev Microbiol* 14:221-34.

14. McHenry ML, Bartlett J, Igo RP, Jr., Wampande EM, Benchek P, Mayanja-Kizza H, Fluegge K, Hall NB, Gagneux S, Tishkoff SA, Wejse C, Sirugo G, Boom WH, Joloba M, Williams SM, Stein CM. 2020. Interaction between host genes and Mycobacterium tuberculosis lineage can affect tuberculosis severity: Evidence for coevolution? PLoS Genet 16:e1008728.
15. Bustamante J, Boisson-Dupuis S, Abel L, Casanova JL. 2014. Mendelian susceptibility to mycobacterial disease: genetic, immunological, and clinical features of inborn errors of IFN-gamma immunity. Semin Immunol 26:454-70.
16. Nathan C, Shiloh MU. 2000. Reactive oxygen and nitrogen intermediates in the relationship between mammalian hosts and microbial pathogens. Proc Natl Acad Sci U S A 97:8841-8.
17. Kimmey JM, Huynh JP, Weiss LA, Park S, Kambal A, Debnath J, Virgin HW, Stallings CL. 2015. Unique role for ATG5 in neutrophil-mediated immunopathology during M. tuberculosis infection. Nature 528:565-9.
18. Olive AJ, Smith CM, Kiritsy MC, Sasseti CM. 2018. The Phagocyte Oxidase Controls Tolerance to Mycobacterium tuberculosis Infection. J Immunol doi:10.4049/jimmunol.1800202.
19. Mayer-Barber KD, Andrade BB, Barber DL, Hieny S, Feng CG, Caspar P, Oland S, Gordon S, Sher A. 2011. Innate and adaptive interferons suppress IL-1alpha and IL-1beta production by distinct pulmonary myeloid subsets during Mycobacterium tuberculosis infection. Immunity 35:1023-34.
20. Panday A, Sahoo MK, Osorio D, Batra S. 2015. NADPH oxidases: an overview from structure to innate immunity-associated pathologies. Cell Mol Immunol 12:5-23.
21. Bustamante J, Arias AA, Vogt G, Picard C, Galicia LB, Prando C, Grant AV, Marchal CC, Hubeau M, Chaggier A, de Beaucoudrey L, Puel A, Feinberg J, Valinetz E, Janniere L, Besse C, Boland A, Brisseau JM, Blanche S, Lortholary O, Fieschi C, Emile JF, Boisson-Dupuis S, Al-Muhsen S, Woda B, Newburger PE, Condino-Neto A, Dinauer MC, Abel L, Casanova JL. 2011. Germline CYBB mutations that selectively affect macrophages in kindreds with X-linked predisposition to tuberculous mycobacterial disease. Nat Immunol 12:213-21.
22. Jung YJ, LaCourse R, Ryan L, North RJ. 2002. Virulent but not avirulent Mycobacterium tuberculosis can evade the growth inhibitory action of a T helper 1-dependent, nitric oxide Synthase 2-independent defense in mice. J Exp Med 196:991-8.
23. Cooper AM, Segal BH, Frank AA, Holland SM, Orme IM. 2000. Transient loss of resistance to pulmonary tuberculosis in p47(phox-/-) mice. Infect Immun 68:1231-4.

24. Ng VH, Cox JS, Sousa AO, MacMicking JD, McKinney JD. 2004. Role of KatG catalase-peroxidase in mycobacterial pathogenesis: countering the phagocyte oxidative burst. *Mol Microbiol* 52:1291-302.
25. Kelley N, Jeltema D, Duan Y, He Y. 2019. The NLRP3 Inflammasome: An Overview of Mechanisms of Activation and Regulation. *Int J Mol Sci* 20.
26. Chan AH, Schroder K. 2020. Inflammasome signaling and regulation of interleukin-1 family cytokines. *J Exp Med* 217.
27. Mayer-Barber KD, Barber DL, Shenderov K, White SD, Wilson MS, Cheever A, Kugler D, Hieny S, Caspar P, Nunez G, Schlueter D, Flavell RA, Sutterwala FS, Sher A. 2010. Caspase-1 independent IL-1 β production is critical for host resistance to mycobacterium tuberculosis and does not require TLR signaling in vivo. *J Immunol* 184:3326-30.
28. McElvania Tekippe E, Allen IC, Hulseberg PD, Sullivan JT, McCann JR, Sandor M, Braunstein M, Ting JP. 2010. Granuloma formation and host defense in chronic Mycobacterium tuberculosis infection requires PYCARD/ASC but not NLRP3 or caspase-1. *PLoS One* 5:e12320.
29. von Moltke J, Ayres JS, Kofoed EM, Chavarria-Smith J, Vance RE. 2013. Recognition of bacteria by inflammasomes. *Annu Rev Immunol* 31:73-106.
30. Canton M, Sanchez-Rodriguez R, Spera I, Venegas FC, Favia M, Viola A, Castegna A. 2021. Reactive Oxygen Species in Macrophages: Sources and Targets. *Front Immunol* 12:734229.
31. Mishra BB, Lovewell RR, Olive AJ, Zhang G, Wang W, Eugenin E, Smith CM, Phuah JY, Long JE, Dubuke ML, Palace SG, Goguen JD, Baker RE, Nambi S, Mishra R, Booty MG, Baer CE, Shaffer SA, Dartois V, McCormick BA, Chen X, Sasseti CM. 2017. Nitric oxide prevents a pathogen-permissive granulocytic inflammation during tuberculosis. *Nat Microbiol* 2:17072.
32. Mishra BB, Rathinam VA, Martens GW, Martinot AJ, Kornfeld H, Fitzgerald KA, Sasseti CM. 2013. Nitric oxide controls the immunopathology of tuberculosis by inhibiting NLRP3 inflammasome-dependent processing of IL-1 β . *Nat Immunol* 14:52-60.
33. Lovewell RR, Baer CE, Mishra BB, Smith CM, Sasseti CM. 2020. Granulocytes act as a niche for Mycobacterium tuberculosis growth. *Mucosal Immunol* doi:10.1038/s41385-020-0300-z.
34. Obregon-Henao A, Henao-Tamayo M, Orme IM, Ordway DJ. 2013. Gr1(int)CD11b+ myeloid-derived suppressor cells in Mycobacterium tuberculosis infection. *PLoS One* 8:e80669.

35. Lee PP, Chan KW, Jiang L, Chen T, Li C, Lee TL, Mak PH, Fok SF, Yang X, Lau YL. 2008. Susceptibility to mycobacterial infections in children with X-linked chronic granulomatous disease: a review of 17 patients living in a region endemic for tuberculosis. *Pediatr Infect Dis J* 27:224-30.
36. Khan TA, Kalsoom K, Iqbal A, Asif H, Rahman H, Farooq SO, Naveed H, Nasir U, Amin MU, Hussain M, Tipu HN, Florea A. 2016. A novel missense mutation in the NADPH binding domain of CYBB abolishes the NADPH oxidase activity in a male patient with increased susceptibility to infections. *Microb Pathog* 100:163-169.
37. Rankin AN, Hendrix SV, Naik SK, Stallings CL. 2022. Exploring the Role of Low-Density Neutrophils During Mycobacterium tuberculosis Infection. *Front Cell Infect Microbiol* 12:901590.
38. Di Paolo NC, Shafiani S, Day T, Papayannopoulou T, Russell DW, Iwakura Y, Sherman D, Urdahl K, Shayakhmetov DM. 2015. Interdependence between Interleukin-1 and Tumor Necrosis Factor Regulates TNF-Dependent Control of Mycobacterium tuberculosis Infection. *Immunity* 43:1125-36.
39. Freigang S, Ampenberger F, Weiss A, Kanneganti TD, Iwakura Y, Hersberger M, Kopf M. 2013. Fatty acid-induced mitochondrial uncoupling elicits inflammasome-independent IL-1 α and sterile vascular inflammation in atherosclerosis. *Nat Immunol* 14:1045-53.
40. Evavold CL, Hafner-Bratkovic I, Devant P, D'Andrea JM, Ngwa EM, Borsic E, Doench JG, LaFleur MW, Sharpe AH, Thiagarajah JR, Kagan JC. 2021. Control of gasdermin D oligomerization and pyroptosis by the Regulator-Rag-mTORC1 pathway. *Cell* 184:4495-4511 e19.
41. Sokolovska A, Becker CE, Ip WK, Rathinam VA, Brudner M, Paquette N, Tanne A, Vanaja SK, Moore KJ, Fitzgerald KA, Lacy-Hulbert A, Stuart LM. 2013. Activation of caspase-1 by the NLRP3 inflammasome regulates the NADPH oxidase NOX2 to control phagosome function. *Nat Immunol* 14:543-53.
42. Dorhoi A, Nouailles G, Jorg S, Hagens K, Heinemann E, Pradl L, Oberbeck-Muller D, Duque-Correa MA, Reece ST, Ruland J, Brosch R, Tschopp J, Gross O, Kaufmann SH. 2012. Activation of the NLRP3 inflammasome by Mycobacterium tuberculosis is uncoupled from susceptibility to active tuberculosis. *Eur J Immunol* 42:374-84.
43. Beckwith KS, Beckwith MS, Ullmann S, Saetra RS, Kim H, Marstad A, Asberg SE, Strand TA, Haug M, Niederweis M, Stenmark HA, Flo TH. 2020. Plasma membrane damage causes NLRP3 activation and pyroptosis during Mycobacterium tuberculosis infection. *Nat Commun* 11:2270.

44. Qian J, Hu Y, Zhang X, Chi M, Xu S, Wang H, Zhang X. 2022. Mycobacterium tuberculosis PE_PGRS19 Induces Pyroptosis through a Non-Classical Caspase-11/GSDMD Pathway in Macrophages. *Microorganisms* 10.
45. Bourigault ML, Segueni N, Rose S, Court N, Vacher R, Vasseur V, Erard F, Le Bert M, Garcia I, Iwakura Y, Jacobs M, Ryffel B, Quesniaux VF. 2013. Relative contribution of IL-1 α , IL-1 β and TNF to the host response to Mycobacterium tuberculosis and attenuated M. bovis BCG. *Immun Inflamm Dis* 1:47-62.
46. Rauch I, Deets KA, Ji DX, von Moltke J, Tenthorey JL, Lee AY, Philip NH, Ayres JS, Brodsky IE, Gronert K, Vance RE. 2017. NAIP-NLRC4 Inflammasomes Coordinate Intestinal Epithelial Cell Expulsion with Eicosanoid and IL-18 Release via Activation of Caspase-1 and -8. *Immunity* 46:649-659.
47. Wang S, Miura M, Jung YK, Zhu H, Li E, Yuan J. 1998. Murine caspase-11, an ICE-interacting protease, is essential for the activation of ICE. *Cell* 92:501-9.
48. Mair B, Moffat J, Boone C, Andrews BJ. 2019. Genetic interaction networks in cancer cells. *Curr Opin Genet Dev* 54:64-72.
49. Wilburn KM, Meade RK, Heckenberg EM, Dockterman J, Coers J, Sasseti CM, Olive AJ, Smith CM. 2023. Differential Requirement for IRGM Proteins during Tuberculosis Infection in Mice. *Infect Immun* doi:10.1128/iai.00510-22:e0051022.

CHAPTER 5: CONCLUDING REMARKS AND FUTURE DIRECTIONS

Respiratory infections and non-communicable chronic respiratory diseases account for 2 of the top 5 causes of death worldwide, with a global burden of 3.59 million and 3.54 million deaths caused per year, respectively(1, 2). Research directed at preventing or curing these diseases has been impeded by an inability to accurately study pulmonary immune cell populations in an efficient, cost-effective manner. In these studies, I developed a novel cell system to model the alveolar macrophage and employed genetic interaction studies to identify a novel immune network that is critical for protection to *Mycobacterium tuberculosis* infection.

We began by creating an ex vivo alveolar macrophage cell model that enabled us to bypass the current obstacles in studying AM biology and explore AM-specific regulation of cellular processes such as metabolism, cell survival, and inflammation. We identified TGF- β as being necessary for the development and long-term stability of these cells and, for the first time, successfully implemented a CRISPR-Cas9-mediated loss-of-function forward genetic screen in a primary, alveolar macrophage-like cell model. We used this forward genetic screen, and functional genetic studies, to begin to uncover AM-specific biological processes and inflammatory responses. We then explored the impact of TGF- β on the inflammatory processes in these cells. Given the ubiquity and importance of TGF- β in the lung and in AM development and maintenance, understanding how it shapes AM biology will allow us to better identify the impacts of variable TGF- β levels in the lungs. We uncover an unexpected role of TGF- β in TLR2 signaling, resulting in a novel method of IFN- β production mediated through MAVS and IRF3/7, further highlighting the uniqueness of pulmonary inflammatory responses. To conclude this work, we investigated genetic interactions between the NADPH phagocyte

oxidase and the inflammasome during Mtb infection in an effort to further understand how these seemingly distinct immune mechanisms interact to protect against pulmonary TB. We discovered, surprisingly, that while loss of either the phagocyte oxidase or catalytic component of the inflammasome, Caspase1, resulted in no changes to susceptibility during early infection, animals lacking both components were extremely susceptible to disease. This susceptibility was characterized by an altered cytokine environment and infiltrating, permissive neutrophil recruitment to the site of infection. This study highlights the necessity for genetic interaction studies for us to identify potentially parallel pathways that are critical for defense against Mtb.

The development of the FLAM model opens the door for extensive exploration of the previously elusive alveolar macrophage. Given that the AM is the primary phagocyte in the lungs, and potentially the first cell that many pathogens encounter, FLAMs could be used to build a more physiologically relevant understanding of host-pathogen interactions of other pathogens that cause pulmonary disease in addition to *Mycobacterium tuberculosis*. Specifically, we have been studying FLAM responses to *Mycobacterium abscessus* (Mab), a rare but deadly lung and skin pathogen that is notoriously recalcitrant to treatment, in parallel with Mtb to learn more about the shared and unique factors of pathogenesis that may help us better understand the mechanisms that contribute to, and fail to contribute to, protection during infection. The FLAM cell model is also currently in use by groups studying mechanisms of disease for other bacterial and fungal lung pathogens. With the scale and efficiency that these collaborators and ourselves can now work with while exploring AM-pathogen interactions, we will be able to synthesize our findings into a more comprehensive,

general understanding of lung inflammation and apply these findings to approach future studies with a more informed research strategy. Furthermore, with the use of FLAMs in numerous research spaces, we will also begin to build a better understanding of differences between these cells and many other cell models that have been previously used to study macrophage responses to pathogens. Parallel infections between FLAMs and other macrophage models would not just improve our understanding of pulmonary responses to these pathogens but allow us to further appreciate the unique mechanisms by which AMs regulate inflammation.

Independent of host-pathogen interactions, this model can also be used to explore AM biology at homeostasis and uncover both what makes these cells so unique and exactly how unique they are from other cell types. Alveolar macrophages are known to rely on fatty acid metabolism and oxidative phosphorylation as their primary means of energy generation(3, 4). It is thought that this metabolic distinction from BMDMs, which primarily use glycolysis unless directed otherwise, plays an important role in the unique inflammatory profile of AMs(5, 6). In our initial genetic screen for regulators of SiglecF to identify pathways necessary for maintaining the AM-like state, we discover that components of the peroxisome biogenesis, cytochrome p450, and oxidative phosphorylation pathways were necessary for SiglecF surface expression. Each of these pathways is directly linked to either fatty acid oxidation or oxidative phosphorylation and suggest similarities between FLAM and AM metabolism(7–10). Peroxisome biogenesis is particularly interesting, as peroxisomes are not only intimately linked with numerous stages of lipid oxidation and biosynthesis but are also able to generate NADH and acetyl-CoA for use in oxidative phosphorylation(11, 12).

Additionally, ongoing work investigating mitochondrial respiration in our model suggests a unique sensitivity of FLAMs to disruption of the electron transport chain and CPT1, an essential enzyme in fatty acid oxidation (data not shown). These findings highlight fatty acid metabolism and mitochondrial respiration as key contributors to AM biology. Further studies exploring AM metabolism are necessary to fully understand the role of these pathways and how they specifically contribute to AM immune activation. The prevalence of fatty acid metabolism in AMs is not surprising, given the lipid-rich environment in which AMs reside. Current strategies culturing AMs and FLAMs *ex vivo*, however, employ traditional cell culture media with a defined nutrient and chemical composition, with added serum. While these conditions permit acceptable AM-like phenotypes *ex-vivo*, they do not recapitulate the levels of lipids in the lungs and prevent us from exploring relevant lipid metabolism in these cells. To better understand AM metabolism in a physiologically relevant setting, future studies will explore supplementing culture media with defined surfactants and measuring cellular processes such as replication, cell survival, and inflammatory responses. Mitochondrial respiration should also be more explicitly studied as an essential metabolic process in these cells. Recently, linezolid (an oxazolidinone antibiotic that is used to treat bacterial infections, but also inhibits mammalian mitochondrial ribosomes) was used to deplete mitochondrial mass within macrophages to study the impact of mitochondria on inflammatory responses(13–16). This strategy, in addition to commonly used staining practices to measure total mitochondria and mitochondrial-derived ROS (a byproduct of mitochondrial respiration) can be used to effectively study the prevalence and activity of mitochondria in FLAMs.

Among macrophages, AMs are distinctive not only in their means of energy generation but also in their ability to self-propagate(3, 5, 17–19). These differences in core cellular processes suggests that these cells also likely have unique requirements for viability. Numerous studies have defined essential genes in various cell types using the previously described CRISPR-Cas9 loss of function screening approach(20–23). This strategy could likewise be employed in FLAMs to identify essential genes in AMs. This is done by generating a genome-wide loss of function library and maintaining the library in culture over time. As the library is maintained, genomic DNA is sampled at numerous timepoints and sequenced. This allows us to track the relative abundance of each sgRNA in the population over time. As the library is passaged, sgRNAs that disrupt genes that are essential or are positive regulators of replication will become less abundant relative to genes that have no effect on replication or growth suppressors. By comparing these abundances at each timepoint, we can identify which sgRNAs become less abundant over time or were never identified in the library at any timepoint. The utility of genetics screens in this model do not end with identifying essential genes, however. Genetic screens have been performed extensively in BMDMs and BMDM-models to identify novel regulators of numerous cellular and immune-based processes(23–31). These studies provide the ideal groundwork to replicate genetic screens in the FLAM model, to systematically and efficiently identify AM-unique regulators of many important processes. Furthermore, the GenomeCRISPR database offers a valuable resource to compare regulators identified in FLAMs with data from >500 other, published CRISPR/Cas9 screens in hundreds of different cell types(32).

Together, these strategies and resources will allow us to elucidate the AM-specific regulation of numerous, key biological processes.

A significant drawback to studies in murine models is the lack of genetic diversity. While human populations possess significant genetic diversity across our genome, nearly all murine models are clonal and inbred, meaning that there is no genetic diversity within the studied populations. While this is ideal for gathering consistent and replicable results, it limits the translatability of any findings to human health and disease. To address this and create human-like randomized genetic diversity in a mouse population, the Collaborative Cross (CC) model was created(33). This model involves randomized breeding between 8, genetically distinct founder strains, followed by multiple generations of interbreeding to create hundreds of recombinant inbred mouse lines that each possess a random assortment of alleles from each of the eight founder strains. This distribution of alleles between the strains allows for determination of allelic contributions to phenotypes through analysis of such phenotypes and correlation of the phenotypes with the allelic combinations present in mice of interest(34, 35). While a powerful tool to model human genetic diversity, a major limitation is the high cost of resources and time to acquire and maintain the mice necessary to make full use of the CC model. Previously, studies of lung health and disease using this model would have necessitated repeated isolation of AMs from each mouse line. Given the already established limitations of studies using AMs, attempting to employ the CC model with AMs would require a massive quantity of time and resources, rendering this approach untenable. The FLAM model, however, addresses these concerns: our ability to generate large numbers of cells and frozen stocks from a

single isolation means that instead of expanding and maintaining a significant colony for each CC line, we instead would need a single viable breeder pair for each line, all but obviating the previously mentioned limitations of the CC model. Combining the CC model with the FLAM cell model would allow us to study the contributions of various alleles in the context of lung health and disease, potentially allowing for more relevant, informative, and impactful findings.

Perhaps the most exciting future direction from these studies is the use of the FLAM model *in vivo* through adoptive transfers. Currently, studying AM-specific knockouts *in vivo* requires the careful and lengthy process of breeding mice with a “floxed” gene of interest with mice containing a Cre-recombinase on a gene expression by AMs (and ideally no or few other tissues). Limitations of this approach include availability of Cre and “floxed” mice for the tissue/genes of interest, respectively, and the time commitment to the multiple generations of breeding that are necessary to generate the appropriate Cre-lox mouse. Furthermore, an AM-specific Cre mouse does not exist, and we are limited to using Cre-mice that affect multiple immune cell populations (such as dendritic cells in Cd11c-Cre and all myeloid cells in LsyM-Cre). Alternatively, with the efficiency and accuracy of CRISPR/Cas9 loss-of-function gene editing that is possible in the FLAM model, I hypothesize that we will be able to create mutants of interest in FLAMs *ex vivo*, and adoptively transfer those cells into the lungs of mice. Previous studies have displayed that transfer of macrophages into the lungs is possible, and that these transferred macrophages populate the lung, adapt to the environment, and persist as a pulmonary macrophage population(36–39). Transferring FLAMs in the lungs of WT mice would permit rapid, low-cost analysis of the function of AM-specific

knockouts in vivo. Inversely, a possibility that is unique to this strategy is the potential to transfer WT FLAMs into the lungs of mice that are mutated for a gene of interest and lacking resident AMs. This two-pronged approach would allow us to definitively investigate the impact of genes specifically in AMs in vivo with a previously impossible efficiency and rigor.

The use of in vivo transfer of FLAMs into the lungs would also further refine our screening approach in identifying genes that contribute to protection during disease. While our ex vivo culture conditions and genetic screening strategies have enabled us to discover new facets of lung biology and inflammatory responses, we are likely not fully appreciating the complexity and importance of the lung environment and how it may impact AMs and their responses. In vivo screening for phenotypes of interest, such as inflammatory cytokine responses or bacterial control would be the gold standard for identifying genes that control immune responses during disease. The use of CRISPR sub-libraries would allow us to transfer a defined pool of FLAMs mutated for genes of interest, perform an experiment, extract the mutated FLAMs, and use flow cytometry and next-generation sequencing to identify physiologically relevant gene candidates for follow-up studies. This in vivo screening strategy would permit high-confidence identification of mechanisms of pathogen response in the lungs.

Independent of strictly AM biology, our studies identifying and dissecting the novel genetic interaction between the phagocyte oxidase and Caspase1 highlight the importance of such studies in uncovering protective host pathways during response to Mtb. A challenge in identifying novel mechanisms of immune protection during disease is the relevance of unidentified, redundant pathways for particularly critical immune

processes. We can use the CRISPR/Cas9 genetic screening approach described in Chapter 2 to address this obstacle in an unbiased way. By screening for an immune-based phenotype (cytokine production, bacterial growth, bacterial uptake, etc) using a loss-of-function library built into a macrophage background knocked out for a central immune component that on its own doesn't appear to play a large role (such as Caspase1 or the phagocyte oxidase), we will be able to identify novel genetic interactions that are essential to protection in an unbiased, large scale manner. Such a model could be built into a FLAM and/or iBMDM model with little effort, and parallel genetic screens by this method would inform follow-up studies regarding myeloid-derived macrophage -based immune responses, AM-based immune responses, and the shared and unique regulation that these populations have over vital protective mechanisms.

In the above-described studies, I illustrate a series of studies and future directions that will further our understanding of physiologically relevant immune responses to lung inflammation and *Mycobacterium tuberculosis*. By setting out to create an improved alveolar macrophage cell culture system before exploring Mtb pathogenesis and host responses, I was able to uncover novel regulators of lung biology regarding the AM-state at baseline, and AM-specific inflammatory responses. Leveraging this model with iterative genetics approaches will allow us to explore the relatively uncharted territory of alveolar macrophage genetic regulatory mechanisms to disease. We will be able to employ these strategies and their findings to identify future targets for Mtb host-directed therapy and contribute in a meaningful way to our ability to prevent and cure tuberculosis.

BIBLIOGRAPHY

1. Bochen Cao by, Stevens GA, Ho J, Ma Fat D, Cao Gretchen Stevens BA, Ma D, Estevez D, Daher J, Ferlay J, Gacic-Dobo M, Gerland P, Glaziou P, Hug L, Ilaych K, Jakob R, Liu L, Lozano R, Mahy M, Mathers C, Moller A-B, Msemburi W, Naghavi M, Noor A, Patel MK, You D. 2000. Global Health Estimates Technical Paper.
2. Murphy SL, Kochanek KD, Xu J, Arias E. 2020. Mortality in the United States, 2020 Key findings Data from the National Vital Statistics System.
3. Woods PS, Kimmig LM, Meliton AY, Sun KA, Tian Y, O'Leary EM, Gökalp GA, Hamanaka RB, Mutlu GM. 2020. Tissue-resident alveolar macrophages do not rely on glycolysis for LPS-induced inflammation. *Am J Respir Cell Mol Biol* 62:243–255.
4. Gao X, Zhu B, Wu Y, Li C, Zhou X, Tang J, Sun J. 2022. TFAM-Dependent Mitochondrial Metabolism Is Required for Alveolar Macrophage Maintenance and Homeostasis. *The Journal of Immunology* 208:1456–1466.
5. Wang T, Liu H, Lian G, Zhang SY, Wang X, Jiang C. 2017. HIF1 α -Induced Glycolysis Metabolism Is Essential to the Activation of Inflammatory Macrophages. *Mediators Inflamm* 2017.
6. Svedberg FR, Brown SL, Krauss MZ, Campbell L, Sharpe C, Clausen M, Howell GJ, Clark H, Madsen J, Evans CM, Sutherland TE, Ivans AC, Thornton DJ, Grecis RK, Hussell T, Cunoosamy DM, Cook PC, MacDonald AS. 2019. The lung environment controls alveolar macrophage metabolism and responsiveness in type 2 inflammation. *Nat Immunol* 20:571–580.
7. Yanai R, Mulki L, Hasegawa E, Takeuchi K, Sweigard H, Suzuki J, Gaissert P, Vavvas DG, Sonoda KH, Rothe M, Schunck WH, Miller JW, Connor KM. 2014. Cytochrome P450-generated metabolites derived from omega-3 fatty acids attenuate neovascularization. *Proc Natl Acad Sci U S A* 2014/07/01. 111:9603–9608.
8. COOPER DY, ESTABROOK RW, ROSENTHAL O. 1963. The stoichiometry of C21 hydroxylation of steroids by adrenocortical. *J Biol Chem* 238:1320–1323.
9. Lu AY, Coon MJ. 1968. Role of hemoprotein P-450 in fatty acid omega-hydroxylation in a soluble enzyme system from liver microsomes. *Journal of Biological Chemistry* 243:1331–1332.
10. Wanders RJA, Waterham HR, Ferdinandusse S. 2016. Metabolic interplay between peroxisomes and other subcellular organelles including mitochondria and the endoplasmic reticulum. *Front Cell Dev Biol* 3:83.

11. Marchesini S, Poirier Y. 2003. Futile Cycling of Intermediates of Fatty Acid Biosynthesis toward Peroxisomal β -Oxidation in *Saccharomyces cerevisiae*. *Journal of Biological Chemistry* 278:32596–32601.
12. He A, Chen X, Tan M, Chen Y, Lu D, Zhang X, Dean JM, Razani B, Lodhi IJ. 2020. Acetyl-CoA Derived from Hepatic Peroxisomal β -Oxidation Inhibits Autophagy and Promotes Steatosis via mTORC1 Activation. *Mol Cell* 79:30.
13. de Vriese AS, van Coster R, Smet J, Seneca S, Lovering A, van Haute LL, Vanopdenbosch LJ, Martin JJ, Ceuterick-De Groote C, Vandecasteele S, Boelaert JR. 2006. Linezolid-induced inhibition of mitochondrial protein synthesis. *Clin Infect Dis* 42:1111–1117.
14. Wilson DN, Schluenzen F, Harms JM, Starosta AL, Connell SR, Fucini P. 2008. The oxazolidinone antibiotics perturb the ribosomal peptidyl-transferase center and effect tRNA positioning. *Proc Natl Acad Sci U S A* 105:13339–13344.
15. Soriano A, Miró O, Mensa J. 2005. Mitochondrial toxicity associated with linezolid. *N Engl J Med* 353:2305–2306.
16. Kiritsy MC, McCann K, Mott D, Holland SM, Behar SM, Sasseti CM, Olive AJ. 2021. Mitochondrial respiration contributes to the interferon gamma response in antigen-presenting cells. *Elife* 10.
17. Hetzel M, Ackermann M, Lachmann N. 2021. Beyond “Big Eaters”: The Versatile Role of Alveolar Macrophages in Health and Disease. *Int J Mol Sci*2021/04/04. 22.
18. Yu X, Buttgereit A, Lelios I, Utz SG, Cansever D, Becher B, Greter M. 2017. The Cytokine TGF-beta Promotes the Development and Homeostasis of Alveolar Macrophages. *Immunity*2017/11/12. 47:903-912 e4.
19. Williams M, de Kleer I, Henri S, Post S, Vanhoutte L, de Prijck S, Deswarte K, Malissen B, Hammad H, Lambrecht BN. 2013. Alveolar macrophages develop from fetal monocytes that differentiate into long-lived cells in the first week of life via GM-CSF. *J Exp Med*2013/09/18. 210:1977–1992.
20. Tzelepis K, Koike-Yusa H, de Braekeleer E, Li Y, Metzakopian E, Dovey OM, Mupo A, Grinkevich V, Li M, Mazan M, Gozdecka M, Ohnishi S, Cooper J, Patel M, McKerrell T, Chen B, Domingues AF, Gallipoli P, Teichmann S, Ponstingl H, McDermott U, Saez-Rodriguez J, Huntly BJP, Iorio F, Pina C, Vassiliou GS, Yusa K. 2016. A CRISPR Dropout Screen Identifies Genetic Vulnerabilities and Therapeutic Targets in Acute Myeloid Leukemia. *Cell Rep* 17:1193.
21. Wang T, Birsoy K, Hughes NW, Krupczak KM, Post Y, Wei JJ, Lander ES, Sabatini DM. 2015. Identification and characterization of essential genes in the human genome. *Science* 350:1096.

22. Bertomeu T, Coulombe-Huntington J, Chatr-aryamontri A, Bourdages KG, Coyaud E, Raught B, Xia Y, Tyers M. 2018. A High-Resolution Genome-Wide CRISPR/Cas9 Viability Screen Reveals Structural Features and Contextual Diversity of the Human Cell-Essential Proteome. *Mol Cell Biol* 38.
23. Covarrubias S, Vollmers AC, Capili A, Boettcher M, Shulkin A, Correa MR, Halasz H, Robinson EK, O'Briain L, Vollmers C, Blau J, Katzman S, McManus MT, Carpenter S. 2020. High-Throughput CRISPR Screening Identifies Genes Involved in Macrophage Viability and Inflammatory Pathways. *Cell Rep* 33.
24. Shi J, Wu X, Wang Z, Li F, Meng Y, Moore RM, Cui J, Xue C, Croce KR, Yurdagul A, Doench JG, Li W, Zarbalis KS, Tabas I, Yamamoto A, Zhang H. 2022. A genome-wide CRISPR screen identifies WDFY3 as a regulator of macrophage efferocytosis. *Nature Communications* 2022 13:1 13:1–19.
25. Lindner B, Martin E, Steininger M, Bundalo A, Lenter M, Zuber J, Schuler M. 2021. A genome-wide CRISPR/Cas9 screen to identify phagocytosis modulators in monocytic THP-1 cells. *Scientific Reports* 2021 11:1 11:1–11.
26. Tong J, Wang X, Liu Y, Ren X, Wang A, Chen Z, Yao J, Mao K, Liu T, Meng FL, Pan W, Zou Q, Liu J, Zhou Y, Xia Q, Flavell RA, Zhu S, Li HB. 2021. Pooled CRISPR screening identifies m6A as a positive regulator of macrophage activation. *Sci Adv* 7:4742–4770.
27. Lai Y, Cui L, Babunovic GH, Fortune SM, Doench JG, Lu TK. 2021. High-Throughput CRISPR Screens To Dissect Macrophage-Shigella Interactions. *mBio* 12.
28. Cohen A, Jeng EE, Voorhies M, Symington J, Ali N, Rodriguez RA, Bassik MC, Sil A. 2022. Genome-scale CRISPR screening reveals that C3aR signaling is critical for rapid capture of fungi by macrophages. *PLoS Pathog* 18:e1010237.
29. Kiritsy MC, Ankley LM, Trombley J, Huizinga GP, Lord AE, Orning P, Elling R, Fitzgerald KA, Olive AJ. A genetic screen in macrophages identifies new regulators of IFN γ -inducible MHCII that contribute to T cell activation <https://doi.org/10.7554/eLife>.
30. Gilliland HN, Beckman OK, Olive AJ. 2023. A Genome-Wide Screen in Macrophages Defines Host Genes Regulating the Uptake of Mycobacterium abscessus. *mSphere* e0066322.
31. Kiritsy MC, McCann K, Mott D, Holland SM, Behar SM, Sasseti CM, Olive AJ. 2021. Mitochondrial respiration contributes to the interferon gamma response in antigen-presenting cells. *Elife* 10.
32. Rauscher B, Heigwer F, Breinig M, Winter J, Boutros M. 2017. GenomeCRISPR - a database for high-throughput CRISPR/Cas9 screens. *Nucleic Acids Res* 45:D679–D686.

33. Chesler EJ, Miller DR, Branstetter LR, Galloway LD, Jackson BL, Philip VM, Voy BH, Culiati CT, Threadgill DW, Williams RW, Churchill GA, Johnson DK, Manly KF. 2008. The Collaborative Cross at Oak Ridge National Laboratory: Developing a powerful resource for systems genetics. *Mammalian Genome* 19:382–389.
34. Threadgill DW, Miller DR, Churchill GA, de Villena FPM. 2011. The collaborative cross: a recombinant inbred mouse population for the systems genetic era. *ILAR J* 52:24–31.
35. Noll KE, Ferris MT, Heise MT. 2019. The Collaborative Cross: A Systems Genetics Resource for Studying Host-Pathogen Interactions. *Cell Host Microbe* 25:484.
36. Careau E, Bissonnette EY. 2004. Adoptive transfer of alveolar macrophages abrogates bronchial hyperresponsiveness. *Am J Respir Cell Mol Biol* 31:22–27.
37. Gorki AD, Symmank D, Zahalka S, Lakovits K, Hladik A, Langer B, Maurer B, Sexl V, Kain R, Knapp S. 2022. Murine Ex Vivo Cultured Alveolar Macrophages Provide a Novel Tool to Study Tissue-Resident Macrophage Behavior and Function. *Am J Respir Cell Mol Biol* 66:64–75.
38. Subramanian S, Busch CJL, Molawi K, Geirsdottir L, Maurizio J, Vargas Aguilar S, Belahbib H, Gimenez G, Yuda RAA, Burkon M, Favret J, Gholamhosseinian Najjar S, de Laval B, Kandalla PK, Sarrazin S, Alexopoulou L, Sieweke MH. 2022. Long-term culture-expanded alveolar macrophages restore their full epigenetic identity after transfer in vivo. *Nature Immunology* 2022 23:3 23:458–468.
39. Eguíluz-Gracia I, Schultz HHL, Sikkeland LIB, Danilova E, Holm AM, Pronk CJH, Agace WW, Iversen M, Andersen C, Jahnsen FL, Baekkevold ES. 2016. Long-term persistence of human donor alveolar macrophages in lung transplant recipients. *Thorax* 71:1006–1011.